CRANFIELD UNIVERSITY

OLGA MURUJEW

TERTIARY PHOSPHORUS REMOVAL FROM WASTEWATER

SCHOOL OF WATER, ENERGY AND ENVIRONMENT

PhD
Academic Year: 2018–2019

Supervisors: Dr. Marc Pidou & Prof. Bruce Jefferson
April 2019

CRANFIELD UNIVERSITY

SCHOOL OF WATER, ENERGY AND ENVIRONMENT

PhD

Academic Year: 2018–2019

OLGA MURUJEW

Tertiary Phosphorus Removal from Wastewater

Supervisors: Dr. Marc Pidou & Prof. Bruce Jefferson
April 2019

Abstract

To protect surface water bodies, final effluents of wastewater treatment works are being regulated with stricter consents. Phosphorus has been identified as a priority compound and according to the Water Framework Directive its levels in wastewater effluents need to be below 1 mg P/L and in some cases as low as 0.1 mg P/L. To meet these consents efficiently and economically, there are several novel or established tertiary P removal technologies.

Chemical P removal is a conventionally applied process. Yet, it requires optimisation in chemical doses and the most appropriate solids liquid separation for tertiary P removal needs yet to be identified to meet the new stricter consents sustainably. Novel tertiary P removal technologies such as immobilised algae beads systems or reactive media constructed wetlands provide a more sustainable approach with no direct use of chemicals on site and the recycling of materials such as the media in the wetland or through conversion of the algal biomass to energy. However, these technologies are not yet fully established and require validation of their viability and cost competitiveness.

In this thesis, tertiary P removal technologies have been evaluated with the aim to resolve existing bottlenecks that are associated with the implementation of these technologies when meeting sub 1 mg P/L levels. Three coagulation-based technologies that have not been operated previously in the UK were assessed on their robustness and resilience under steady-state and dynamic conditions against a 0.3 mg P/L target. It was found that ballasted coagulation was the most robust and could consistently deliver effluent concentrations as low as 0.1 mg P/L. Pile cloth media filtration and ultrafiltration were shown to be less robust yet effective at reaching 0.3 and 0.5 mg P/L targets, respectively. The importance of the solid liquid separation step as well as optimisation of dosing and coagulation-flocculation was highlighted. Further it was found that in a ballasted coagulation system, weaker and bigger flocs are generated through the addition of polymer which are efficiently separated through the incorporation of a ballasting agent. Ultimately, guidance on suitable choice of polymers and their doses was given as anionic polymers at doses as low as 0.1 mg/L.

From the novel alternatives, a reactive media (steel slag) constructed wetland was operated at full-scale under real conditions and has reached the highest reported P retention capacity to date with very low P effluent concentrations ($<$1 mg/L from an average of about 8 mg/L) achieved in the first year of operation. During the life cycle of the wetland, P removal decreased substantially, and it was highlighted that the underlying mechanisms

are more complex than previously assumed. To address the bottleneck of high costs of beads production in immobilised algae systems, a proof-of-concept has been given where 69.1% alginate recovery was achieved, and algae beads made from recycled alginate were further reused in P removal trials. Ultimately, a cost reduction of 34% of operational costs could be achieved.
Finally, the insights were translated into a P removal strategy where the most suitable technologies are recommended for differently scaled wastewater treatment works (WWTW) and different effluent P targets based on their performance, costs and sustainability. For large WWTW, ballasted coagulation appeared to be the most suitable technology while for small WWTW pile cloth media filtration is recommended. Based on this research, ultrafiltration cannot be recommended for tertiary P removal. The novel technologies were highlighted as more sustainable options for small WWTW which still need further understanding and development.

Keywords

P removal; Coagulation; Steel slag; Alginate recovery

Acknowledgements

I will be forever grateful to both my supervisors who had more perseverance and tenacity in this than me. Especially, I would like to thank my first supervisor Marc Pidou for being so supportive until the very end, reading this stuff countless times and for keeping a positive attitude no matter what. Then I would like to express my deepest gratitude to Bruce Jefferson who not only gave me the chance to go to Australia but also guided me throughout this project and especially at the end, for giving the final push.
I am also very thankful for the financial sponsorship from Severn Trent Water and I am grateful for having been given the chance to be part of the Packington Team. Secondly, I am thankful for financial support that was given by the RSC Alan Tetlow Memorial Bursary for my placement in Australia.
I cannot give enough thanks the Innovation team at Severn Trent Water for their support. I am so grateful for having had the chance to meet Andrea Wilson who was an incredibly strong and brave woman and who has made priceless contributions to the success of the Packington Low P project. Your passing has left an empty hole that will never be filled and I will never forget about you.
I am also very grateful for the support from Pete Vale for always being friendly and supportive. I would also like to thank Bob, Ali, John, Keiron, Justin, Yadira, Luca and the stakeholder team of this project for their support throughout. A big thank you also to Martin for helping with admin stuff and sorting things out.
At Cranfield, I would like to thank the lab technicians team: Jane for managing the lab so well; Richard Andrews, Alan Nelson, Paul Barton and Monika Jodkowska for the always friendly, patient and efficient response to all my questions and for all the help. I would like to thank Ana Soares and Giuseppina Di Lorenzo for being my advisors and giving valuable input. I would like to thank Monica Rivas Casado for the support in statistics and finally, I would like to thank Tania Rice plainly for being awesome at her job.
At RMIT, I would like to thank Felicity Roddick and Linhua Fan for welcoming me to their research group and guiding me through the way of the alginate project. Further, I would like to thank the RMIT technician team Peggy, Cameron and Sandro (especially for the nice coffees!). A big thank you to Chaitali for teaching me how to take decent SEM images and Nadia for the support in freeze-drying techniques.
Also, I would like to thank Matthew Kube, my B1, for brightening up the sometimes dull lab work and for reminding that a thesis has to be written only once. Many thanks also to Dr Rachel Whitton for the friendly chats and of course teaching me how to count algae. I

would also like to thank Dr Kristell Le Corre Pidou for the super support on the reactive media part of the project.
I want to express my endless gratitude to all the people who have been in my life during these last years.
"Being sent to Coventry" was not so bad after all, because I was lucky enough to meet my *Couchsurfing* family. I am thankful for all the beautiful people I have met who have enabled me to have a life (maybe too) far away from science. Thank you for all the great memories of all the parties, trips and dinners. A huge thank you to my lovely sister-by-choice, Bertha Du bist mein Sonnenschein im Leben! To Ledicia Pereira Gomez who is one of the kindest people I have ever met. Thank you for being a friend. I will miss our roadtrips, dinners and talks about the *intriguing* quirks of English grammar and pronunciation. I am also thankful to Craig and Eleanor who were my first "real" English friends. Thank you for the dinners, (climbing) trips and showing me the English way of living! Then I am thankful for the awesome climbing family: Thank you for being great friends and creating wonderful memories. I am especially thankful for being able to call Justyna, a wonderful, strong woman in all ways, and her two pirate princesses my friends. Thank you to Fabrizio, the eternal traveler and role model when it comes to life-wisdom, who can always make me laugh and understands the level of people making life difficult. I know that you'll find your place someday. My biggest thank you also to Ionut and Markus for being a wonderful and cheerful company and always up for climbs and jokes. Merci beaucop à Simon, who loves when I speak French, for being a good friend and for making me a better climber. Last but not least, I am so thankful for my friend Steve, the most kindhearted punk of the UK, for taking me climbing, for the dinners and for taking me out on your motorbike. I would also like to thank the Crackley Woods volunteer group: Jon for being a great work party leader, for teaching me how to use a saw and how to lay traditional English hedges. You have been trying hard to teach me trees and birds as well but I am a learning-resistant student. Many, many thanks also to Dave and his weekly cake treats. Then I would like to say thank you to Sarah Gunn who not only gave me a room in Melbourne but also a friendly and welcoming home. Thank you for educating me about timber and logging, taking me out to my first "Anti-logging protest", showing me the beautiful rainforest and Aussie-style sandwich-making, providing me with books and for keeping my spirits up when I was down (I think, the wine helped, too). I would also like to thank Paul O'Callaghan and my colleagues at BlueTech Research for being so supportive during this time.
Großer Dank geht auch an meine Freunde von daheim, insbesondere Robert Hausmann, der mein Gejammer zum Ende hin ertragen musste und mich immer zum Lachen bringen kann.
Mein größter Dank geht auch an meine Eltern, die mich immer bei allem unterstützt haben (auch wenn manchmal widerwillig). Ihr habt auf Vieles verzichten müssen, um mir meinen Weg zu ermöglichen und dafür werde ich ewig dankbar sein.
Unglaublich dankbar bin ich auch für meine wundervolle, schlaue Schwester, Natalia, auf die ich unheimlich stolz bin. Danke auch an Vitalja, der mit seiner Lebenseinstellung, das

Leben nicht so ernst zu nehmen, inspririert und mich immer zum Lachen bringen kann. Eure beiden Kinder sind euch ganz besonders gut gelungen! Maksim, mein Schatz, ich bin unendlich dankbar, dafür dass es dich gibt und liebe dich über Alles.
Irina, du bist einer der wichigsten Menschen in meinem Leben. Mit niemandem verreise ich so gerne wie mit dir, mit niemandem lache ich so viel wie mit dir und niemand versteht mich so sehr wie du. Auf viele weitere gemeinsame LeKu Jahre! Ich kann unsere gemeinsame große Reise nicht erwarten!!
Finally, Daniel- thank you for making me part of Team Humboldt, for being so considerate during ”this situation” and for everything else.

Contents

List of Figures

List of Tables

List of Abbreviations

AB	Algae beads
B	Ballast only
BC	Ballasted coagulation
BOF	Blast oxygen furnace
BP	Ballast and Polymer
CB	Coagulant and Ballast
CBP	Coagulant, Ballast and Polymer
CD	Charge density
CF	Cloth filtration
Co	Coagulant only
COD	Chemical oxygen demand
CP	Coagulant and Polymer
CW	Constructed wetlands
DEFRA	Department for Environment, Food and Rural Affairs
EAF	Electric arc furnace
EB	Empty beads
EBCT	Empty bed contact time
EBPR	Enhanced biological P removal
EDX	Energy Dispersive X-Ray Diffraction

FU	Fresh un-used
FW	Fresh washed
HAP	Hydroxyapatite
HCT	Hydraulic conductivity test
HRAP	High-rate algal pond
HRT	Hydraulic retention time
IAP	Ion activity product
IBR	Immobilised algae (bio-)reactor
K_{sp}	Solubility product
MF	Membrane filtration
nOPEX	Net operational expenditure
O & M	Operation and Maintenance
OD	Oxidation ditch
PAO	Phosphate accumulating organism
PBR	Photobioreactor
PE	Population equivalent
RA	Recycled/recovered alginate
RI	Robustness index
SEM	Scanning Electron Microscopy
SF	Sand filter
SI	Saturation index
TAG	Technical advisory group
TF	Trickling filter
TP	Total P
TRL	Technology readiness level
TSS	Total suspended solids

UWWTD	Urban Wastewater Treatment Directive
VA	Virgin alginate
WFD	Water Framework Directive
WWTW	Wastewater treatment works

Chapter 1

Introduction

1.1 Background

Although phosphorus (P) is an essential nutrient and naturally present in the environment, its accumulation in fresh waters can lead to eutrophication which causes blooms of algae. These create toxic conditions for aquatic organisms and are therefore harmful for the environment and its biodiversity (Desmidt et al. 2015; Paerl et al. 2001; Schaum 2018). P concentrations above natural levels come from anthropogenic sources with wastewater effluents being a main contributor (Cordell et al. 2011; Desmidt et al. 2015; Neal et al. 2010).

In the UK, 588 sensitive areas have been recognised of which 914 km^2 are already or close to be eutrophic caused by excess phosphorus and nitrogen (N) concentrations (DEFRA 2012). To support the Department for Environment, Food and Rural Affairs (DEFRA) a technical advisory group (TAG) has been initiated which reviews River Basin Management Plans in periodic phases to facilitate the implementation of the Water Framework Directive (WFD) (Chave 2001; DEFRA 2014; UK TAG 2013). The goal is to achieve "good ecological status" in surface waters (Andrews et al. 2008; Chave 2001). This qual-

itative term refers to the presence of substances at concentrations that can be ascribed to human impact but that ”deviate only slightly from those normally associated with the surface water body type under undisturbed conditions” (EU Water Framework Directive 2000). The discharge of final effluents from wastewater treatment works (WWTWs) has been previously regulated by the Urban Wastewater Treatment Directive (UWWTD) (Urban Wastewater Treatment Directive 1998). However, with adoption of the WFD the protection of surface (rivers, lakes, bathing waters) and ground waters was put into focus and new discharge limits have been determined. The previous discharge consents for P were 1 mg P/L for WWTWs of more than 100 000 population equivalent (PE) and 2 mg P/L for works with PE between 10 000 and 100 000 (Urban Wastewater Treatment Directive 1998). Therefore, from the implementation of the WFD and the latest River Basin Management Plan (2015-2021), P has been highlighted as one of the priority substances to be regulated and the discharge limits for P will be stricter at levels below 1 mg/L and with some sites expected to be set target levels as low as 0.1 mg/L (EU Water Framework Directive 2000). New P consents will depend on the P levels at ”near natural conditions” (UK TAG 2013), environmental sensitivity, altitude, alkalinity of sites and on upstream dilution rates (Chave 2001). Therefore, utilities are receiving regulatory pressure from the implementation of the WFD to remove P and need to reconsider current P removal options to ensure that the new consents will be met (Chave 2001).

On average, WWTWs receive P concentrations of 7-9 mg P/L and P can be either removed chemically or biologically (De-Bashan and Bashan 2004; Morse et al. 1998; Pratt et al. 2012). In chemical P removal, a metal salt (based on iron or aluminium) is added which reacts with phosphate species to form flocs. These flocs are removed as sludge from the wastewater through settling or filtration (Bratby 2016; Yeoman et al. 1988). Generally, it is possible to chemically achieve effluent P concentrations below 1 mg P/L. However, doing so requires disproportionately high coagulant doses with associated larger sludge

volumes and ultimately an increase in costs (Bratby 2016; Murthy et al. 2005). Accordingly, it is considered better practice to add a tertiary stage that utilises coagulant to reduce the final P concentration from 1-2 mg P/L down to the required target of 0.1-1.0 mg P/L. This approach benefits in two major ways. Firstly, in wastewater phosphorus occurs in different forms such as ortho-phosphate, pyrophosphates, triphosphates and poly-phosphates, in varying concentrations depending on pH, ligand reactions and concentrations of the other constituents in the wastewater. During the wastewater treatment process and especially during the aerobic stage phosphorus species are transformed into the the predominant form of ortho-phosphate. This species is more easily removed by chemical precipitation than the other forms it exists in (Bratby 2016). Secondly, the required dose is greatly reduced compared to dosing just upstream with reported savings of tens of mg/L of coagulant (Bratby 2016).

Alternatively, P can be removed through enhanced biological P removal (EBPR) which is more sustainable. With EBPR favourable growth conditions for phosphate accumulating organisms (PAOs) are generated. In the initial anaerobic stage, PAOs take up carbon compounds for intracellular storage while releasing internal polyphosphates as soluble phosphates. This is then followed by an aerobic stage where the PAOs take up phosphates to transform them into intracellular polyphosphate. This process has been known for more than 30 years and since then various configurations have been developed to enhance its efficiency and reliability. In comparison to chemical P removal, the EBPR process is more sustainable because it produces relatively small amounts of sludge. Low phosphorus concentrations can be achieved with EBPR if specific conditions are maintained, e.g. low carbohydrate levels in the sludge (De-Bashan and Bashan 2004). The dynamics of wastewater composition and conditions at WWTWs can negatively affect the performance of the EBPR process therefore additional coagulant dosing is usually required when targeting low effluent phosphorus concentrations (Oehmen et al. 2007). Coagulant is also

added at some sites to reduce the risk of downstream struvite precipitation form the excess sludge.

However, importantly P is a major plant nutrient and its derivatives are used as fertilisers in agriculture. Fertilisers are mainly produced from mined phosphate rock whose reserves are finite and non-renewable. Phosphate rock is anticipated to reach its peak production around the year 2030 (Cordell et al. 2011). Accordingly, technologies that just remove phosphorus from wastewater can be viewed as ultimately unsustainable. Therefore, technologies that enable recovery alongside removal are the next logical step as part of a switch toward a circular economic strategy (Melia et al. 2017, Pratt and Shilton 2009, Schaum 2018). Nutrient recovery can be applied at various stages of wastewater treatment. A concentrated stream of P is required for an efficient and economic recovery (Morse et al. 1998). This has been already studied extensively by various researchers who reported on precipitation of struvite or calcium phosphate from sludge, sludge ash and sludge digestion liquor (Desmidt et al. 2015).

At tertiary stage, alternative technologies that not only remove P but also have an added value such as generating fertiliser, producing energy or reusing waste media would move wastewater treatment facilities further towards resource recovery facilities (Schaum 2018). Research has been on-going in the field of P sorption media and subsequent P-based fertilisers (Acelas et al. 2015; Martin et al. 2013), the use of microalgae for treatment and anaerobic digestion of the biomass (Whitton 2019) and the use of reactive media that would otherwise go to waste (Blanco et al. 2016; Yang et al. 2018). Despite promising results, adoption of these technologies has not yet taken place in full-scale WWTWs. While further development in these fields are much required and continuing, the time until full-scale implementation needs to be covered by already existing and chemically-based tertiary P removal technologies while focusing on minimal chemical consumption and ensuring that consents are met at WWTWs.

1.1.1 Technology readiness levels of tertiary P removal

Different sizes of wastewater treatment plants will require individually suitable solutions. At small WWTWs, technologies that require no or very little maintenance, such as constructed wetlands and rotating biological contactors are usually installed while at large WWTWs, operation-intense technologies that can treat large flow rates are implemented. With traditional P removal, the required levels below $<$1 mg P/L will be difficult to achieve economically and therefore advanced tertiary P removal will need to be investigated.

There are emerging coagulation-based technologies that would be suitable for large works and that have already been tested at demonstration scale against ultra-low effluent P concentrations, i.e. $<$0.1 mg/L, and a number of full-scale plants exist in the USA (DeBarbadillo et al. 2010; Ragsdale 2007). Yet, these developments cannot be directly translated towards meeting consents between 1-0.1 mg P/L as is required in the UK and therefore research in this area is needed.

To evaluate the development stage of new technologies and reduce risks for implementation, NASA introduced the concept of ”technology readiness levels” (TRLs). These range between TRL 1 to TRL 9 to signify early research to successful deployment and operation, respectively (Mankins 2009). Although coagulation-based technologies are commercially available and can therefore be classified to a high TRL (Mankins 2009) they are not a long term sustainable choice since they consume large amounts of chemicals and energy throughout their life-time (Table 1.1). Nevertheless, advanced tertiary solid liquid separation technologies offer an opportunity for optimisation of operational conditions towards minimum required chemical doses while achieving low effluent P concentrations. For instance, a high rate sedimentation process -ballasted coagulation- uses a polymer as one of the components and many products are available. Because there is

currently a lack of scientific guidance on the impact of polymers and their doses, a better understanding of P removal in ballasted coagulation is needed.

Sustainable alternatives consuming less energy and no chemicals are currently under development. For instance, an immobilised algae reactor (IBR), where algal biomass is contained in solid alginate beads, has been shown to achieve effluent P levels of 0.1 mg/L at hydraulic retention times between 3-20 h (Whitton et al. 2018). This technology would be suitable for small WWTW but is yet to be tested in large scale and is currently at TRL 5 (Table 1.1). Importantly, the costs for implementation of a full-scale reactor have been shown not to be cost-competitive at the current time, mainly because of the high cost associated with the production of the algae beads (Whitton 2016), suggesting that an investigation into cost-reduction potential is essential.

Another typical technology at small WWTW are constructed wetlands which are currently not used for P removal. However, there has been increasing interest in replacing the commonly used gravel with reactive media to enhance P removal (Vohla et al. 2011), where steel slag has been identified as the most promising media (Drizo et al. 1999). This technology can be seen at TRL 6 because there have been already full-scale trials with another media, melter slag, for example (Shilton et al. 2006). Existing literature of the use of steel slag has predominately been undertaken at small scale laboratory and pilot trials using synthetic waters that are dissimilar to real wastewater. Whilst these have shown reactive media to be effective and have proposed removal mechanisms by which the technology operates, this has not been validated at large scale and in long-term using real wastewater. In addition, there are still existing barriers such as high effluent pH and leaching of toxic metals. Accordingly, there is concern over the translation of the existing knowledge base to enable confidence in its use at full-scale.

Utilities throughout the UK have collaborated in recent years to investigate tertiary P removal technologies on their efficacy and viability for full-scale implementation. How-

ever, as Severn Trent Water acknowledged the criticality of implementing more efficient and sustainable P removal technologies they decided to fund a dedicated trial. The work presented in this thesis was then developed in conjunction with the sponsoring partner Severn Trent Water as well as Atkins. At a WWTW in Leicestershire, UK, with 28 344 PE, four novel and emerging technologies have been tested at demonstration scale side by side. This site was chosen because it discharges into an ecologically sensitive area. Commercially available, yet new to the UK, coagulation technologies -a pile cloth media filter, a ballasted coagulation process, an ultrafiltration membrane- at higher TRLs will be assessed against their performance and robustness. Further, an outlook toward tertiary P removal of the future will be given through evaluating a large-scale long-term trial with a reactive media constructed wetland and through an attempt to improve the overall economics of an immobilised algae system.

Table 1.1: Technology overview

Technology	TRL	Size of WWTW	Additional chemicals	Operation and Maintenance	Bottlenecks of technologies
Immobilised algae reactor	5	S	None	Medium	Cost of bead production
Steel slag constructed wetland	6	S	None	Low	Validating viability
Ballasted coagulation	9	L	Coagulant, Polymer, Ballast	Medium	Optimised chemical use, Identification of most appropriate solid liquid separation
Pile cloth filtration	9	S-L	Coagulant	Low	
Membrane filtration	9	M-L	Coagulant, Cleaning chemicals	Medium	

1.2 Aims and Objectives

The overall aim of the thesis was to understand how to resolve the bottlenecks associated with implementation of tertiary P technologies when meeting sub 1 mg P/L concentrations.

A Compare the robustness and efficacy of commercial coagulation-based technologies with different solid liquid separation processes in meeting sub 1 mg P/L consents under UK conditions.

B Analyse the impact of different polymers and their doses on P removal and floc properties in a ballasted coagulation process.

C Validate existing understanding of the efficacy of reactive media in large scale, long-term constructed wetland trials for P removal.

D Evaluate the potential to recover and reuse alginate in an immobilised algal bio-reactor process.

1.3 Thesis Plan

This thesis is presented as a series of chapters formatted as journal papers. All papers were written by the primary author, Olga Murujew and edited by Dr Marc Pidou and Prof. Bruce Jefferson. All experimental work was designed, co-ordinated and completed by Olga Murujew at Severn Trent Water (UK), Cranfield University (UK) and RMIT University (Australia) with contributions from research fellows, PhD and visiting students as follows. Support in plant operation for the demonstration trial described in Chapter 2 and the reactive media wetland in Chapter 4 was given by WatsTech Ltd. The evaluation of polymers and their impact on P removal as described in Chapter 3 was assisted by Jordan Geoffroy, Emeline Fournie and Elisa Socionovo Gioacchini. In addition, support was given by Dr. Kristell Le Corre Pidou for the calculations of saturation indices described in Chapter 4. For the alginate related research in Chapter 5, microalgal cultivation and harvesting was aided by Matthew Kube and Dr. Rachel Whitton for experiments undertaken at RMIT University and Cranfield University, respectively. Support for SEM imaging of

algae beads was given by Dr. Chaitali Dekiwadia from RMIT University.

In Chapter 2, three coagulation-based technologies were assessed against their robustness and resilience towards meeting a <0.3 mg/L P target. The technologies were a ballasted coagulation, a pile cloth media filter and an ultrafiltration membrane, all operated at demonstration scale at the same WWTW. Resilience and robustness were tested against a range of operational conditions which were steady state, storm and diurnal simulation and variation of the wastewater feed. The findings highlighted the importance of solids liquid separation and informed the P removal strategy for tertiary P removal (Chapter 2, *Paper 1*, -submitted: Murujew, O., Wilson, A., Vale, P., Jefferson, B. and Pidou, M., Tertiary treatment of phosphorus using coagulants with different solid liquid separation technologies: Comparison of robustness and resilience, Journal of Chemical Engineering).

Since there is a gap in literature on the importance of polymer choice and dose specifically for ballasted coagulation systems, a detailed laboratory scale study was conducted with seven, anionic and cationic, polymers. P removal efficiency was compared as well as floc growth and structure were assessed. The results highlighted that polymers resulted in different performance and gave a guidance towards a suitable choice in wastewaters with 1 mg P/L influent and high alkalinity content (Chapter 3, *Paper 2*, -submitted: Murujew, O., Geoffroy, J., Fournie, E., Socionovo Gioacchini, E., Wilson, A., Vale, P., Jefferson, B. and Pidou, M., The impact of polymer selection and dose on the incorporation of ballasting agents onto wastewater aggregates, Water Research).

To validate existing knowledge on reactive media, a full-scale constructed wetland with basic oxygen furnace steel slag media was operated in long-term (>2 years) at the same site of the coagulant-based technologies. The outcomes of this study showed the broad range of potential P removal pathways and will further inform the P removal strategy for small scale WWTW (Chapter 4, *Paper 3*- submitted: Murujew, O., Le Corre Pidou, K., Wilson, A., Vale, P., Jefferson, B. and Pidou, M., Reactive media constructed wetland for

phosphorus removal: Assessing the opportunity and challenges, Journal of Environmental Management).

The potential of alginate recovery from immobilised algae beads was studied to deliver a proof-of-concept and to evaluate the potential towards reduction of operational costs of an IBR. The results from this research inform a tertiary P removal strategy for sustainable solutions that are currently under development (Chapter 5, *Paper 4*- submitted: Murujew, O., Whitton, R., Fan, L., Roddick, F., Jefferson, B. and Pidou, M., Recycling and reuse of alginate in an immobilised algae system, Environmental Technology).

The implications of the work were overall discussed and a UK-based P removal strategy for small, medium and large WWTW is presented. The insights from the thesis are evaluated against currently available technologies and those that have potential to be implemented in the future with their current challenges.

Finally, the last chapter summarises the key findings and presents an outlook for potential further work in the areas of coagulation-based P removal, reactive media applications and alginate recycling. The thesis plan summarises the individual papers, the objectives and their status of journal submissions (Table 1.2).

Table 1.2: Thesis structure

Chapter	Paper	Objective	Title	Journal	Status
1	-	-	Introduction	-	-
2	1	A	Tertiary treatment of phosphorus using coagulants with different solid liquid separation technologies: Comparison of robustness and resilience	Journal of Chemical Engineering	Submitted
3	2	A,B	The impact of polymer selection and dose on the incorporation of ballasting agents onto wastewater aggregates	Water Research	Submitted
4	3	C	Reactive media constructed wetland for phosphorus removal: Assessing the opportunity and challenges	Journal of Environmental Management	Submitted
5	4	D	Recycling and reuse of alginate in an immobilised algae system	Environmental Technology	Submitted
6	-	A,B,C,D	Implications of the work: Implementation of advanced tertiary P removal	-	-
7	-	-	Conclusions and future work	-	-

References

Acelas, N. Y., Martin, B. D., López, D., and Jefferson, B. (2015). "Selective removal of phosphate from wastewater using hydrated metal oxides dispersed within anionic exchange media". *Chemosphere* 119, pp. 1353–1360.

Andrews, J., Hobson, J., Hunt, D., and Shepherd, D. (2008). *Water Framework Directive: Sustainable Treatment Solutions for Achieving Good Ecological Status*. Tech. rep. London: UKWIR.

De-Bashan, L. E. and Bashan, Y. (2004). "Recent advances in removing phosphorus from wastewater and its future use as fertilizer (1997-2003)". *Water Research* 38.19, pp. 4222–4246.

Blanco, I., Molle, P., Sáenz de Miera, L. E., and Ansola, G. (2016). "Basic Oxygen Furnace steel slag aggregates for phosphorus treatment: Evaluation of its potential use as a substrate in constructed wetlands". *Water Research* 89, pp. 355–365.

Bratby, J. (2016). *Coagulation and Flocculation in Water and Wastewater Treatment - Second Edition*. Vol. 3. IWA Publishing.

Chave, P. A. (2001). *The EU Water Framework Directive- An Introduction*. IWA Publishing.

Cordell, D., Rosemarin, A., Schröder, J. J., and Smit, A. L. (2011). "Towards global phosphorus security: a systems framework for phosphorus recovery and reuse options." *Chemosphere* 84.6, pp. 747–58.

DeBarbadillo, C., Shellswell, G., Cyr, W., Edwards, B., Waite, R., Mullan, J., and Mitchell, R. (2010). "Pilot Testing of Four Tertiary Phosphorus Removal Processes To Achieve Ultra-Low Phosphorus Limits At the Lakeshore WPCP in the Town of Innisfil , Ontario". *WEFTEC*. Black & Veatch, pp. 1–10.

DEFRA (2012). *Waste water treatment in the United Kingdom -2012- Implementation of the European Union Urban Waste Water Treatment Directive- 91/271/EEC*. Tech. rep. Department of Environment, Food & Rural Affairs.

(2014). *Water Framework Directive implementation in England and Wales: new and updated standards to protect the water environment*. Tech. rep. Department of Environment, Food & Rural Affairs.

Desmidt, E., Ghyselbrecht, K., Zhang, Y., Pinoy, L., Van der Bruggen, B., Verstraete, W., Rabaey, K., and Meesschaert, B. (2015). "Global Phosphorus Scarcity and Full-Scale P-Recovery Techniques: A Review". *Critical Reviews in Environmental Science and Technology* 45.4, pp. 336–384.

Drizo, A., Frost, C. A., Grace, J., and Smith, K. A. (1999). "Physico-chemical screening of phosphate-removing substrates for use in constructed wetland systems". *Water Research* 33.17, pp. 3595–3602.

EU Water Framework Directive (2000). *2000/60/EC*.

Mankins, J. C. (2009). "Technology readiness assessments: A retrospective". *Acta Astronautica* 65.9-10, pp. 1216–1223.

Martin, B. D., De Kock, L., Stephenson, T., Parsons, S. a., and Jefferson, B. (2013). "The impact of contactor scale on a ferric nanoparticle adsorbent process for the removal of phosphorus from municipal wastewater". *Chemical Engineering Journal* 215-216, pp. 209–215.

Melia, P. M., Cundy, A. B., Sohi, S. P., Hooda, P. S., and Busquets, R. (2017). *Trends in the recovery of phosphorus in bioavailable forms from wastewater*.

Morse, G. K., Brett, S. W., Guy, J. A., and Lester, J. N. (1998). "Review: Phosphorus removal and recovery technologies". *Science of the Total Environment* 212.1, pp. 69–81.

Murthy, S., Takacs, I., Dold, P., and Al-Omari, A. (2005). "Examining the bioavailability of chemically removed phosphorus at the blue plains advanced wastewater treatment plant". *Proceedings of the Water Environment Federation*. WEFTEC, pp. 4279–4287.

Neal, C., Jarvie, H. P., Withers, P. J. A., Whitton, B. A., and Neal, M. (2010). "The strategic significance of wastewater sources to pollutant phosphorus levels in English rivers and to environmental management for rural, agricultural and urban catchments". *Science of the Total Environment* 408.7, pp. 1485–1500.

Oehmen, A., Lemos, P. C., Carvalho, G., Yuan, Z., Keller, J., Blackall, L. L., and Reis, M. A. M. (2007). "Advances in enhanced biological phosphorus removal: From micro to macro scale". *Water Research* 41.11, pp. 2271–2300.

Paerl, H. W., Fulton, R. S., Moisander, P. H., and Dyble, J. (2001). "Harmful Freshwater Algal Blooms, With an Emphasis on Cyanobacteria". *The Scientific World* 1, pp. 76–113.

Pratt, C. and Shilton, A. (2009). "Suitability of adsorption isotherms for predicting the retention capacity of active slag filters removing phosphorus from wastewater". *Water Science and Technology* 59.8, pp. 1673–1678.

Pratt, C., Parsons, S., Soares, A., and Martin, B. D. (2012). "Biologically and chemically mediated adsorption and precipitation of phosphorus from wastewater." *Current opinion in biotechnology* 23.6, pp. 890–6.

Ragsdale, D. (2007). *Advanced wastewater treatment to achieve low concentration of phosphorus*. Tech. rep. Seattle: US EPA.

Schaum, C. (2018). "Wastewater treatment of the future: Health, water and resource protection". *Phosphorus: Polluter and Resource of the Future – Removal and Recovery from Wastewater*. Vol. 17. International Water Association, pp. 535–554.

Shilton, A. N., Elmetri, I., Drizo, A., Pratt, S., Haverkamp, R. G., and Bilby, S. C. (2006). "Phosphorus removal by an 'active' slag filter-a decade of full scale experience". *Water Research* 40.1, pp. 113–118.

UK TAG (2013). *Updated Recommendations on Phosphorus Standards for Rivers- River Basin Management (2015-2021)*. Tech. rep. UKWIR.

Urban Wastewater Treatment Directive (1998). *98/15/EC*.

Vohla, C., Kõiv, M., Bavor, H. J., Chazarenc, F., and Mander, Ü. (2011). "Filter materials for phosphorus removal from wastewater in treatment wetlands-A review". *Ecological Engineering* 37.1, pp. 70–89.

Whitton, R. L. (2016). "Algae Reactors for Wastewater Treatment". PhD thesis. Cranfield University.

Whitton, R., Santinelli, M., Pidou, M., Ometto, F., Henderson, R., Roddick, F., Jarvis, P., Villa, R., and Jefferson, B. (2018). "Tertiary nutrient removal from wastewater by immobilised microalgae: impact of wastewater nutrient characteristics and hydraulic retention time (HRT)". *H2Open Journal* 1.1, pp. 12–25.

Yang, Y., Zhao, Y., Liu, R., and Morgan, D. (2018). "Global development of various emerged substrates utilized in constructed wetlands". *Bioresource Technology* 261, pp. 441–452.

Yeoman, S., Stephenson, T., Lester, J. N., and Perry, R. (1988). "The removal of phosphorus during wastewater treatment: A review". *Environmental Pollution* 49.3, pp. 183–233.

Chapter 2

Tertiary treatment of phosphorus using coagulants with different solid liquid separation technologies: Comparison of Robustness and Resilience

Olga Murujew[1], Andrea Wilson[2,3], Peter Vale[2], Bruce Jefferson[1], Marc Pidou[1,*]

[1] Cranfield University, College Road, Cranfield, Bedfordshire, MK43 0AL, UK

[2] Severn Trent Water, 2 St Johns Street, Coventry, CV1 2LZ, UK

[3] Atkins Global, Woodcote Grove, Epsom, Surrey, KT18 5BW, UK

[*]Corresponding author: m.pidou@cranfield.ac.uk

Abstract

In this work, three tertiary solid separation technologies have been assessed on their robustness and resilience against an effluent P target <0.3 mg/L at steady state and

dynamic conditions. Overall, ballasted coagulation was shown to be the most robust technology whereas an ultrafiltration membrane with Alum coagulant outperformed the ballasted coagulation system for a wastewater feed with higher suspended solids for P removal. Pile cloth filtration improved with the higher solids feed as well yet being most suitable for less stringent targets <0.5 mg P/L. A molar ratio of 1.37 Fe:P was shown to be sufficient to meet the P target at short contact times as with the ballasted coagulation process. Overall, it was highlighted that optimisation of up-stream flocculation can be a considerable factor for consistent performance.

Keywords: P removal, coagulation, solids liquid separation

2.1 Introduction

Phosphorus discharge standards from sewage works relate to the need to manage the potential ecological impacts of effluent discharge. The specific levels vary considerably across the world and the characteristics of the receiving waterbody. In Europe, recent revision of the required standards is seeing a reduction in the annual average phosphorus concentration from levels of 1.0-2.0 mg P/L to between 0.1 and 1.0 mg P/L with many sites expected to meet levels around 0.3 mg P/L (EU Water Framework Directive 2000). Traditional practice for targets of 1 mg P/L and above is to design and operate treatment works to meet 50% of the target level to ensure compliance. However, below 1 mg P/L, targets of 70-80% of the permitted value are considered operationally appropriate such that for a 0.3 mg P/L, the site would need to deliver an effluent with an annual average of between 0.21 and 0.24 mg P/L. Stricter discharge consents are common place in the USA where levels can be significantly below 0.1 mg P/L (Lee et al. 2015; Ragsdale 2007).

A large proportion of the wastewater treatment sites utilise chemical precipitation with metal salts (Fe or Al) for all, or part, of the required removal. The mechanisms of removal

comprise a combination of precipitation of metal-phosphate-hydroxo complexes, adsorption onto precipitated surfaces and aggregation of colloids (Bratby 2016). Phosphorus exists in many forms including ortho-phosphate, condensed forms (pyrophosphates, triphosphates) and poly-phosphates with the relative distribution impacted by concentration, pH and ligand reactions with the other components in the wastewater. Further, transformation occurs during the aerobic secondary processes such that the majority of phosphorus is in the ortho-phosphate form once it reaches the tertiary stage (Bratby 2016). The efficacy of coagulation is highest when the P is in the ortho-P form. Therefore, it is common practice to dose during or after the biological process rather than in the primary stage so that dose requirements can be minimised. The dose expressed as a stoichiometric mole ratio is reported to vary between 1.4 and 4.3 of Al_{added}: $P_{removed}$ (Baillod et al. 1977). The relative importance of direct precipitation decreases as the target residual levels becomes lower with removal to below 1 mg P/L thought to be predominantly associated with adsorption and colloidal aggregation. Accordingly, the relative dose requirements increase significantly as the target level is reduced (Figure 2.1). To illustrate in the case of alum dosing, 83.5 mg/L were required to reduce phosphorus levels from 5.17 to 0.97 mg/L at the head of a contact stabilisation plant. In comparison, 125 mg/L were required to reduce the phosphorus levels from 2 to 0.05 mg/L in an oxidation pond effluent (Bratby 2016). Consequently, whilst compliance is possible through single point dosing into the crude wastewater and/or the main biological process, the coagulant doses to reach sub 1 mg P/L are substantial (Bratby 2016; Murthy et al. 2005). Accordingly, it is becoming more common to meet sub 1.0 mg P/L standards by incorporating a tertiary coagulation step linked to a range of different solid liquid separation systems (Table A.1). These include traditional tertiary treatment technology used for solids removal such as depth filters and cloth filters as well as advanced filtration with membranes as well as, a relatively recent technology, ballasted sedimentation. The different options operate with different removal

mechanisms for the precipitated solids and are effective over different particle size ranges. For instance, ultrafiltration membranes sieve out particles larger than the opening, typically 0.05 µm. In contrast, depth filters work by a combination of collision and attachment mechanisms with minimum removal associated with particles sizes around the 0.45 µm level (Hahn and O'Melia 2004). Cloth filters sit in between the two with the formation of a dynamic cake layer aiding removal during the filter cycle and an effective cut size in the microns range. In contrast, ballasted systems operate through sedimentation and hence small particles are poorly removed in line with Stokes' law.

The fact that they operate under different mechanisms suggests that they will be impacted differently by variations in the feed water flow and composition during steady state operation and respond differently to external or internal perturbations. Consideration of such issues connects to concepts of robustness and resilience as commonly used in ecological systems (Janssen et al. 2007). Whilst different definitions are used the most appropriate to the current discussion are that robustness relates to the consistency of the output against a variable input and resilience relates to the ability of a technology to recover from a perturbation that has caused a deterioration in the output (Nazif and Karamouz 2009). There is a paucity of translation to treatment technology assessment, especially in relation to predicting future capability. However, examples exist for depth filters in drinking water treatment (Hartshorn et al. 2015; Y. Li et al. 2008), clarifiers (Huck and Coffey 2004) and aerated constructed wetlands (Butterworth et al. 2013). Assessment of robustness is derived by examining the cumulative distribution of the effluent concentration whilst operated under steady state conditions. This can be converted in a quantifiable index through a number of performance indices (Hartshorn et al. 2015). The most common is the robustness index although it is known to being heavily dependent on the goal target and the percentile levels chosen (Huck and Coffey 2004). However, when comparing different options, these weaknesses are less important as the comparison is set to the same param-

eters and as such focus can be given to the relative difference and the overall profiles. Many of the reported trials have been associated with achieving ultra low effluents of between 0.014 and 0.15 mg TP/L from influent levels that varied between 0.22 and 3.5 mg TP/L. There is also a paucity of direct comparison between technology options limiting decisions making based on performance efficacy. Where these do exist (DeBarbadillo et al. 2010; Lee et al. 2015) the trials are focused on delivering ultra low discharge standards (sub 0.1 mg P/l), using high coagulant doses making transition to the current challenges to meet sub 1 mg P/L in Europe very difficult. Accordingly, the current paper compares three demonstration scale, coagulant based, tertiary treatment options during steady state and dynamic operation. The target to be achieved was a residual phosphorus concentration of 0.3 mg P/L and this was assessed against two wastewaters and varying coagulant dose.

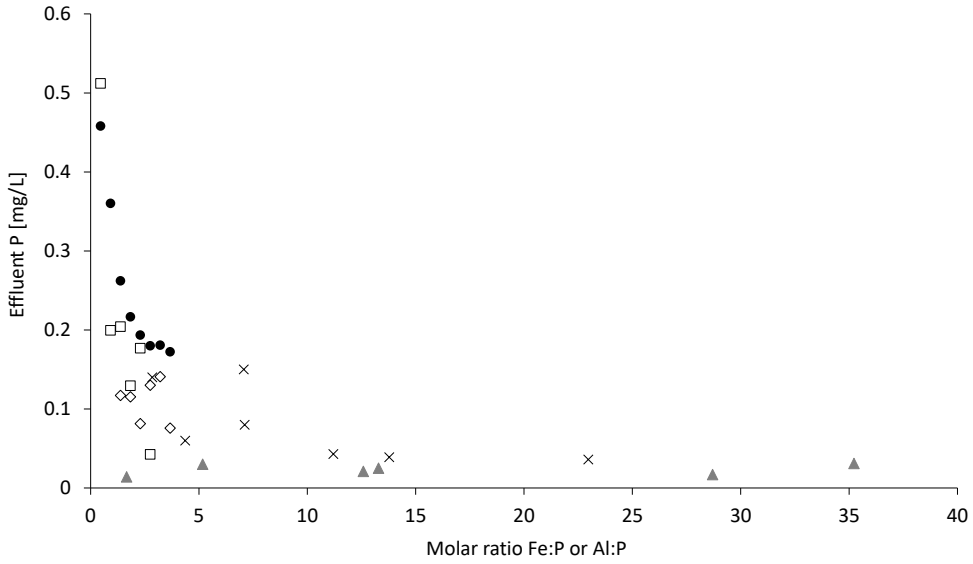

Figure 2.1: Comparison of effluent total P levels in correlation with varied molar Me:P ratio for Fe (▲) or Al (X) coagulants reported in literature. Comparison against effluent ortho-P levels reported in this study using $FeCl_3$ for cloth filter (●), ballasted coagulation (◇) and membrane filtration (□)

2.2 Materials and Methods

2.2.1 Materials

Three coagulant based technologies: ballasted coagulation, pile cloth filtration and membrane filtration, were installed as tertiary treatment at a wastewater treatment plant in Leicestershire, UK. All the technologies were operated as per the supplier's instructions. The site has iron-dosed oxidation ditches (OD) as secondary treatment. For the trial, influent ortho-P to the pilot systems was supplemented to 1 or 2 mg P/L with KH_2PO_4 as required (Table 2.1). A second set of tests were performed using tankered secondary treated wastewater from the site that contained the benchmark depth filter technology.

Table 2.1: Influent wastewater characteristics of the oxidation ditch and trickling filter wastewaters. Data given as Average ± 1 standard deviation and number of total samples taken (n).

WWTP	ortho-P [mg/L]	TP [mg/L]	Fe [mg/L]	TSS [mg/L]	NH4-N [mg/L]	COD[mg/L]	pH
OD	1.09 ± 0.38 (79)	1.21 ± 0.36 (66)	0.67 ± 0.3 (72)	7.27 ± 3.42 (76)	0.1 ± 0.24 (79)	21.25 ± 2.77 (78)	7.42 ± 0.17 (79)
TF	1.25 ± 0.54 (13)	1.75 ± 0.39 (13)	2.5 ± 0.52 (8)	35.17 ± 20.03 (12)	4.75 ± 0.45 (8)	59.17 ± 14.08 (13)	7.39 ± 0.22 (11)

The ballasted coagulation technology (BC) (CoMag®, Evoqua Water Technologies, UK) consisted of three mixing tanks and a clarifier (each 270 L) (Figure 2.2). Over the total range of tested flow rates, the hydraulic residence times ranged between 5.5 and 15 minutes and the surface overflow rates between 5 and 15 m/h. Two coagulants were used, ferric chloride ($FeCl_3$) and $Fe_2(SO_4)_3$ (Fe-S) which were dosed in an in-line static mixer (Table 2.2). The ballast (magnetite, Fe_3O_4) and a polymer (anionic polyacrylamide) were dosed at 4 g/L and 0.5-1 mg/L, respectively. Each of the chemical compounds was added subsequently to each of the mixing tanks. In the clarifier, 25% of settled sludge was recycled back into the system and the other part underwent shear mixing to recycle the ballast through a magnetic drum back into the treatment train.

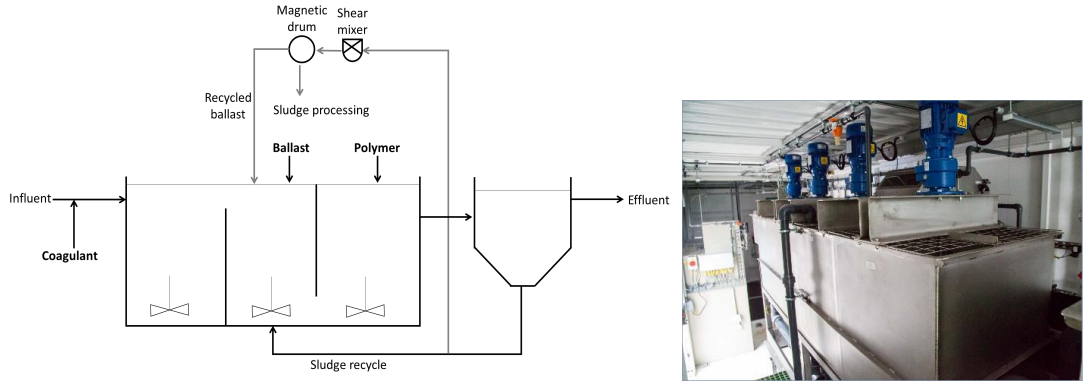

(a) (b)

Figure 2.2: Ballasted coagulation technology (a) flow sheet and (b) photo.

The cloth media filtration technology (CF) had a fast mixing coagulation (330 L) and a flocculation tank (1650 L) upfront. The mixing speeds were optimised throughout the trial. The mixing rate of the fast mixing coagulation tank was 200 RPM for the first 185 days and was then increased to 290 RPM for the remaining 22 days of the trial. In the flocculation tank, the mixing rate was 130 RPM during the first 125 days of operation which was then reduced to 35 RPM for 4 days and after that to 25 RPM for the remaining 78 days of the trial. Over the range of tested flow rates the hydraulic residence times varied between 1.4-5.5 and 6.9-27.5 minutes in the fast mixing and flocculation tank, respectively.

A microfibre pile cloth (Mecana®, Hydrok, UK) with a surface area 2 m^2 was fixed on a drum which was placed inside an open tank (Figure 2.3). Under operation solids accumulate on the cloth restricting flow through the cloth until the water level rises until triggering a sensor initiating backwash during which the drum takes a full turn and deposited solids are removed with a suction pump from the surface. $FeCl_3$ was the coagulant used for this technology. For the tested flow rates, the hydraulic and solids loading rates ranged between 1.8-7.2 m/h and 0.013-0.052 kg TSS/(m^2.h), respectively.

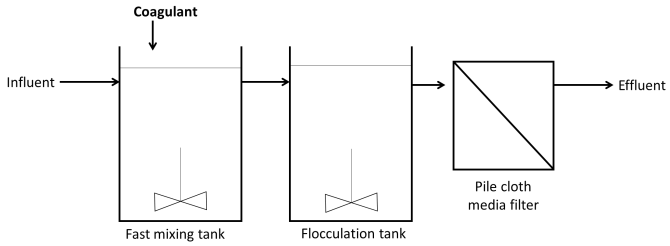

(a)

(b)

Figure 2.3: Cloth media filter (a) flow sheet and (b) photo.

The membrane filtration technology consisted of an ultrafiltration hollow fibre membrane cartridge (Puron MP®, Koch Membrane Systems, Germany) (pore size = 0.03 µm, Polyester reinforced PVDF) with the same fast mixing (330 L, 290 RPM) and slow mixing (1650 L, 25 RPM) tanks upstream as with the cloth filter (Figure 2.4). The mixing rates were not varied during this trial. The membrane had a surface area of 51 m^2 and was configured in an outside-in flow and operated in dead end mode. Every 20-30 minutes of filtration, backwashes were induced for 170 s. Every 2 days, acid chemical cleans (pH 2-2.5) were carried out to reduce transmembrane pressure below 600 mbar, remove remaining deposits from the membrane surface and to maintain permeability. The membrane filtration (MF) was operated with two coagulants $FeCl_3$ and dialuminium chloride pentahydroxide ($Al_2Cl(OH)_5$, PAC).

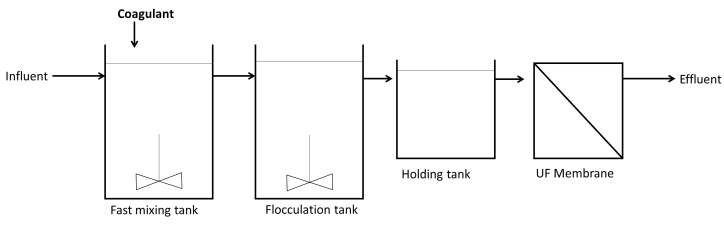

(a)

(b)

Figure 2.4: Membrane filtration

The technologies were benchmarked against a full-scale depth filter which was adapted to include upstream coagulant dosing located at a site that uses trickling filters as the main biological process. The filter was a continuous backwash upflow moving bed filter containing 1 mm sand operated at a surface loading rate of 8.96 $m^3/m^2/h$ (Blue Pro®, Blue Water, USA) (Figure 2.5). At the TF site, the sand filter (SF) consisted of 5 filters (each 25 m^3, 3 m diameter) which were operated at an average flow rate of 17.6 L/s per filter. The flow rate was adapted to the flow on the main site. The coagulant, $Fe_2(SO_4)_3$, was dosed flow proportionally and ranged between 10 to 13 mg Fe/L.

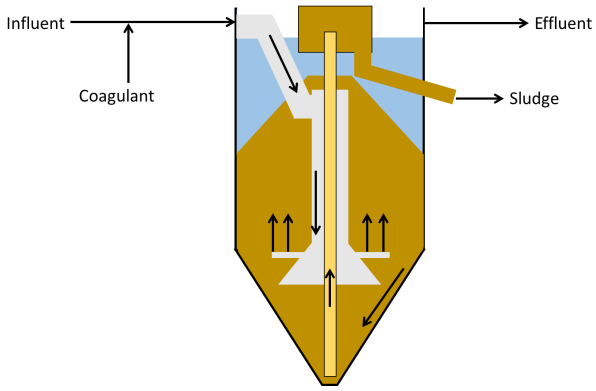

Figure 2.5: Sand filter flow chart

2.2.2 Methods

The trials were split into a number of categories: Steady state treating wastewater from both sites, coagulant dose response, storm response, diurnal flow pattern response and high influent P response (Table 2.2). Results were evaluated against an effluent P target of 0.3 mg/L unless otherwise noted. Influent and effluent samples were taken every 15 minutes and analysed for ortho-P and ferric concentrations as well as turbidity (online analysers, ABB, UK). Additionally, grab samples were taken periodically to be further analysed on TP, COD and NH_4-N using test kits (Hach Lange, UK). Suspended solids

(TSS) were determined by filtering 250 mL of a sample through a 1.2 µm glass fibre filter and drying in the oven at 105°C.

Table 2.2: Set parameters for tests done with coagulation technologies. The used coagulant was $FeCl_3$ for CF, BC and MF unless otherwise noted. The SF was operated with Fe-S.

Operational test	Technology	Influent ortho-P [mg/L]	Coagulant dose[mg Fe/L]	Polymer dose [mg/L]	Flow rate [L/s]
Steady state	CF (19 days)	1	5	NA	2.5
	BC (17 days)		8	1	1.5
	MF (37 days)		5	NA	0.57
	SF (15 days)	0.93[a]	10-14	NA	17.6[b]
Coagulant dose response	CF (49 days)	1	1-9	NA	2.5
	BC (45 days)		3-8	1	1.5
	MF (77 days)		1-6	NA	0.57
Storm	CF (3 days)	0.5-2	12-6	NA	1-4
	BC (3 days)		8	1	1.5-3
Diurnal flow profile	CF (10 days)	1	4	NA	1.3-3.3
	BC (8 days)		5 (Fe-S)	1	1.2-2.9
High Influent P	CF (6 days)	2	8-10	NA	2.5
	BC (6 days)		8	0.5	2
	MF (5 days)		6-7 (PAC)	NA	0.57
TF feed	CF (1 day)	1.25[c]	9	NA	1
	BC (1 day)		8	1	1.5
	MF (1 day)		6 (PAC)	NA	0.57
	SF (15 days)	0.93	10-14	NA	17.6

[a] The influent P concentration was not altered on this site and therefore the measured value of soluble reactive P is given here.

[b] This was the average flow of each sandfilter cell. There were 5 cells in total with variable on/off depending on flow pattern on main site.

[c] Based on average measured ortho-P concentration.

Coagulant dose response

Coagulant dose response curves were plotted from operating the systems at varied coagulant doses. The data from these tests were analysed statistically (Statistica 13) using a Box-Cox transformation for effluent P values. The transformed results were then plotted

with an ANOVA factorial general linear model where coagulant doses and technology type were used as categorical variables. A post-hoc Fisher LSD analysis was used to determine significant differences ($P<0.05$) between the three technologies.

Steady state and varied wastewater feed

CF, BC and MF were run at unchanged operational conditions for at least two weeks to evaluate their robustness. The robustness index was calculated according to Hartshorn et al. (2015) for a range of P targets between 0.05 and 0.9 mg P/L using equation 2.1.

$$RI = \left[\left(1 - \frac{G\%}{100}\right) \times \frac{P_{90}}{P_{50}}\right] + \left[\frac{P_{50}}{P_{Goal}} \times \frac{G\%}{100}\right] \tag{2.1}$$

where G% represents the percentile at target effluent P concentration, P_{Goal}. P_{90} and P_{50} are P concentrations at the 90th and 50th percentile, respectively. A lower RI value represents more robustness towards the set goal. Performance of CF, BC and MF were also compared to the previously described SF and the wastewater from this site was fed to the CF, BC and MF to trial performance and compare to the SF (Table 2.2).

Dynamic operation

Storm tests were run for 4h and 24h with a rapid increase from a low flow rate (CF: 1 L/s and BC: 1.5 L/s) to a high flow rate (CF: 4 L/s, BC: 3 L/s) while simultaneously diluting influent P from 2 mg/L to 0.5 mg/L (Figure 2.6). Diurnal flow tests were run for 4 days to simulate a real-life wastewater flow with higher flows in the mornings and evenings and lower flows during the day (Figure 2.12). Flows varied between 1.3 and 3.3 L/s and 1.2 and 2.9 L/s for CF and BC, respectively. The MF was not operated under storm or diurnal flows. An increase in influent P concentration from 1 to 2 mg/L was tested for 4-6 days at fixed flow rates.

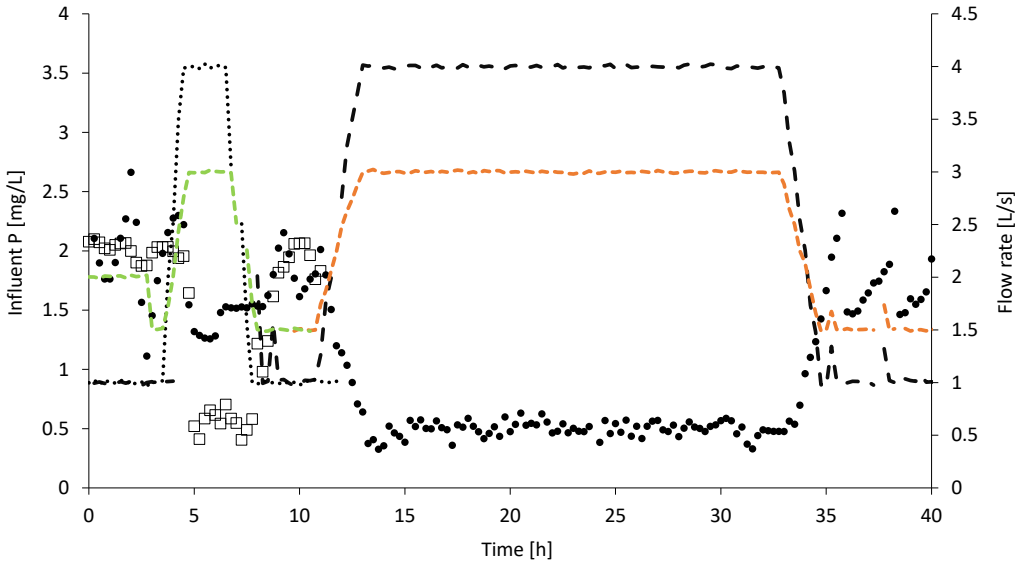

Figure 2.6: Influent P pattern for 4h (□) and 24h storm duration (●). Flow pattern for 4h storm for cloth filter (CF) (·····) and ballasted coagulation (BC) (------) and for 24h storm for CF (- - - -) and BC (- - - -).

2.3 Results and Discussion

2.3.1 Steady-state operation and robustness

All four technologies demonstrated the ability to meet a 0.3 mg P/L discharge level during the steady state trials (Figure 2.7). To illustrate, the 50th Percentile, used here as a proxy for the annual average, was 0.02, <0.05[1] , 0.14 and 0.18 mg P/L (as ortho-phosphate) for the SF, BC, MF and CF respectively. Fractionation tests revealed that 81% of the incoming P was in the dissolved form, 1% was colloidal P and 18% P was associated to solid matter. Conversion of the data to an operational TP standard is most conservatively assessed by subtracting the difference between TP and ortho-P in the influent, adding this value onto the effluent ortho-P values (assuming no non ortho-P removal) and then reducing to 70% of that value to provide an operational buffer. This would set the ortho-P

[1]Below detection limit of 0.05 mg/L. The detection limit for SF P analysis was stated as 0 mg/L.

effluent target to 0.21 mg P/L. In this case, the SF and BC are still effective, but the CF is not, and the MF is marginal. Effluent total phosphorus spot sample measurements during the steady state trials reported median levels of 0.05 ±0.003, 0.083 ±0.094[2] , 0.174 ±0.176[3] and 0.3 ±0.04 mg/L for the BC, MF, SF and CF, respectively, reversing the observations based on on-line ortho-P measurements in which case the BC and MF would meet the 0.3 mg/L TP consent and the SF (considering the standard deviation) would not. Consideration of the robustness curves indicates robust profiles for the SF and BC with a larger proportion of the data associated to a steep vertical curve followed by a tail at very high percentile values (Figure 2.7). For instance, the 90th percentile values were 0.03 and 0.07 for the SF and BC respectively with maximum values of 0.54 and 0.84 mg P/L. In contrast, the MF and CF profiles were indicative of less robust systems where the curves were less vertically inclined and spread over a broader range of effluent ortho-P values.

The corresponding robustness index values (Figure 2.8), assuming a target of 0.21 mg P/L as ortho-P at the 50th percentile, were 0.18, 0.24, 0.95 and 0.97 for the SF, BC, MF and CF, respectively. Overall, big differences in robustness can be seen between the technologies at lower targets. The RI values converge at higher target values with larger difference observed once the target level was reduced below 0.2 mg P/L (Figure 2.8). Between effluent P targets of 0.05 and 0.3 mg/L, the SF and BC RI curves showed decreasing robustness indices from 0.42 and 0.91 to 0.16 and 0.21, respectively. In the case of MF and CF the indices were 2 and 1.36 with decreasing values down to 0.54 and 0.64, respectively.

It has to be noted though that the SF was operated at higher coagulant doses (10-14 mg Fe/L, 15.9-22.3 Fe:P molar ratio) than the other technologies (5-8 mg Fe/L, 2.29-3.67 Fe:P molar ratio). In addition, the flocculation set up used in the BC appears better opti-

[2]This was based on 7 samples taken during steady state operation that varied between 0.07 and 0.28 mg TP/L.

[3]Variation of total P values between 0.06 and 0.82, minimum and maximum, respectively. The reason for the relatively big difference between SF ortho-P and TP values is that ortho-P analysis was filtered through 0.45μm prior to analysis.

mised than that used for the MF and CF such that sub optimal flocculation and excessive floc breakage may have contributed to the poorer performance of the two filtration processes (Zheng et al. 2011). As such, when the mixing speed in the upstream flocculation tank to the CF was reduced from 135 rpm over 35 rpm to 25 rpm, average P removal changed from 70.7% over 80.6% to 71%, respectively indicating the importance of the mixer speed on final P concentration. Previous trials exploring the different components within the BC have revealed that the combination of coagulant, polymer and ballast are able to remove more phosphorus than coagulant alone (Chapter 3) (Kängsepp et al. 2016). This is attributed to the polymer sweeping up colloids that were originally in the water and those generated by the chemical precipitation (Li et al. 2017). The combination results in large particle sizes with small number of fines compared to coagulant alone and thus is well suited to achieve very low residual phosphorus concentrations. This is supported by the respective residual solids levels observed during the trials which were 8.47 $\pm$ 5.09, 4.13 $\pm$ 1.35, 1.03 $\pm$ 0.78 and 9.00 $\pm$ 1.11 mg/L for the SF, BC, MF and CF respectively. However, the SF was also able to meet a very low effluent P concentration and achieved this with coagulant alone, albeit at a much higher dose. Either way this suggests that effective flocculation is critical in ensuring robust treatment (Rossini et al. 1999).

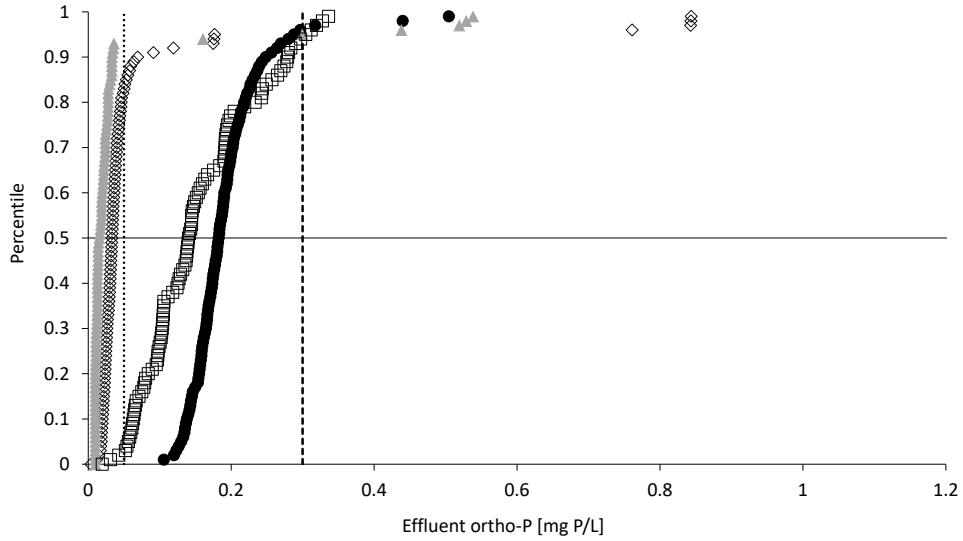

Figure 2.7: Steady state for the sand filter (▲), cloth filter (●), ballasted coagulation (◇) and membrane filtration (□) with P detection limit (·····) and P target (------).

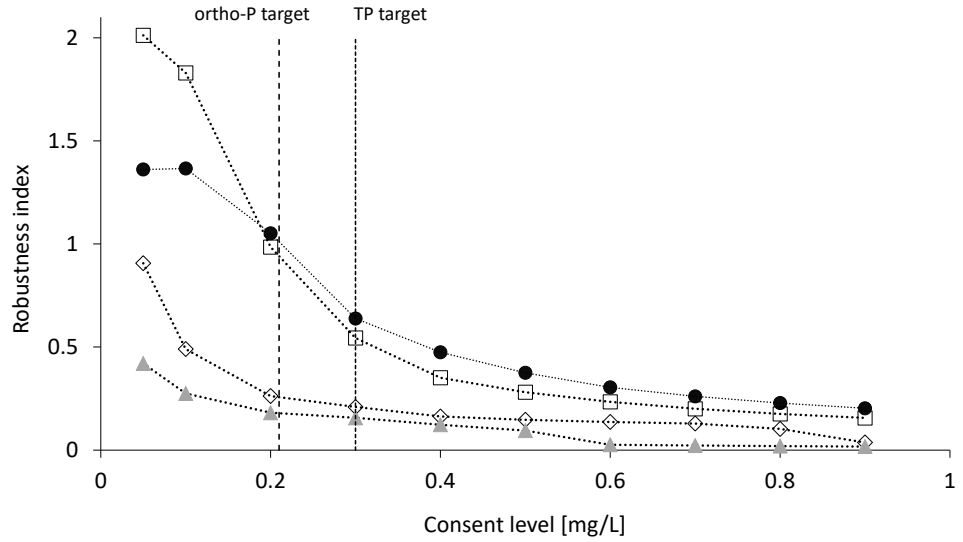

Figure 2.8: Robustness indices against potential P consents for the sand filter (▲), cloth filter (●), ballasted coagulation (◇) and membrane filtration (□)

2.3.2 Varied influent characteristics

The wastewater at the test site was low in suspended solids and this has been shown to inhibit effective flocculation (Havlicek 2018) and may impact the observed results from the steady state trials especially in relation to the CF and MF systems as the BC adds

additional particles in the form of a ballast and recycled sludge (Chapter 3). Accordingly, wastewater was tankered from the site where the SF was located and then run through the other technologies (Table 2.3). Although the influent was from the same site, a difference in ferric, TSS, ammonia-N and COD concentration was observed between the influent analysed directly at that site and when it was analysed after transport and so the results are presented relative to the specific influent that was treated (Table 2.3).

Ortho-P removal, based on median concentrations, was 98.2%, 92%, 84.7% and 83.9% for SF, MF, BC and CF, respectively showing a better performance for the membrane than the ballasted coagulation process which is likely due to the change to an aluminium based coagulant in the MF (Langer and Scherman 2013; Qin et al. 2012). This is further highlighted when seeing the MF P removal with Al coagulant and oxidation ditch feed which was the highest of all technologies. At equivalent conditions, values of 94.5%, 88.9% and 81.8% for MF, BC and CF, respectively were observed during the trials with the oxidation ditch effluent indicating that the more polluted wastewater from the trickling filter site resulted in a slight deterioration in treatment performance. The difference is congruent with the TP to ortho-P ratio which were 1.79 and 1.32 for the trickling filter and oxidation ditch sites respectively corresponding to non-ortho-P fractions of 0.66 and 0.42 mg P/L. The levels observed at the trickling filter site are high for a biologically treated effluent and this fraction is known to be much more difficult to remove by chemical precipitation requiring much higher doses to enable removal (Bratby 2016). Interestingly, more similarity between the different technologies was observed regarding total P removal which were observed to be 91.3%, 88.4%, 84.0% and 81.1% for MF, SF, CF and BC, respectively. The associated median value for TP were 0.15, 0.17, 0.27 and 0.33 mg P/L for MF, SF, CF and BC, respectively indicating that only the BC and potentially the CF were not able to meet the operational target of 0.3 mg P/L although this is for a low sample number. Importantly, it revealed a difference in the relative efficacy of the plants which,

if based on TP removal, was MF, SF, CF and BC last.

Previously reported data on trials of individual processes indicates better performance than observed in the current trial. For instance, a ballasted coagulation trial with an influent of 1 mg TP/L was reduced to 0.04 mg TP/L with a coagulant dose of 20 mg Al/L of PACl and 0.8 mg/L of polymer (Lee et al. 2015). Similarly, in a pilot scale depth filter trial using a 5.7 mg Al/L dose of polyaluminium silicate sulfate a residual of 0.06 mg TP/L was achieved from an initial concentration of 1.5 mg TP/L (Bratby 2016). However, the required conditions vary considerably due to the phosphorus species present and the nature of the coagulant. For instance, another depth filter trial treating a 0.135 mg TP/L influent required up to 7 mg Fe/L (28.7 Fe:P molar ratio) of ferric chloride to reduce the phosphorus concentration down to 0.017 mg TP/L. When elevated concentrations of coagulant are used, the resultant speciation changes with increasing production of polymeric species and a reduction in the efficacy of removal such that higher Fe:P dose ratios are required (El Samrani et al. 2004).

Table 2.3: Effluent wastewater characteristics with TF as influent. Data given as median values with total number of samples. CF: Cloth filter, BC: Ballasted coagulation, MF: Membrane filtration, SF: Sand filtration

	ortho-P [mg/L]	TP [mg/L]	Fe [mg/L]	TSS [mg/L]	NH4-N [mg/L]	COD [mg/L]
Influent SF (n=30)	0.84 [a]	1.50	0.28 [b]	13.75	3.24	45.00
SF (n=30)	0.02	0.17	0.33	6.99	2.85	19.50
Influent CF/ BC/ MF	1.30 (13)	1.72 (13)	2.51 (8)	27.30 (12)	4.67 (8)	52.70 (13)
CF	0.21 (23)	0.27 (2)	1.50 (23)	10.35 (24)	5.28 (2)	28 (2)
BC	0.20 (19)	0.33 (3)	1.67 (20)	7.50 (19)	4.30 (3)	26.20 (3)
MF	0.10 (8)	0.15 (8)	0.14 (42)	1.9 (8)	-	19.8 (8)
Removal rates [%]						
SF	98.2	88.4	-	49.2	12.1	56.7
CF	83.9	84.0	40.2	62.1	-	46.9
BC	84.7	81.1	33.7	72.5	7.8	50.3
MF	92.0	91.3	94.3	93	-	62.4

[a] In this case soluble reactive P was measured where the sample is filtered through a 0.45 µm filter and then analysed using a colorimetric method.

[b] Ferric was analysed with ICP instead of a colorimetric method.

2.3.3 Coagulant dose response

Dose response trials with the three pilot technologies revealed a decrease in residual ortho-P at low doses which thereafter stabilised (Figure 2.9). To illustrate, in the case of the CF, the ortho-P concentration decreased from 0.46 mg P/L to 0.26 mg P/L between doses of 1 and 3 mg Fe/L. Whereas, between doses of 4 to 8 mg Fe/L the residual concentration stabilised between 0.17 and 0.22 mg P/L (Figure 2.9). A similar response was observed in the case of the MF where the effluent concentration dropped from 0.51 mg P/L to 0.2 mg P/L between coagulant doses 1 and 2 mg Fe/L. At higher doses of 3 to 8 mg Fe/L the residual concentration fluctuated between 0.2 and 0.04 mg P/L. In the case of BC, only doses of 3 mg Fe/L and above were tested and at these doses a fluctuating residual con-

centration of between 0.12 and 0.08 mg P/L was observed. Previous jar test trials with the different BC components revealed that performance was stable down to coagulant doses of 5 mg Fe/L, consistent with the current findings (Chapter 3). Overall to meet an ortho-P target of 0.21 mg P/L, a coagulant dose of 3 to 4 mg Fe/L appears appropriate for the BC and MF and a minimum dose of 5 mg Fe/L seems necessary in the case of CF. This equates to dose ratios of between 1.37 and 1.83 and of 2.29 respectively which is towards the lower end commonly reported for tertiary treatment but consistent with standard practice in general phosphorus precipitation (Table A.1, Figure 2.1). At these doses the ferric species are predominately iron dimers linked to a single phosphate anion (El Samrani et al. 2004). To achieve sub 0.1 mg P/L residual substantially higher doses are required as the incorporation of phosphate into the precipitate becomes less effective and the coagulant starts to form progressively more poly hydrolysed species (Gu 2014). Interestingly, statistical analysis showed that there are significant differences in the data set of varied coagulant doses for BC, MF and CF indicating that the different solid liquid separation mechanisms involved result in different treatment efficacies. Detailed understanding of this linkage is currently limited and represents an area of important future activity to fully optimise such systems by properly tailoring the coagulation-flocculation process to the downstream mechanism of separation.

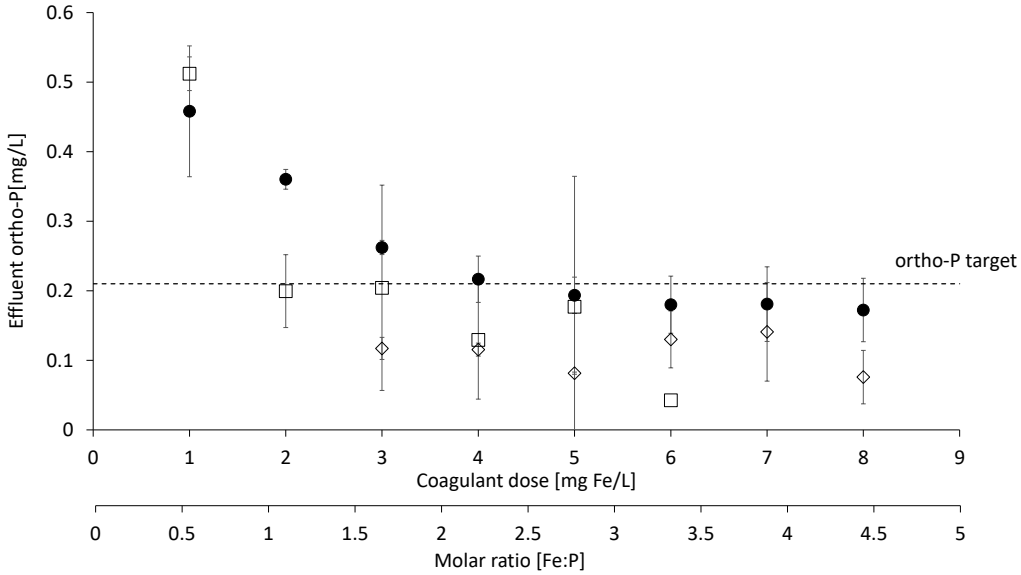

Figure 2.9: Coagulant dose response for CF (●), BC (◇) and MF (□) against TP target of 0.3 mg/L (------) and ortho-P target of 0.21 mg/L (– – – –). Average values with error bars ± 1 standard deviation. CF: Cloth filter, BC: Ballasted coagulation, MF: Membrane filtration

2.3.4 Dynamic operation and stress testing

The systems where then tested against dynamic response to a change in phosphorus concentration, dose or flow (Figures 2.10, 2.11, 2.12). A step change in the influent phosphorus concentration from 1 to 2 mg P/L resulted in a sharp increase in the effluent phosphorus concentration with the CF but was not observed for the MF or the BC systems. In the case of the CF, the effluent concentration increased to 0.49-1.15 mg P/L which compares to the slight increase seen for the other technologies with peaks of 0.07 and 0.17 mg P/L as ortho-P (Figure 2.10a). In response, the coagulant dose to the CF was increased from an initial value of 4 to 8 mg Fe/L. The residual phosphorus initially declined to a low of 0.57 mg P/L before increasing again. The coagulant doses were then increased to 9 and 10 mg Fe/L on days 2.5 and 5.5, respectively. This resulted again in decreasing effluent P concentrations for a short time but overall the concentrations fluctuated between 0.63 and 1.5 mg P/L, clearly above the effluent target. In the case of the MF, it is noteworthy when

the coagulant was changed to PACl an improved performance was observed compared to tests with $FeCl_3$ during the dose response test (Figure 2.10b). Although analysis of the impact of coagulant type on performance was not an objective of this work, this highlights an aspect worth examining in the future (Bill et al. 2011; Langer and Scherman 2013; Qin et al. 2012).

The BC and CF were then exposed to dynamic flow events in the form of a 4- or 24-hour storm whereby the flow increased by 300 and 400% for the BC and CF respectively and the phosphorus concentration decreased by 25%. During the 4 h storm simulation, the increase of the flow started at 4.25 h reaching maximum flow at 5.25 h, then starting to decrease at 7.25 h and reaching the original flow at 8.5 h (Figure 2.6 and 2.11).

Before the storm simulation started, effluent P from the CF ranged between 0.35 and 0.5 mg P/L, thus already above the target of 0.3 mg P/L (Figure 2.11a). At 5.75 h, half an hour after the maximum flow rate was reached, the effluent P dropped down to 0.135 mg P/L and decreased further to 0.075 mg P/L at 7.25 h. At the end of the storm simulation, i.e. 8.5 h, the effluent P was 0.07 mg P/L and started increasing up to 0.3 mg P/L at 11h. Because the highest P values have been reached outside of the storm flow conditions, i.e. before 4.25 h and after 8.5 h, but during the high influent P setting of 2 mg/L, it appears that the P concentration plays a more significant role in CF performance than the flow rate. It has to be noted that the coagulant dose was adjusted between 6 and 12 mg Fe/L when the P was at minimum or maximum, respectively (Table 2.2). This equates to molar ratios between 3.32 and 6.64 Fe/P for high and low influent P, respectively, suggesting that under-dosing occurred at 2 mg/L influent P conditions. Nevertheless, the performance of the CF system remained relatively stable during the storm simulation showing that the technology can be robust in dynamic situations. The response to the prolonged storm was similar to the 4h storm simulation, effluent P ranged above the P target before and after the 24h storm at values between 0.33-1.11 mg P/L and 0.33-1.01 mg P/L, respectively

(Figure 2.11b). At 12.75 h, i.e. 0.15 h before reaching maximum flow, the CF reached a peak of 0.78 mg P/L in the effluent which quickly decreased down to 0.13 mg P/L at 13.75 h. The flow rate decreased between 32.75 h and 34.75 h, the end of the storm simulation, and during that time the effluent P ranged between 0.12 and 0.33 mg P/L.

For the BC, the effluent P ranged between 0.04 and 0.14 mg P/L during the 4 h storm simulation which suggests that this system is robust to sudden flow changes (Figure 2.11c). During the 24h storm, the BC showed an increase in effluent concentration to 0.3 mg P/L at 10.75 h with a subsequent decrease to 0.08 mg P/L at 14.75 h (Figure 2.11d). Performance was kept stable until the end of the storm at 34.75 h but was followed by an increase to 0.35 mg P/L at 36.25 h which does not seem to be a dosing issue (2.21 Fe:P molar ratio) because the "High influent P" test was conducted at the same coagulant dose (8 mg Fe/L) and did not show adverse impact on performance (Figure 2.10a).

Overall, storm conditions did not appear to cause performance disruptions in the BC suggesting that the flocculation system is adequate for the changes presented (DeBarbadillo et al. 2010). This aligns to the reported fast reaction time of the hydrolysing ferric coagulant which forms its precipitate within seconds (Bratby 2016). The same was observed for the CF system where the change in influent concentration appeared to have more impact than flow dynamics. Ultimately this reflects the need to optimise both the dose and the mixing conditions for effective flocculation (Takács et al. 2011).

The final tests exposed both technologies to diurnal flow operation (Figure 2.12). As before, the BC system demonstrated a greater robustness to the changes with only minor increases in effluent phosphorus concentration occurring at two points leading to peaks of 0.07 and 0.08 mg P/L. These coincided with the largest variations in flow and indicate that the level of change poises the greatest risk. In the case of the CF the levels fluctuated between 0.16 and 0.44 mg P/L although the peaks in concentration did not necessarily coincide with the peaks in flow. Interestingly, the largest changes in flow did not have the

same impact as seen for the BC system and largely indicating that the CF is less sensitive to flow variation. However, the effluent concentration was higher and fluctuated more than the BC indicating that the systems requires further optimisation of the technology to consistently deliver sub 0.3 mg P/L effluents and this is likely related to the pre-flocculation system. The flow variations during this test may have impacted floc formation and breakage through changes in retention time and velocity in the flocculation tanks. This can be supported through previously reported trials of a 10 µm microsieve technology that achieved very low effluent P concentrations (Langer and Scherman 2013). This system compared ferric and aluminium coagulants in combination with polymer dosing to reduce a wastewater phosphorus concentration from approximately 0.5 mg P/L as total phosphorus down to 60 µg P/L.

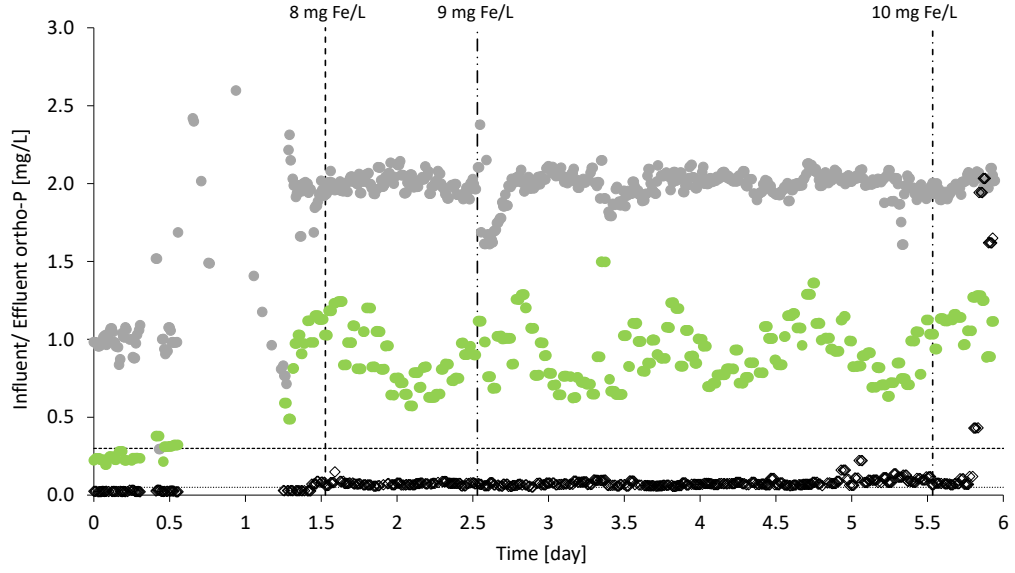

(a)

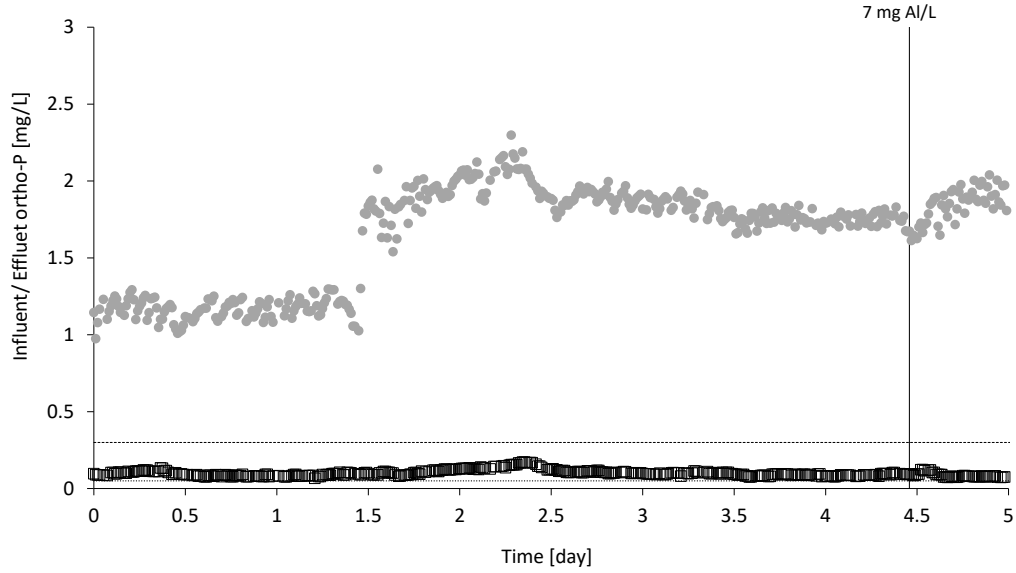

(b)

Figure 2.10: Impact of increased influent P concentration from 1 to 2 mgP/L on treatment performance. Influent P (●), P effluent target (------) and P detection limit (·····) for (a) CF (●) and BC (◇). For CF, coagulant dose was 4 mg Fe/L first and then increased to 8 mg Fe/L (- - - -), 9 mg Fe/L (–··–··) and 10 mg Fe/L (–·–·–·); BC was dosed with 8 mg Fe/L and 0.5 mg/L polymer, (b) MF (□) had a coagulant dose of 6 mg Al/L and later 7 mg Al/L (——). CF: Cloth filter, BC: Ballasted coagulation, MF: Membrane filtration

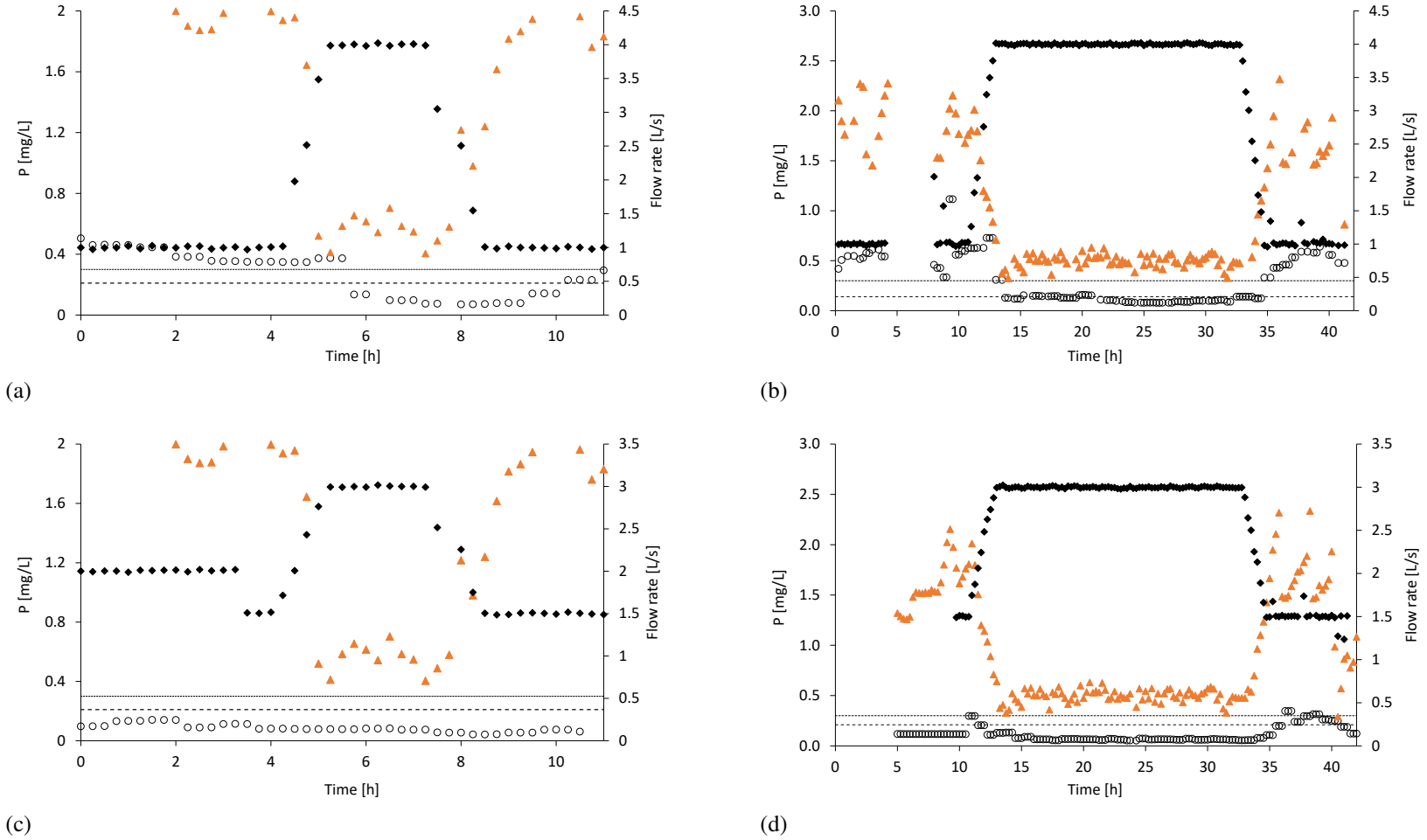

Figure 2.11: Impact of storm simulations on performance of CF and BC. Influent P (▲), effluent P (●) and flow rates (◆) for CF and BC during (a) 4h Storm test CF (b) 24h Storm test CF (c) 4h Storm test BC (d) 24h Storm test BC with TP target (------) and ortho-P target (----). Gap of data for BC occurred due to a shutdown from high combined phosphate. CF: Cloth filter, BC: Ballasted coagulation

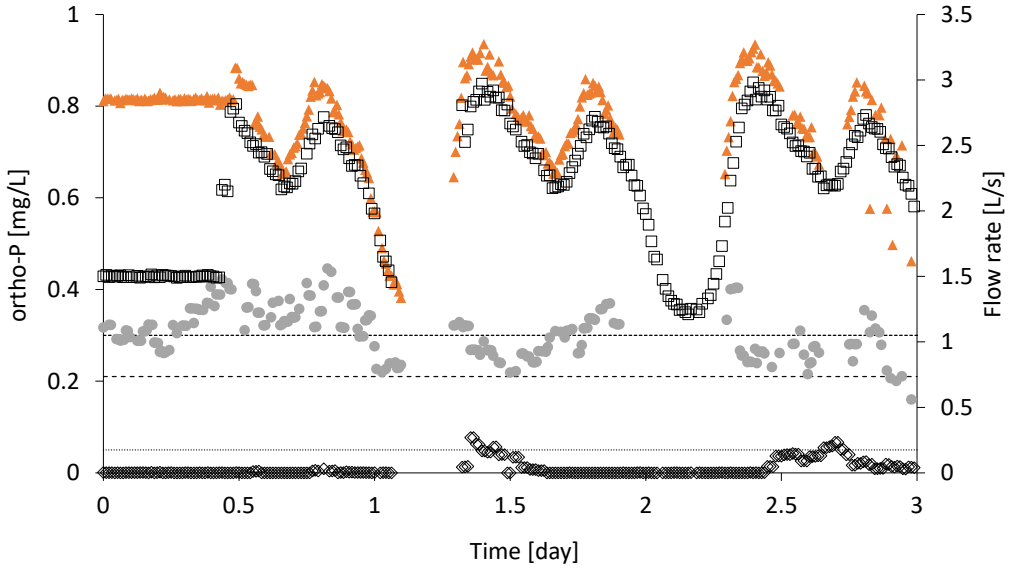

Figure 2.12: Diurnal operation with effluent P (y1) for cloth filter (●) and ballasted coagulation (◇) and flow rates (y2) for cloth filter(▲) and ballasted coagulation (□).TP target (-------), ortho-P target (- - - -) and P detection limit (·····).

2.4 Conclusions

This work has shown that the choice for solids retention technologies can be decisive to achieve effluent P below 0.3 mg/L. From the three technologies tested, the ballasted coagulation process was found to perform most consistently during steady state and dynamic operations reaching effluent P values below the ortho-P target of 0.21 mg/L. Especially during storm and diurnal tests the technology achieved consistently low effluent P concentrations suggesting that the system consists of optimised coagulation-flocculation system. Both the cloth filtration and ultrafiltration membrane were able to achieve the effluent target though at higher coagulant doses (Figure 2.9). Additionally, the upstream coagulation and flocculation system was suggested to be an important factor.

In tests with a high solids feed from a trickling filter site, the ultrafiltration membrane was shown to outperform the ballasted coagulation system and it is assumed that the higher

solids content resulted in larger flocs that were more prone to break in the ballasted system. It was shown in laboratory trials that polymer-ballast flocs break faster (Chapter 3) and therefore short contact times are essential to achieve low effluent P. Improved performance with a different feed was observed for the cloth filtration technology suggesting that more adsorption sites are available through the higher solids content.

When it comes to implementation in full-scale not only performance, but also capital and operational costs will be considered. A previously published life cycle assessment for tertiary P removal technologies revealed that energy demand increases when moving from high rate sedimentation over a microsieve to UF (Remy et al. 2014). Translated to this study, this means that ballasted coagulation (i.e. high rate sedimentation) can be a sensible choice for medium to large wastewater treatment plants where effluent consents below $<$0.3 mg P/L are set. The cloth filtration technology can be also implemented at smaller sites that have consents between 0.3 and 0.5 mg P/L. Based on this work and the projected costs, the ultrafiltration technology will likely not be a suitable solution at this stage because it still requires more understanding into impacts of coagulant types and up-stream flocculation to achieve resilient performance at conservative chemical consumption.

To deliver the required effluent P concentrations, coagulant doses at minimum molar ratios of 1.37 Fe:P were shown to be sufficient at short contact times as has been seen for the ballasted coagulation process. Moreover, cloth filtration and ultrafiltration were observed to have limitations which were not only influenced by coagulant doses but also coagulant types and up-stream flocculation conditions.

2.5 Acknowledgements

Funding for this study was gratefully received by Severn Trent Water. The authors would also like to acknowledge the provision of the demonstration plants from Evoqua Water

Technologies, Hydrok and Koch Membranes.

References

Baillod, C., Cressey, G., and Beaupre, R. (1977). "Influence of Phosphorus Removal on Solids Budget". *Journal of the Water Pollution Control Federation* 49.1, pp. 131–145.

Bill, K., Benisch, M., Falconer, H., Pellegrin, M.-L., Fredrickson, H. S., Fisher, C., Carleton, B., Neethling, J., and Clark, D. (2011). "Evaluation of a Tertiary Membrane Filter Demonstration Pilot to Achieve Ultra-Low Effluent Phosphorus Concentrations". *Proceedings of Annual WEFTEC- National Conference of WEF*, pp. 306–319.

Bratby, J. (2016). *Coagulation and Flocculation in Water and Wastewater Treatment - Second Edition*. Vol. 3. IWA Publishing.

Butterworth, E., Dotro, G., Jones, M., Richards, A., Onunkwo, P., Narroway, Y., and Jefferson, B. (2013). "Effect of artificial aeration on tertiary nitrification in a full-scale subsurface horizontal flow constructed wetland". *Ecological Engineering* 54, pp. 236–244.

DeBarbadillo, C., Shellswell, G., Cyr, W., Edwards, B., Waite, R., Mullan, J., and Mitchell, R. (2010). "Pilot Testing of Four Tertiary Phosphorus Removal Processes To Achieve Ultra-Low Phosphorus Limits At the Lakeshore WPCP in the Town of Innisfil , Ontario". *WEFTEC*. Black & Veatch, pp. 1–10.

El Samrani, A. G., Lartiges, B. S., Montargès-Pelletier, E., Kazpard, V., Barrès, O., and Ghanbaja, J. (2004). "Clarification of municipal sewage with ferric chloride: The nature of coagulant species". *Water Research* 38.3, pp. 756–768.

EU Water Framework Directive (2000). *2000/60/EC*.

Gu, A. Z. (2014). *Phosphorus Fractionation and Removal in Wastewater Treatment - Implications for Minimizing Effluent Phosphorus*. International Water Association.

Hahn, M. W. and O'Melia, C. R. (2004). "Deposition and Reentrainment of Brownian Particles in Porous Media under Unfavorable Chemical Conditions: Some Concepts and Applications". *Environmental Science and Technology* 38.1, pp. 210–220.

Hartshorn, A. J., Prpich, G., Upton, A., Macadam, J., Jefferson, B., and Jarvis, P. (2015). "Assessing filter robustness at drinking water treatment plants". *Water and Environment Journal* 29.1, pp. 16–26.

Havlicek, M. (2018). "Direct coagulant dosing on sand filters for low phosphorus consents". PhD thesis. Cranfield University.

Huck, P. M. and Coffey, B. M. (2004). "The Importance of Robustness in Drinking Water Systems". *Journal of Toxicology and Environmental Health, Part A* 67.20-22, pp. 1581–1590.

Janssen, M. A., Anderies, J. M., and Ostrom, E. (2007). "Robustness of Social-Ecological Systems to Spatial and Temporal Variability". *Society & Natural Resources* 20.4, pp. 307–322.

Kängsepp, P., Väänänen, J., Örning, K., Sjölin, M., Olsson, P., Rönnberg, J., Wallebäck, F., Cimbritz, M., and Pellicer-Nàcher, C. (2016). "Performance and operating experiences of the first scandinavian full-scale discfilter installation for tertiary phosphorus polishing with preceding coagulation and flocculation". *Water Practice and Technology* 11.2, pp. 459–468.

Langer, M. and Scherman, A. (2013). *Feasibility of the Microsieve technology for advanced phosphorus removal Project acronym: OXERAM 2*. Tech. rep. Berlin: Kompetenzzentrum Wasser Berlin gGmbh.

Lee, R. M., Carlson, J. M., Bril, J., Cramer, J., and Harenda, J. (2015). "Pilot Testing Reveals Alternative Methods to Meet Wisconsin's Low Level Phosphorus Limits". *Proceedings of Annual WEFTEC- National Conference of WEF*, pp. 3238–3252.

Li, J., Liu, X., and Cheng, F. (2017). “Bio-refractory organics removal and floc characteristics of poly-silicic-cation coagulants in tertiary-treatment of coking wastewater”. *Chemical Engineering Journal* 324.September, pp. 10–18.

Li, Y., Gao, B., Wu, T., Chen, W., Li, X., and Wang, B. (2008). “Adsorption kinetics for removal of thiocyanate from aqueous solution by calcined hydrotalcite”. *Colloids and Surfaces A: Physicochemical and Engineering Aspects* 325.1-2, pp. 38–43.

Murthy, S., Takacs, I., Dold, P., and Al-Omari, A. (2005). “Examining the bioavailability of chemically removed phosphorus at the blue plains advanced wastewater treatment plant”. *Proceedings of the Water Environment Federation*. WEFTEC, pp. 4279–4287.

Nazif, S. and Karamouz, M. (2009). “Algorithm for Assessment of Water Distribution System’s Readiness: Planning for Disasters”. *Journal of Water Resources Planning and Management* 135.4, pp. 244–252.

Qin, J.-J., Oo, M. H., Kekre, K. A., and Knops, F. (2012). “Integrated coagulation–ultrafiltration for enhanced removals of phosphate and organic in tertiary treatment”. *Desalination and Water Treatment* 44.1-3, pp. 284–288.

Ragsdale, D. (2007). *Advanced wastewater treatment to achieve low concentration of phosphorus*. Tech. rep. Seattle: US EPA.

Remy, C., Miehe, U., Lesjean, B., and Bartholomäus, C. (2014). “Comparing environmental impacts of tertiary wastewater treatment technologies for advanced phosphorus removal and disinfection with life cycle assessment”. *Water Science and Technology* 69.8, pp. 1742–1750.

Rossini, M., Garrido, J., and Galluzzo, M. (1999). “Optimization of the coagulation–flocculation treatment: influence of rapid mix parameters”. *Water Research* 33.8, pp. 1817–1826.

Takács, I., Johnson, B. R., Smith, S., Szabó, A., and Murthy, S. (2011). “Chemical P removal – from lab tests through model understanding to full-scale demonstration”. *IWA*

Specialized Conference on Design, Operation and Economics of Large Watstewater Treatment Plants, pp. 101–108.

Zheng, H., Zhu, G., Jiang, S., Tshukudu, T., Xiang, X., Zhang, P., and He, Q. (2011). "Investigations of coagulation-flocculation process by performance optimization, model prediction and fractal structure of flocs". *Desalination*.

Chapter 3

The impact of polymer selection and dose on the incorporation of ballasting agents onto wastewater aggregates

Olga Murujew[1], Jordan Geoffroy[1], Emeline Fournie[1], Elisa Socionovo Gioacchini[1], Andrea Wilson[2,3], Peter Vale[2], Bruce Jefferson[1], Marc Pidou[1,*]

[1] Cranfield University, College Road, Cranfield, Bedfordshire, MK43 0AL, UK

[2] Severn Trent Water, 2 St Johns Street, Coventry, CV1 2LZ, UK

[3] Atkins Global, Woodcote Grove, Epsom, Surrey, KT18 5BW, UK

[*]Corresponding author: m.pidou@cranfield.ac.uk

Abstract

Ballasted coagulation is an efficient high-rate sedimentation process gaining more attention as an advanced P removal technology for levels below 0.1 mg/L. The process is well-known, yet interactions within the matrix of wastewater, coagulant,

polymer and ballast remains unclear, especially when it comes to polymer doses and types which are rather based on recommendations rather than scientific evidence. In this work, the impact of anionic and cationic polymers has been investigated on P removal and floc properties. Anionic polymers were shown to be superior to cationic ones when it comes to P removal and doses even as low as 0.01 mg/L yield better results than coagulant alone. There appears to be a "best-case" floc size with which very good P removal (>90%) can be achieved and flocs of sufficient strength can be generated.

Keywords: Polymer, phosphorus removal, magnetite, ballasted coagulation

3.1 Introduction

Established approaches to manage phosphorus concentrations in wastewater use either enhanced biological P removal (EBPR), or more commonly, chemical precipitation (Yeoman et al. 1988). The resultant final effluent concentration ranges between 1 and 2 mg P/L. The situation is changing with increasing numbers of sites requiring to further lower their effluent P concentration to below 1 mg P/L and potentially as low as 0.1 mg P/L (EU Water Framework Directive 2000). Chemical P removal is undertaken through the addition of a metal salt (e.g. $FeCl_3$) to wastewater prior to either the primary or secondary treatment stage to precipitate the available phosphorus into aggregates which can then be easily removed. P concentrations below 1 mg P/L can be achieved by increasing the dose of coagulant, but very large doses are required. The alternative is to dose ahead of a tertiary solid liquid separation process with current examples including depth sand filtration, drum cloth filtration and ballasted coagulation. In such cases, doses of 4 mg/L to 15 mg/L have been reported for full-scale operations, generating a significant saving in total chemical usage compared to increasing the dose at earlier stages in the treatment

train (Bratby 2016; Hook and Ott 2001; Ragsdale 2007).

In the US, ballasted coagulation – a high-rate sedimentation process- has been able to achieve very low effluent P (<0.1 mg/L) concentrations which makes it an interesting technology for the UK (DeBarbadillo et al. 2010; Lee et al. 2015). The inclusion of a ballasting agent such as sand or magnetite, i.e. Fe_3O_4, into the flocs significantly enhances their settling rate enabling removal in high rate clarification setups characterised by surface overflow rates of 33.6-80 $m^3/m^2/h$ (DeBarbadillo et al. 2010; Imasuen et al. 2004; Lee et al. 2015). The ballast is typically recycled to reduce costs and sludge production by passing the collected sludge through a hydrocyclone (Desjardins et al. 2002; Gasperi et al. 2012; Imasuen et al. 2004). In the case of Fe_3O_4 (magnetite) the hydrocyclone is followed by a magnetic drum to recover and recycle the ballast (Anderson and Priestley 1983).

For the process to work, a polyelectrolyte is added to ensure the ballasting agent is maintained within the floc structure (Bolto et al. 1996; Jarvis et al. 2009). The polymers used are usually characterised by their molecular structure, molecular weight (MW) and charge density (CD) and work under three potential and simultaneous mechanisms: bridging, charge neutralisation and polymer adsorption (Bolto and Gregory, 2007; Rabiee, 2010). Accordingly, polymers may be uncharged, similarly (anionic) or oppositely charged (cationic) to the negatively charged particles in wastewater. Current recommendations concerning the system are agnostic to polymer selection although cationic polymer has been suggested at a dose of 1 mg/L coupled to a coagulant dose of 8 mg/L. However, in some regions of the world, such as the UK, cationic polymers are discouraged by the local environment agency raising questions as to which polymers are most appropriate and what dose level should be applied.

Previous reported trials of ballasted coagulation utilised a $FeCl_3$ coagulant dose of

14 mg/L and an anionic polymer[1] dose of 1 mg/L to achieve a P reduction from 0.22 mg/L to 0.031 mg/L total P during a four-week trial (DeBarbadillo et al. 2010). Similarly, a pilot trial treating 11 m^3/h real wastewater with initial P concentration of 1 mg TP/L achieved a final concentration of 0.025-0.039 mg TP/L with coagulant doses between 12-24 mg/L[2] and a polymer dose of 0.7 mg/L (Lee et al. 2015). However, these trials are based on validating the ability to meet very low P concentrations rather than optimising dose requirements such that further savings are posited. To fully optimise the system, it is important to elucidate the roles of the ballast and polymers although unfortunately there is a paucity of information relating to the topic. A previously published study demonstrated that the inclusion of the ballast reduced coagulant demand by a factor of ten whilst still increasing COD removal by a factor of five compared to an unballasted system (Imasuen et al. 2004). However, there remains no clear basis for selection of the type and dose of polymers in such systems. The current paper resolves this by examining the performance of seven different polymers in terms of both removal and resultant floc properties to inform a guide to selection for use in tertiary P removal systems.

[1] Anionic polyacrylamides of very high MW and low charge density.

[2] Three coagulants were used: Alum 12 mg/L, PACl 20 mg/L, $FeCl_3$ 24 mg/L.

3.2 Materials and Methods

3.2.1 Materials

Wastewater was taken from a sewage works in the UK that has no primary treatment and utilizes oxidation ditches as secondary treatment. The site was being utilised as part of a large-scale demonstration trial of tertiary P removal technologies such that the samples were withdrawn from within the sampling points of the trials (Table 3.1; Chapter 2). The P concentration was maintained at approximately 1 mg/L throughout by addition of KH_2PO_4 (Sigma-Aldrich, Dorset, UK) where required.

Table 3.1: Wastewater characteristics

	COD [mg/L]	Total P [mg/L]	ortho-P [mg/L]	Suspended solids [mg/L]	Alkalinity [mg $CaCO_3$/L]	pH	Zeta potential [mV] near pH 7.4	Turbidity [NTU]
Average ± Standard deviation	21.25 ± 2.77	1.21 ± 0.36	1.09 ± 0.38	7.27 ± 3.42	178.08 ± 16.34	7.42 ± 0.17	-11.01 ± 1.40	2.45 ± 0.88
Number of samples (n)	78	66	79	76	15	79	9	44

Ferric chloride ($FeCl_3$, 60% w/w) was used as coagulant (Brenntag, Leeds, UK), magnetite was used as ballast (LKAB, Luleå, Sweden) and in total seven polymers were used (supplied by Goldcrest (Dodworth, Barnsley, UK), Kemira (Bradford, UK) and BASF (Bradford, UK)). They were all polyacrylamides and were chosen to have a wide range of characteristics (Table 3.2).

Table 3.2: Polymers and their properties used in this study. Information was given by suppliers unless otherwise noted.

Polymer	Charge	Degree of charge	Molecular weight	Apparent viscosity* [mPa· s] at 6 s^{-1} shear rate	Zetapotential* [mV] near pH 7.4	Chemical structure
A1	anionic	low	NA	57.7	-17.4 ± 10.10	NA
A2	anionic	low-medium	medium	182.7	-43.6 ± 10.0	linear
A3	anionic	low	ultra high	17.9	-12.5 ± 6.9	linear
A4	anionic	low	NA	28.8	-7.5 ± 2.53	NA
C1	cationic	low-medium	very high	113.4	17.4 ± 4.6	linear
C2	cationic	high	very high	127.1	32.7 ± 1.5	cross-linked
C3	cationic	medium	very high	69.7	16.4 ± 6.2	linear

*: measured, NA: not available

3.2.2 Methods

Jar test procedures

Experiments on P removal were performed with jar tests (Phipps & Bird, Richmond, Virginia, USA) with a standard and ballasted jar test method. The standard method was used when tests with coagulant only were done. The procedure consisted of 2 minutes stirring at 200 rpm at the point of coagulant addition followed by 15 minutes stirring at 30 rpm and finished by 30 minutes of settling. Coagulant only tests were run at 5 and 8 mg Fe/L with samples taken after 5, 10 and 15 minutes to assess floc settling over time. The ballasted jar test method was used when ballasted coagulation experiments were performed simulating the conditions in real systems. At the point of coagulant addition, the mixture was stirred at 200 rpm for 2 minutes. After that magnetite (ballast) was added with the stirrer continuing at 200 rpm stirring for 1 minute followed by polymer addition and again stirring at 200 rpm for 1 minute. At the end, the mixture settled for 5 minutes. For selected jar tests, pre-treated magnetite was used to simulate used ballast. This was prepared by stirring unused (fresh) magnetite in wastewater for 1h and drying it at 105°C.

Water analysis

Samples were taken after stirring at 0.5, 1, 3, 5, 15 and 30 minutes for the time dependent settling analysis (Figure 3.1). The impact of different combinations of the coagulation components was sampled after 5 minutes settling and filtered over 0.45 µm (Figure 3.2, 3.3 and 3.4.). Ortho-phosphate was measured following a standard colorimetric method using cell tests (Hach, Sheffield, UK and Merck, Nottingham, UK). Turbidity was measured using a turbidimeter (Model 2100N, Hach, Sheffield, UK). Floc growth and properties were analysed with a particle analyser (Malvern Mastersizer, Malvern, UK). Floc strength (FS) was calculated according to

$$FS = \frac{d_{\text{stable}}}{d_{\text{peak}}} \tag{3.1}$$

with d_{stable}: floc size at 60 minutes and d_{peak}: peak floc size.

Polymer characterisation

Viscosity of polymers was measured with a Viscometer (Brookfield DV-E, UK) with the concentrations of the polymers adjusted to 0.5% and measurements carried out at a range of spindle rotation speeds between 0-100 s^{-1}. Zeta potential was measured using a Malvern Zetasizer (Nano Series, Nano ZS, UK). The polymers were diluted in DI water to obtain a solution of 1 mg/L and the pH was then adjusted between 2 and 12 using HCl and NaOH. Structural analysis of polymers was carried out with FTIR and NMR by Tun Abdul Razak Research Centre (Brickendonbury, Hertford, SG13 8NL). Prior to FTIR scanning, the polymers were dried, dissolved in chloroform and then cast into a film on potassium bromide plates. The FTIR spectra were obtained in a region of 4000-650 cm^{-1} with a single scan per spectrum (Perkin Elmer Spectrum 100). For NMR measurements,

polymers were dried and dissolved in deuterated water (D_2O) with trimethyl-silyl (TSP) agent. ^{13}C NMR spectra were obtained with composite pulse with ^{1}H decoupled and a 30°pulse (8.2 ms) with a pulse delay of 3 seconds was applied (Bruker Avance II 300MZ NMR spectrometer with QNP probe).

3.3 Results and Discussion

3.3.1 Impact of polymer choice and dose on P removal

Phosphorus removal varied for unfiltered samples between 88% and 98% when using the seven different polymers in conjunction with coagulant and ballast (Figure 3.1). Three anionic (A1, A2 and A4) and one cationic polymer (C3) achieved the maximum recorded removal which corresponded to residual phosphorus concentrations below the level of detection of the analytical method (0.05 mg/L). In comparison, the other polymers achieved lower removal levels at 91%, 89% and 88% for polymers C1, C2 and A3 respectively. The other observable difference between the polymers relates to the kinetics of removal where polymers C3, A1 and A4 achieved their maximum removal within 30 seconds as opposed to between 3-5 minutes for the other polymers.
In contrast, the use of coagulant only resulted in a significantly slower overall settling rate and a lower final removal (Figure 3.1). To illustrate, phosphorus removal was 14.8%, 50.9% and 72.9% after 5, 15 and 30 minutes respectively. The significantly faster kinetics in the case of the polymers is congruent with previous trials in drinking water production and highlights the impact of the ballasting agent (Dixon 1991).

To elucidate the role of the polymer, a series of jar tests were conducted utilising the different components that make up the combined system using polymer A1 and filtering the samples over 0.45 µm (Figure 3.2). Phosphorus removal for coagulation only (Co), ballast only (B), coagulant and ballast (CB) and ballast, coagulant and polymer (BCP) were 94%, 8%, 70% and 98% respectively when using 8 mg/L of coagulant. Decreasing the coagulant dose to 5 mg/L decreased P removal for the coagulation system only to 86% but increased removal for the CB system to 86%. However, in the BCP case, the removal was not impacted by lowering the coagulant dose by 38% offering a potential for

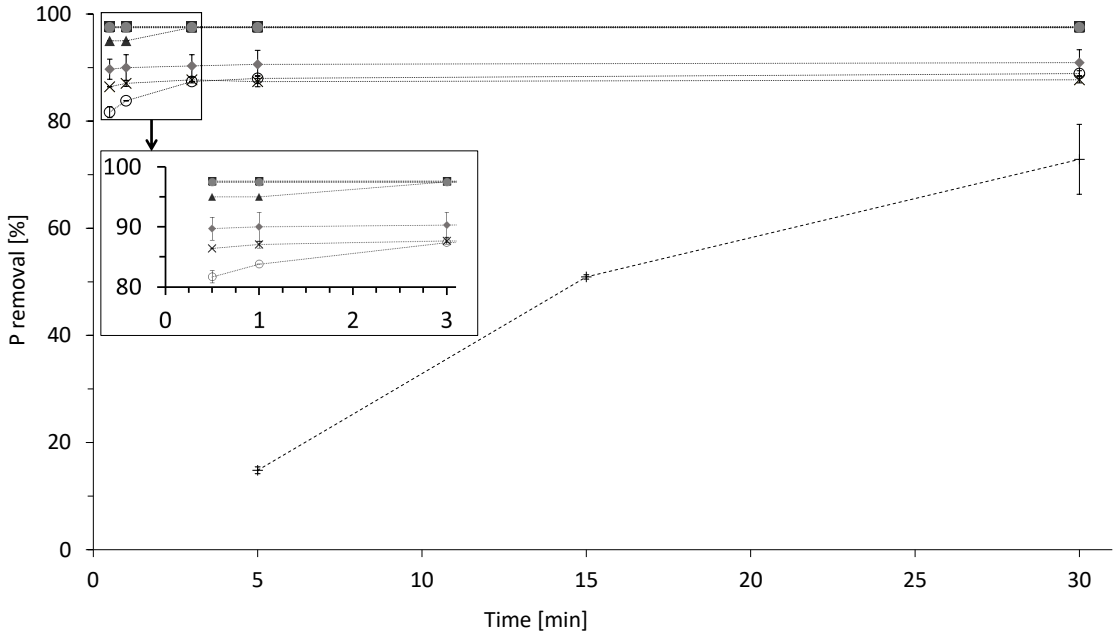

Figure 3.1: P removal from initial 1 mg P/L in relation to settling time between 0.5 and 30 minutes at 5 mg Fe/L and 0.5 mg/L polymer dose and used magnetite. Polymers: A1 (■), A2 (▲), A3 (x), A4 (□), C1 (◆), C2 (○), and C3 (●) and only coagulant (+).

substantial chemical savings.

A second series of trials were conducted with two anionic (A1 and A2) and two cationic polymers (C1 and C2) to further explore the role of the polymer by comparing its use alone (P) in conjunction with the ballast (BP), the coagulant (CP) or both (BCP) and filtering the samples over 0.45 µm (Figure 3.3). Comparison of the phosphorus removal achieved with the four polymers when used alone (P) revealed that none of the polymers were effective as a primary precipitating agent (Figure 3.3). To illustrate, when used alone phosphorus removals of 34%, 7%, 3% and 1% were observed for polymers A1, A2, C1 and C2, respectively. Combining the polymer with the ballast switched the sequence of efficacy of the polymers with the two cationic polymers being more effective with phosphorus removal levels of 44% and 69% C1 and C2, respectively. In contrast, the anionic polymers, A1 and A2 resulted in phosphorus removal levels of 14% and 22%,

respectively. Significantly improved removal was observed when the polymer was used in conjunction with a ferric coagulant with phosphorus removal levels of 28-36%, 77-84%, 46-55% and 39-76% for A1, A2, C1 and C2, respectively. Interestingly, the removal with coagulant alone is higher than in conjunction with polymer suggesting the polymer is either inhibiting precipitation or is exerting a demand on the coagulant irrespective of its charge. Further, improved removal was observed when the coagulant dose was increased from 5 mg/L to 8 mg/L yielding an improvement in removal efficiency between 7-9% for A1, A2 and C1 with a much greater enhancement with C2 of an additional 37% phosphorus removal. When all components (BCP) were added to the process very high phosphorous removal (97.7%) was achieved for A1 and A2. This demonstrates that the ballasted coagulation process is more efficient than coagulation alone and enables very low residual phosphorus levels to be achieved. However, this observation only applies to the two anionic polymers tested (A1, A2) as reduced performance was observed for C1 and C2 such that it was comparable to coagulation alone at 87-92% as BCP compared to 86-95% when just using coagulant.

No discernible impact was observed when reducing the polymer dose from 1 mg/L down to 0.3 mg/L with all four polymers at both 5 mg/L and 8 mg/L of coagulant and with fresh or reused ballast and with unfiltered samples (Figure 3.4). In the case of the two anionic polymers and a coagulant dose of 8 mg/L, no impact was seen when reducing the polymer dose down to the lowest level tested, 0.01 mg/L or a 99% saving in polymer. When using the lower coagulant dose of 5 mg/L, a different profile was observed whereby the removal increased as a function of polymer doses up to around 0.3 mg/L. To illustrate, in the case of A1, phosphorus removal increased from 80% at 0.01 mg/L to 95.7% at 0.3 mg/L and then to 98% at 1 mg/L. Equivalent variation in removal was observed with the other three polymers at polymer doses below 0.3 mg/L but all systems then delivered stable removal irrespective of dose.

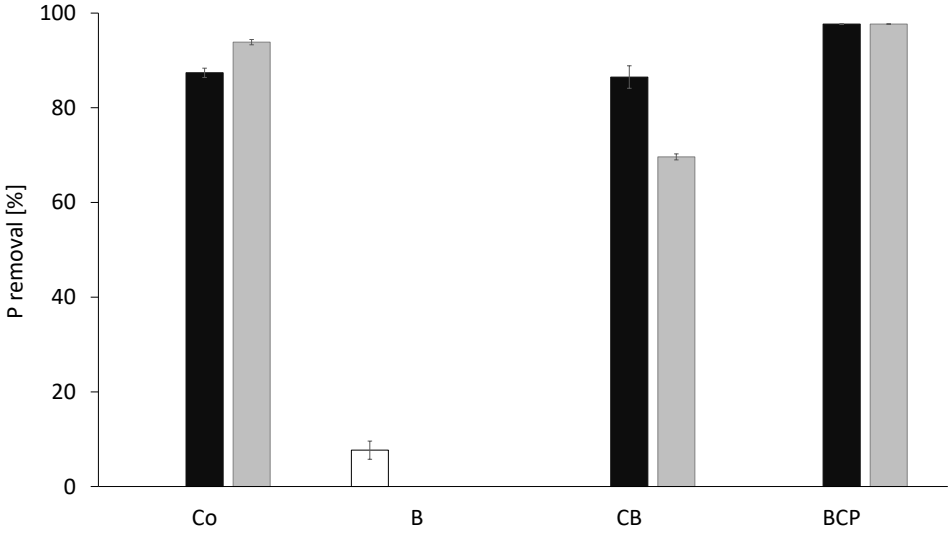

Figure 3.2: P removal from initial 1 mg P/L with coagulant only (Co), ballast only (B), combination of coagulant and ballast (CB) and all components (CBP, 1 mg/L A1 polymer dose) at 0 mg Fe/L (□), 5 mg Fe/L (■) and 8 mg Fe/L (■) after 5 minutes of settling with filtered samples over 0.45 µm.

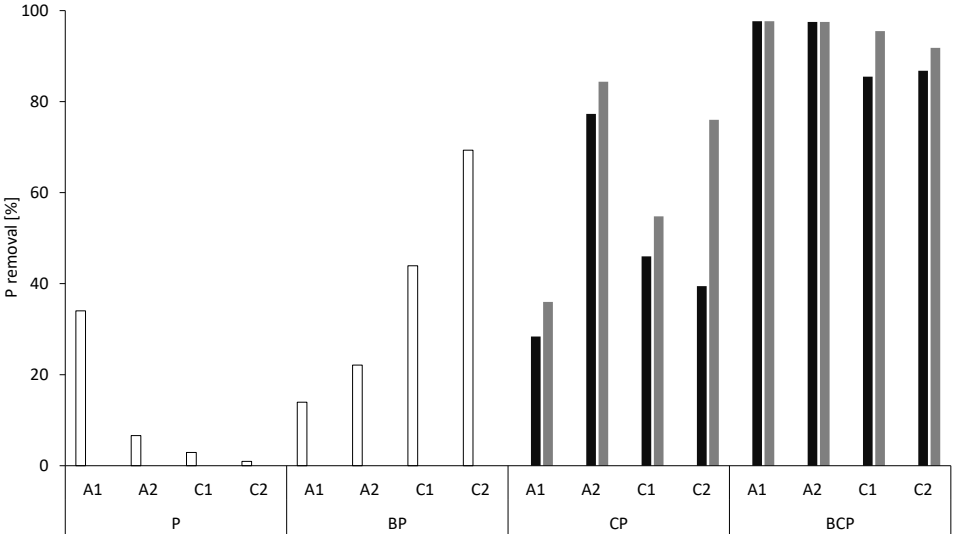

Figure 3.3: P Removal from initial 1 mg P/L at different coagulation combinations: polymer only (P), ballast and polymer (BP), coagulant and polymer (CP), coagulant, ballast and polymer (CBP). Coagulant doses: 0 mg Fe/L (□), 5 mg Fe/L (■) and 8 mg Fe/L (■), polymer dose: 1 mg/L, ballast (used) dose: 5 g/L, settling time: 5 minutes and filtration over 0.45 µm.

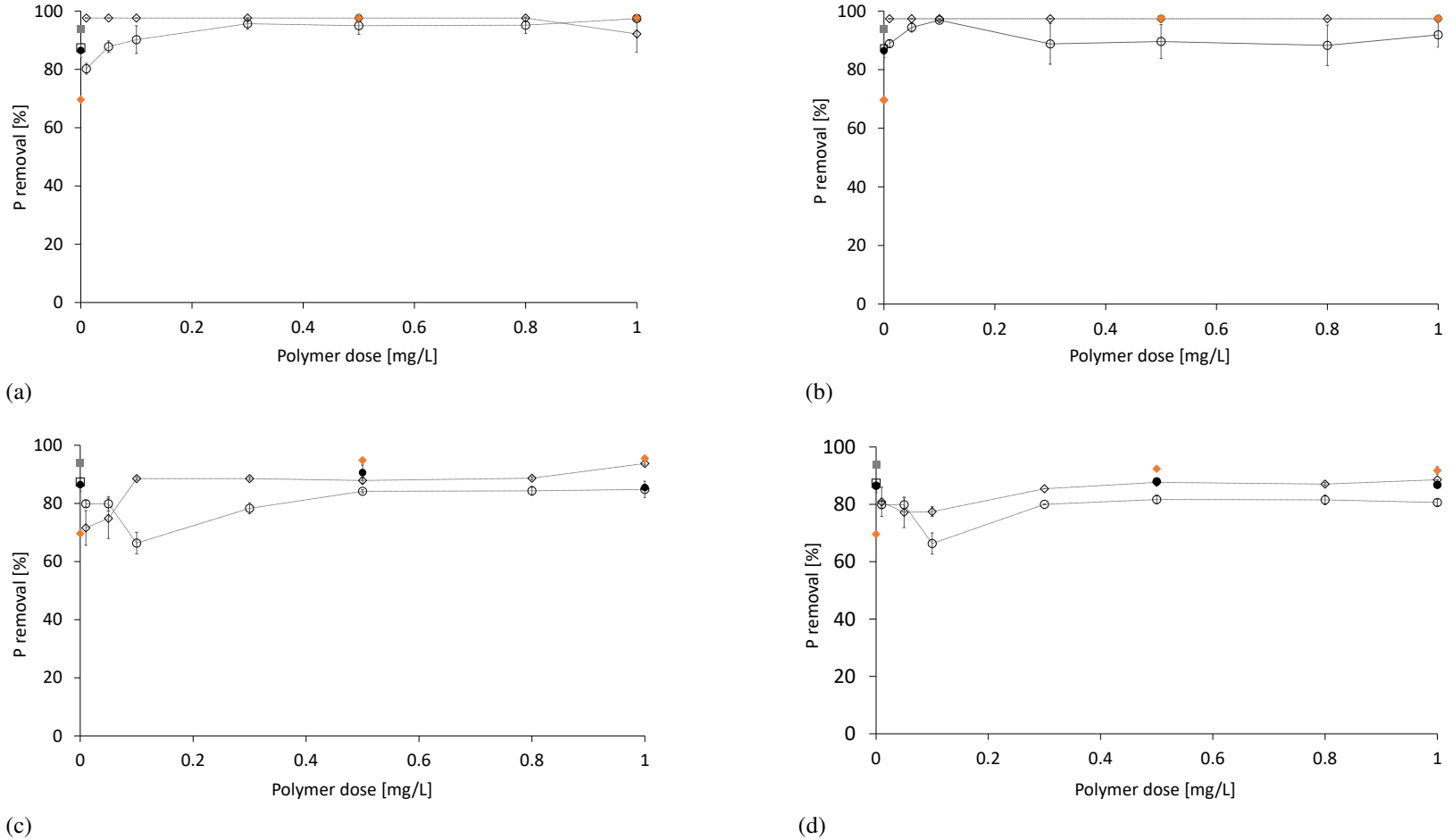

Figure 3.4: Polymer dose response curves after 5 minutes settling time at 5 mg Fe/L with fresh magnetite (○), 8 mg Fe/L with fresh magnetite (◇), at 5 mg Fe/L with used magnetite (●) and 8 mg Fe/L with used magnetite (◆) for (a) A1, (b) A2, (c) C1, (d) C2 . In comparison to coagulant only at 5 mg Fe/L (□) and 8 mg Fe/L (■).

3.3.2 Impact of polymer choice and dose on floc size

For all polymers, the floc growth profiles followed a pattern of rapid growth reaching a peak size after 4-5 minutes followed by gradual decline until a steady state floc size was established (Figure 3.5). The choice of polymer has a significant impact on the maximum floc size achieved, the rate of erosion and hence the time taken to reach a stable floc size. For instance, the maximum d_{50} floc size was 274 µm, 737 µm, 866 µm and 1443 µm for polymers C2, A1, C1 and A2, respectively. After 60 minutes all flocs had stabilised to similar size with a d_{50} between 165 and 197 µm (Figure 3.5). However, the rate of breakage was significantly different with the d_{50} floc size reaching 40% of its difference between peak and final size within 12, 18 and 45 minutes for polymers C1, A2 and A1, respectively. The flocs made by polymer C2 were the smallest, eroded at a slower rate and decreased in total only by 41% compared to the others which decreased in size by 73-86%. Interestingly, polymer C1 showed a different breakage pattern to the others with a much greater initial fragmentation breakage profile (Jarvis et al. 2005a). To illustrate the d_{50} floc size decreased by 499 µm in the 3 minutes after the peak value was observed, equivalent to a 58% reduction in the floc size. In comparison polymers C2, A1 and A2 decreased by 27 µm, (10%), 84 µm (11%) and 107 µm (7%) in the same time.

In comparison, when coagulant alone is used, the d_{50} flocs grow to a stable d_{50} size of approximately 610-600 µm for a period of 30 minutes before gradually eroding to a final size of between 510-530 µm. Accordingly, inclusion of polymer significantly impacts on the formation and breakage profiles of the flocs. This is illustrated through their respective floc strength factors of 0.14, 0.19, 0.26 and 0.59 for polymers A2, C1, A1 and C2 compared to coagulation alone with a floc strength factor of 0.83. A tendency for increasing floc strength factors with decreasing d_{50} peak floc sizes and with slower breakage rates can be seen for all polymers. This indicates that there may be an equilibrium size for the

BCP system at which the flocs are big enough for very good P removal while producing large enough flocs of sufficient strength.

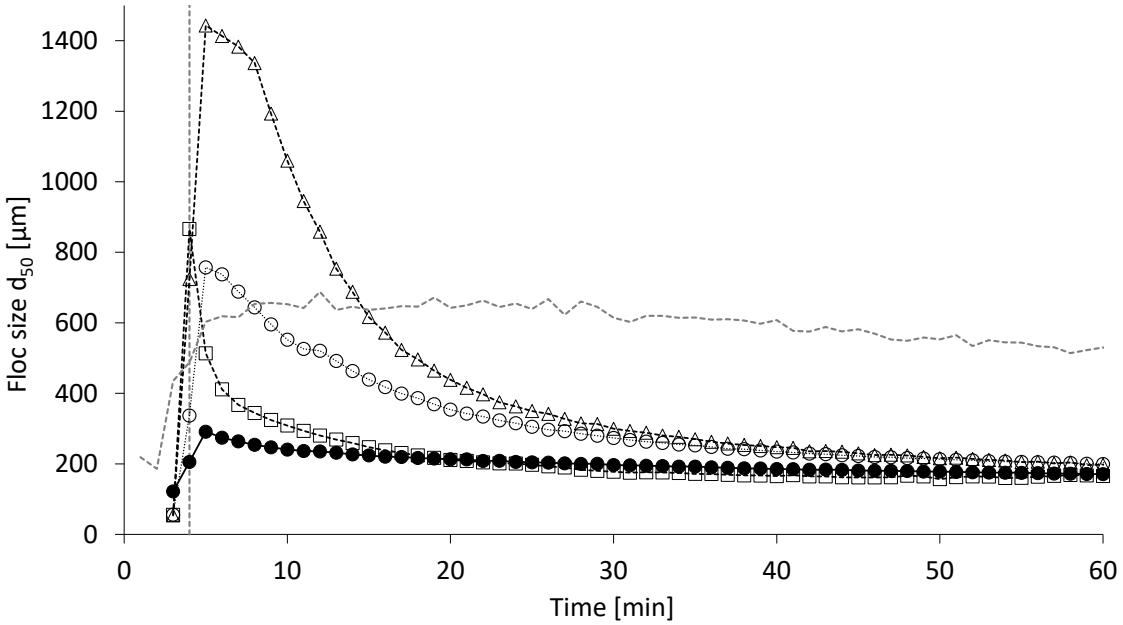

Figure 3.5: Floc growth with time at 8 mg Fe/L, 5 g/L fresh magnetite and 1 mg/L polymer dose. Polymers: A1 (∘), A2 (△), C1 (□), C2 (●), coagulant only: ------. Vertical dotted line indicates 4 minutes, i.e. when stirring was stopped in jar test procedure.

An increase in polymer dose resulted in an increased floc size in all cases (Table 3.3). To illustrate, in the case of polymer A1, the d_{50} floc size increased from 68.3 µm at a polymer dose of 0.01 mg/L to 154.3 µm, 413.7 µm and 337.0 µm at polymer doses of 0.1, 0.5 and 1 mg/L, respectively. This equates to a size increase factor of 4.9 between the low and high doses. Similar trends were observed for the other polymers with equivalent size increase factors of 10.9, 15.2 and 3.5 for polymers A2, C1 and C2, respectively. The impact in dose appeared to be more sensitive for the anionic polymer where a change in dose from 0.01 to 0.1 mg/L resulted in a 226% increase in the d_{50} for A1 and a 346% increase for A2. In comparison, an increase in d_{50} of 127% and 112% was measured for the cationic polymers C1 and C2. In all cases, the increased polymer dose generated more open, dendritic structures as evidenced by the change in the fractal dimension. To illustrate, in the case of the polymer A1, the fractal dimension decreased from a value of 2.7 at a polymer dose of 0.01 mg/L to 2.6, 2.2 and 2.3 for polymer doses of 0.1, 0.5 and 1.0 mg/L respectively. Similar changes occurred with the other polymers except for C1 where the shape of the flocs remained more stable across the polymer doses tested.

The impact of polymer dose was further elucidated by comparing the particle size distributions at the peak size (roughly 4 minutes) and after 60 minutes to explore how the flocs break (Figure 3.6). Comparison of the PSDs for low doses revealed that the shape of the size distribution remained similar and that only a small shift in the size was observed congruent with an erosion mechanism dominating as is common with small flocs (Jarvis et al. 2005b). This was seen in the case of polymers A2, C1 and C2 with shifts in the mode size from 68.1 µm to 47.5 µm for A2, 56.5 µm to 45.6 µm for C1 and 61.2 µm to 55.5 µm for C2 (Figure 3.6). In the case of the higher polymer dose a different response can be seen where larger scale shift in particle size distribution can be observed which is more indicative of a fragmentation mechanism that occurs with large flocs that are bigger than the Kolmogorov scale of turbulence (Jarvis et al. 2005b). Previous research using

similar jar testers have estimated the size of the turbulent eddies to be of a similar size to the flocs at the energy dissipation rate being used (Jarvis et al. 2005b). Accordingly, flocs bigger than this size are more likely to fragment. This is seen in the case of polymers A1, A2 and C1 but not C2. For instance, the mode size decreased from 782 µm to 199 µm when using 1 mg/L of A1 and from 1673.3 µm to 288 µm when using A2. In contrast the mode size changed from 322 µm to 178.7 µm when using 1 mg/L of C2. The impact of the polymer dose can be also considered in terms of the colloids by examining the d_{10} and the residual turbidity and the end of the settling phase (Table 3.3). Both data sets indicate a coherent observation in that higher doses increase the d_{10} floc size and reduce the residual turbidity. For instance, in the case of the anionic polymers the d_{10} size increased from 31.1 µm to 69 µm for A1 and 27.2 µm to 75.9 µm for A2 as the polymer dose increased from 0.01 to 1.0 mg/L. The corresponding residual turbidities were from 1.8 to 0.9 NTU for A1 and from 1.7 to 0.7 NTU for A2. Whilst the same pattern was observed with the cationic polymers the d_{10} floc sizes were larger but the residual turbidities were higher indicating that either the polymers were less effective at capturing colloids or more breakage was occurring that generated fine particles. The evolution of the d_{10} floc size showed a sharp increase to a peak at 5 minutes with a steady decrease to a stable size at the end. Therefore, it suggests that the more likely explanation is that of greater fines generation during erosive floc breakage. Similarly, as with d_{50}, higher polymer doses resulted in larger flocs which then break down more quickly the larger the peak size was.

Table 3.3: P removal and turbidity after 5 minutes of settling. Floc sizes and fractal dimensions after 4 minutes of stirring. Floc strength factor (FS) based on d_{50} peak and stable sizes. All at coagulant dose 8 mg Fe/L, 5 g/L fresh magnetite, 200 rpm stirring.

Polymer	Dose [mg/L]	P removal [%]	Turbidity [NTU]	d_{50} [µm]	d_{10} [µm]	Mode [µm]	D_f	FS
A1	0.01	97.6 ± 0	1.8	68.3 ± 8.3	31.1 ±3.1	71.6 ± 9.8	2.7	0.73
	0.1	97.6 ±0	1.0	154.3 ± 7.5	49.5 ± 4.2	195.3 ± 32.9	2.6	0.42
	0.5	97.6 ± 0	0.8	413.7 ± 204.9	89.8 ± 41.2	411.7 ± 381.7	2.2	0.24
	1	92.2 ± 6.3	0.9	337.0 ± 17.8	69.0 ± 9.6	583.0 ± 86.1	2.3	0.26
A2	0.01	97.4 ± 0	1.7	66.2 ± 7.3	27.2 ± 3.1	68.1 ± 11.4	2.7	0.8
	0.1	97.4 ± 0	1.4	229.3 ± 14.0	61.8 ± 3.7	316.0 ± 16.0	2.6	0.32
	0.5	97.4 ± 0	0.7	714.0 ± 120.4	90.2 ± 15.4	974.7 ± 307.0	2.5	0.12
	1	97.4 ± 0	0.7	724.3 ± 94.2	75.9 ± 9.7	1476.7 ± 170.1	2.2	0.14
C1	0.01	71.6 ± 6.0	3.6	57.0 ± 4.1	24.4 ± 1.7	56.5 ± 6.2	2.8	0.97
	0.1	88.6 ± 0.6		72.6 ± 2.3	28.8 ± 2.3	73.6 ± 10.1	2.7	1.15
	0.5	87.9 ± 1.0	1.6	219.5*	56.8*	299.0*	2.6	0.62
	1	93.7 ± 0.6	1.1	866.0 ± 99.0	139.0 ± 20.7	1070.0 ± 177.2	2.5	0.19
C2	0.01	80.9 ± 5.1	2.3	59.0 ± 6.4	25.0 ± 2.3	61.2 ± 9.3	2.8	0.9
	0.1	77.5 ± 1.7	3.6	66.4 ± 4.3	24.8 ± 2.0	65.4 ± 7.8	2.7	1.24
	0.5	87.7 ± 0.6	1.6	159.5 ± 29.5	45.6 ± 5.7	231.7 ± 118.0	2.5	0.41
	1	88.6 ± 0	1.7	205.6 ± 98.2	92.1 ± 81.0	270.7 ± 154.1	2.3	0.59

*: No standard deviation as only two repetitions were done

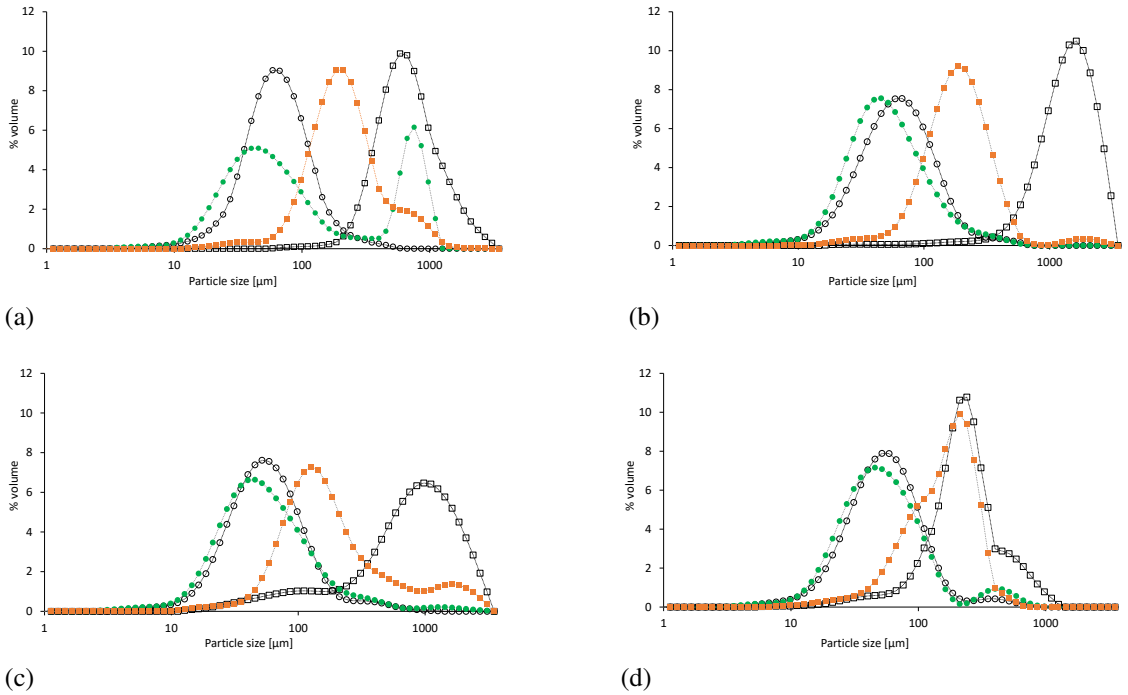

Figure 3.6: PSD at 8 mg Fe/L, 5 g/L fresh magnetite. Peak floc size (4-5 min) at polymer doses 0.01 mg/L (∘) and 1 mg/L (□). Stable floc size (60 min) at 0.01 mg/L (●) and 1 mg/L (■) for (a) A1, (b) A2, (c) C1, (d) C2.

3.3.3 Polymer properties and comparison to performance

The cationic polymers were all defined by the manufacturers as high molecular weight and have measured apparent viscosities of 113.4, 127.1 and 68.7 mPa.s for C1, C2 and C3, respectively when used at a shear rate of 6 s^{-1} (Table 3.2). Less information was available for the anionic polymers where A2 was described as a medium molecular weight and A3 as an ultra-high molecular weight polymer. The corresponding apparent viscosities at a shear rate of 6 s^{-1} were 57.7, 182.7, 17.9 and 28.8 mPa.s for A1, A2, A3 and A4, respectively. All the anionic polymers were described as low or low-medium charge and had measured zeta potentials at pH 7.4 of -17.4, -43.6, -12.5, and -7.5 mV for A1, A2, A3 and A4, respectively (Table 3.2). Measurement of the zeta potential across a pH spectrum revealed that only polymers A1 and A2 had a degree of acid dissociation where the

zeta potential becomes more negative as the pH was increased up to around a pH of 5-6 (Figure B.2). The other anionic polymers (A3 and A4) showed only marginal increase in zeta potential as the pH was increased showing that their charges were predominately fixed in nature. In comparison, the cationic polymers were described as more charged with corresponding zeta potential values at pH 7.4 of 17.4, 32.7 and 16.4 mV at a dose of 1 mg/L. C1 and C2 demonstrated an amphoteric dissociation whereby the zeta potential changed as a function of pH and crossed the zero zeta potential line at a pH of 9.8 and 10.1, respectively. In contrast, C3, exhibited a stable zeta potential over acidic pH which then reduced under alkaline conditions to cross the zero zeta potential line at pH 9.8. Most of the polymers were described as conforming to a linear structure (A2, A3, C1 and C3) with C2 cross-linked and A1 and A4 of unknown structure.

The main functional groups were identified to be acrylamide carbonyl, acrylic carbonyl and quaternary ammonium, ester and ether (Figure 3.7). All of these except of the latter one (ether) belong to regular cationic or anionic polyacrylamides (Bolto and Gregory 2007). The ether group peak (72 ppm) was only linked to A2 and A3. The polymers A4 and A1 had no ether group peak assigned to them and both had a similar NMR spectrum. In the group of the cationic polymers, all had strong peaks between 53.9 and 56.3 ppm which could be attributed to quaternary ammonium groups which would confirm the cationic charge of the polymers (Table 3.2 and 3.4). The peak ratios, obtained from integration of the peak area, show big differences in structural composition between the polymers yet complete examination of the chemical structures was not possible due to their complexity.

The addition of polymer added considerably to P removal performance as was shown with varied combinations of components of the BCP and only combination of all three –coagulant, ballast, polymer– achieved the highest P removal (Figure 3.2). Experiments on the individual components revealed that the polymer does not act as the primary precipitating

agent and so its function related more to the effective incorporation of the ballast into the precipitated aggregate formed by the addition of coagulant. Further, the magnetite does not contribute significantly to phosphorus removal. This is observed through the direct experiment and the comparison of fresh and reused ballast. This is expected as magnetite is a spinel crystal structure with a formula of $Fe^{+II}Fe_2{}^{+III}O_4$ with the majority of Fe ions at their highest oxidation state (+III). In other cases where iron is used as an adsorbent for phosphorus such as hybrid ion exchange resins, iron ions are in their lower oxidation state +II which is more favourable for adsorption (Anderson and Priestley 1983; Zi-li et al. 2004; Martin et al. 2009).

The assessment of the impact of polymer selection and dose has indicated that phosphorus removal performance in a ballasted coagulation system is best served with anionic polymers. Whilst this implies the predominant mechanism is not likely to be electrostatic, the presence of calcium ions in the water are known to act as bridging ions (Rabiee 2010). Furthermore, the recommended polymer dose of 1 mg/L could not be justified with these experiments as doses as low as 0.01 mg/L were shown to be effective and as seen in the cases of C1 and C2, polymer addition can lead to lower phosphorus removal than adding coagulant alone (Figure 3.3). However, the dose did impact the flocs characteristics with higher doses leading to larger flocs and lower residual turbidities. In such cases, bridging mechanisms are likely to be important and these are best served by large MW linear polymers. The poorer removal and smaller floc sizes achieved with C2 supports this due to its crosslinked structure. The enhancement with anionic polymer may also reflect the stronger influence of bridging as direct electrostatic connections will not be made, instead favouring patchwork bridging (Bache and Gregory 2007). Overall the work has outlined that effective tertiary ballasted coagulation for phosphorus removal is best served with low doses of medium to large MW linear anionic polymers.

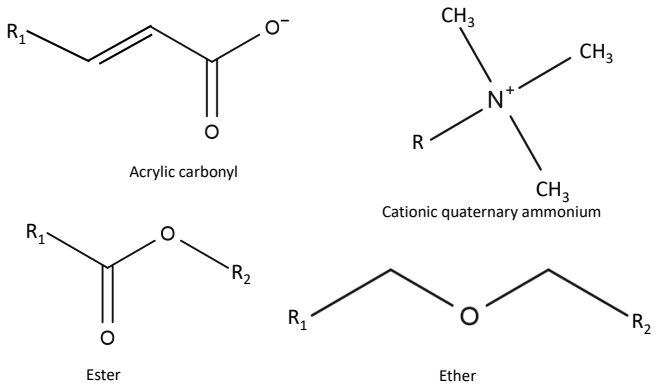

Figure 3.7: Functional groups identified from FTIR and NMR analysis.

Table 3.4: Peak ratios for functional groups determined from ^{13}C-NMR with the respective pK_a values

Polymer	Degree of charge	Acrylic acid	Acrylamide carbonyl	Ether
Chemical shift [ppm]		185-186	182, 44-45, 37	72
A1	Low	0.1	0.3	
A2	Low-medium	0.15	0.28	0.09
A3	Low	2.2	19.5	8
A4	Low	0.2	1	
		Cationic quaternary ammonium	Acrylamide carbonyl	Ester
Chemical shift [ppm]		53.9-56.3	179-182, 41.5-/45, 34-37	175-177, 64.2
C1	Low-medium	1	1.4	0.4
C2	High	1	1.4	8.6
C3	Medium	1.53	0.4	2.62

3.4 Conclusions

The results of this work have shown that the complete BCP system achieves higher P removal when compared to coagulant alone and within shorter time frames (Figure 3.1 and 3.2). However, when cross-comparing the polymers it appeared that polymers C1 and C2 resulted in worse P removal than A1 and A2 (Figure 3.2). At varying polymer doses, overall performance did not deteriorate much even at doses as low as 0.01 mg/L

and therefore the general guidance on using doses of 1 mg/L cannot be supported (Figure 3.4). Nevertheless, P removal was dependent of polymer dose at a lower coagulant dose which indicated towards a mutual relationship between polymer and coagulant doses with potential to save on both chemicals.

When it comes to floc properties, higher polymer doses resulted in larger flocs, lower turbidity and lower fractal dimension values which points towards more open flocs that are potentially better at sweeping particles (Table 3.3). When looking at floc breakage rates, it appears that there might be an ideal floc size at which the floc strength is sufficient enough for achieving excellent P removal. Rather than being a precipitating agent, polymers seem to be acting as the connection between coagulant-wastewater flocs and the ballast particles. These flocs are much weaker compared to coagulant alone (0.8 FS) but strength does not seem to be the crucial factor for efficiency in wastewater treatment.

The guidance that can be taken from this work is that anionic polymers work best in high alkalinity wastewaters (>170 mg $CaCO_3$/L) when they are at doses below 1 mg/L and coagulant dose between 5-8 mg Fe/L which can achieve more than 90% P removal.

3.5 Acknowledgements

Funding for this study was gratefully received by Severn Trent Water. The authors also gratefully acknowledge the supply of polymers from Kemira, BASF and Goldcrest.

References

Anderson, N. J. and Priestley, A. J. (1983). “Colour and turbidity removal with reusable magnetite particles-V. Process Development”. *Water Research* 17.10, pp. 1227–1233.

Bache, D. H. and Gregory, R. (2007). *Flocs in Water Treatment*. 1st ed. London: IWA Publishing.

Bolto, B. A., Dixon, D. R., Gray, S. R., Chee, H., Harbour, P. J., Ngoc, L., and Ware, A. J. (1996). "The use of soluble organic polymers in waste treatment". *Water Science and Technology*. Vol. 34. 9 pt 5, pp. 117–124.

Bolto, B. and Gregory, J. (2007). "Organic polyelectrolytes in water treatment". *Water Research* 41.11, pp. 2301–2324.

Bratby, J. (2016). *Coagulation and Flocculation in Water and Wastewater Treatment - Second Edition*. Vol. 3. IWA Publishing.

DeBarbadillo, C., Shellswell, G., Cyr, W., Edwards, B., Waite, R., Mullan, J., and Mitchell, R. (2010). "Pilot Testing of Four Tertiary Phosphorus Removal Processes To Achieve Ultra-Low Phosphorus Limits At the Lakeshore WPCP in the Town of Innisfil , Ontario". *WEFTEC*. Black & Veatch, pp. 1–10.

Desjardins, C., Koudjonou, B., and Desjardins, R. (2002). "Laboratory study of ballasted flocculation". *Water Research* 36.3, pp. 744–754.

Dixon, D. (1991). "The sirofloc process for water clarification". *Water Supply* 9.1, S33–S36.

EU Water Framework Directive (2000). *2000/60/EC*.

Gasperi, J., Laborie, B., and Rocher, V. (2012). "Treatment of combined sewer overflows by ballasted flocculation: Removal study of a large broad spectrum of pollutants". *Chemical Engineering Journal* 211-212.2012, pp. 293–301.

Hook, G. and Ott, R. (2001). "The Ultimate Challenge for Technology: 0.02 mg/L effluent total phosphorus". *Proceedings of the Water Environment Federation* 2001.12, pp. 113–132.

Imasuen, E., Judd, S., and Sauvignet, P. (2004). "High-rate clarification of municipal wastewaters: A brief". *Journal of Chemical Technology and Biotechnology* 79.8, pp. 914–917.

Jarvis, P., Jefferson, B., Gregory, J., and Parsons, S. (2005a). "A review of floc strength and breakage". *Water Research* 39.14, pp. 3121–3137.

Jarvis, P., Jefferson, B., and Parsons, S. A. (2005b). "Breakage, Regrowth, and Fractal Nature of Natural Organic Matter Flocs". *Environmental Science & Technology* 39.7, pp. 2307–2314.

Jarvis, P., Parsons, S. A., Henderson, R., Nixson, N., and Jefferson, B. (2008). "The practical application of fractal dimension in water treatment practice - the impact of polymer dosing". *Separation Science and Technology* 43.7, pp. 1785–1797.

Lee, R. M., Carlson, J. M., Bril, J., Cramer, J., and Harenda, J. (2015). "Pilot Testing Reveals Alternative Methods to Meet Wisconsin's Low Level Phosphorus Limits". *Proceedings of Annual WEFTEC- National Conference of WEF*, pp. 3238–3252.

Zi-li, H., Yue-hua, H., Jing, X., and Chun-hua, Z. (2004). "Removal of phosphate from municipal sewage by high gradient magnetic separation". *Journal of Central South University of Technology* 11.4, pp. 391–394.

Martin, B. D., Parsons, S. A., and Jefferson, B. (2009). "Removal and recovery of phosphate from municipal wastewaters using a polymeric anion exchanger bound with hydrated ferric oxide nanoparticles". *Water Science and Technology* 60.10, pp. 2637–2645.

Rabiee, A. (2010). "Acrylamide-based anionic polyelectrolytes and their applications: A survey". *Journal of Vinyl and Additive Technology* 21.2, pp. 111–119.

Ragsdale, D. (2007). *Advanced wastewater treatment to achieve low concentration of phosphorus*. Tech. rep. Seattle: US EPA.

Yeoman, S., Stephenson, T., Lester, J. N., and Perry, R. (1988). “The removal of phosphorus during wastewater treatment: A review”. *Environmental Pollution* 49.3, pp. 183–233.

Chapter 4

Reactive media constructed wetland for phosphorus removal: Assessing the opportunity and challenges

Olga Murujew[1], Kristell Le Corre Pidou[1], Andrea Wilson[2,3], Peter Vale[2], Bruce Jefferson[1], Marc Pidou[1,*]

[1] Cranfield University, College Road, Cranfield, Bedfordshire, MK43 0AL, UK

[2] Severn Trent Water, 2 St Johns Street, Coventry, CV1 2LZ, UK

[3] Atkins Global, Woodcote Grove, Epsom, Surrey, KT18 5BW, UK

[*]Corresponding author: m.pidou@cranfield.ac.uk

Abstract

Reactive media present an alternative to gravel in constructed wetlands and have potential to sustainably and efficiently remove P from wastewater. In this study a full-scale steel slag wetland has been operated for its whole lifecycle at which 1.39 mg P/g media were retained. During its lifecycle, this wetland met strict consents

below 0.5 mg P/L for the first 6 months and was operated for 266 and 353 days before the effluent P concentration rose above the typical P consents of 1 and 2 mg P/L, respectively. P removal appears to be impacted not only by calcium concentrations and pH but also temperature and precipitation of other competing minerals such as calcium carbonate. Ultimately, the current study has indicated that current description of the use of reactive media requires amendment to account for the greater complexity that is observed in real systems.

Keywords: Steel slag, reactive media, constructed wetland, P removal

4.1 Introduction

Wastewater treatment in rural areas usually consists of passive or low maintenance processes, such as trickling filters, rotating biological contactors and/or constructed wetlands. However, these have limited ability to remove phosphorus (P) to the low levels (≤1 mg/L) that will be required from the newly implemented Water Framework Directive (WFD) (EU Water Framework Directive 2000). Therefore, alternative options that can remove P whilst maintaining the low maintenance and chemical inputs in an economically viable way are highly desired. Adaptation of constructed wetlands (CW) using reactive media to replace gravel has been investigated in this regard due to the media's ability to remove P from wastewater through precipitation and adsorption mechanisms (Vohla et al. 2011). Comparison of the media previously tested indicates that those rich in Ca/CaO, such as slags, show higher P retention capacities than the alternative media. Particular attention has been given to blast oxygen furnace (BOF) slags which are a waste material from steel making and hence offer a solution aligned to circular economic thinking.

Previous research into the use of steel slag has involved a range of scales from laboratory to pilot trials (0.98-6000 L) operating across a wide range of contact times (empty

bed contact time, EBCT = 3-226 hours) and treating predominately synthetic wastewater with only a few studies using real wastewater (Table 4.1). The media size used (0.1-50 mm) and the initial phosphorus concentration (2.3-300 mg/L) also vary widely making comparison between these different studies difficult (Johansson Westholm 2006; Vohla et al. 2011). For instance, reported P retention capacities ranged for not saturated media from 0.085 mg P/g media (Hussain et al. 2015) up to >10.52 mg P/g media (Dunets et al. 2015) and the highest reported value for saturated media was 3.1 mg P/g media (Blanco et al. 2016). A study comparing samples from 10 European production sites revealed basic oxygen furnace slag (BOF) to deliver a higher phosphorus retention of 2.49 mg P/g media compared to 0.28 mg P/g media for electric arc furnace slag (EAF) (Barca et al. 2012). Further, the study showed that the samples from the different sites lead to variation in performance as illustrated in the range of retention capacity for BOF between 1.14 and 2.49 mg P/g media. To date, there has been one reported trial with real wastewater in a pilot constructed wetland with BOF where performance was greatly reduced relative to that reported for synthetic trials (Barca et al. 2012). The other large scale, long term study, utilised melter slag which removed 70% of the incoming phosphorus for five years when operating at a 7-day EBCT. Thereafter, performance deteriorated reaching a final retention capacity of 1.23 mg P/g media (Shilton et al. 2006).

A number of the studies have proposed potential mechanisms by which the phosphorus is removed. They all indicate the predominant mechanism is calcium oxide dissolution followed by calcium phosphate precipitation resulting in the formation of hydroxyapatite (Figure 4.1; (Barca et al. 2012; Claveau-Mallet et al. 2018)). In addition, adsorption onto the formed hydroxyapatite (HAP) and ligand exchange with metal hydroxides have been identified but are assumed to be relatively minor. However, the experiments leading to the proposed mechanisms were conducted in synthetic waters with elevated phosphorus concentrations, potentially generating misrepresentative findings (Molle et al. 2003). The

role of plants in P removal can be neglected as only one of the 9 compared studies on BOF slag had a wetland with plants (Table 4.1).

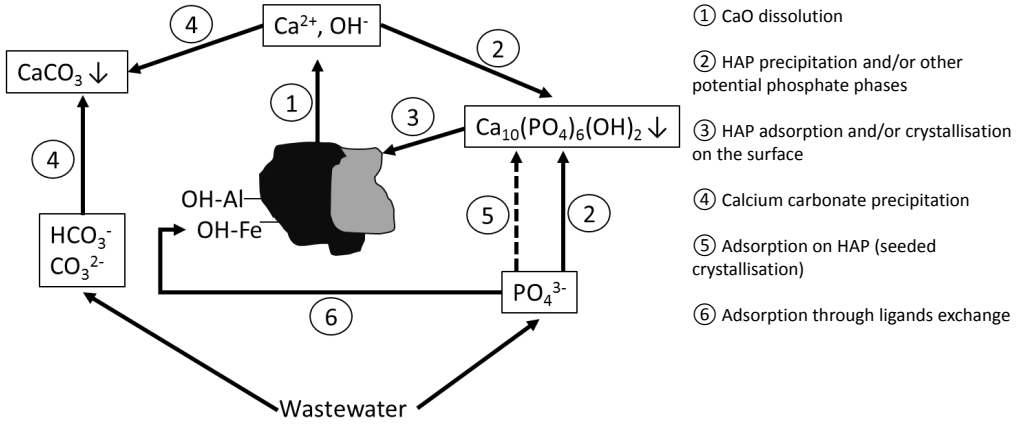

Figure 4.1: Proposed mechanisms based on literature. Adapted from Barca et al. (2012).

Accordingly, there is need to examine the performance of BOF slag under realistic scales and conditions to establish the potential for the technology to be used at full scale and to validate the proposed mechanisms. The current paper aims to achieve this through examination of a full scale constructed wetland containing BOF slag (from a source not previously reported on) treating realistic conditions on wastewater characteristics and phosphorus concentrations. The study lasted for 782 days and included examination of the effluent quality, mineralogical properties of the media and the impact on the reed development. To the authors knowledge this is the largest and longest reported study on using BOF slag for phosphorus removal in constructed wetlands.

Table 4.1: Recent studies on BOF slags in continuous operation. Where possible, retention times were converted by the authors to EBCT for ease of comparison.

Set-up	Particle size [mm]	Scale and Volume	Type of wastewater	Influent P [mg P/L]	P capacity [mg P/g media]	Alkalinity [mg Ca/L]	EBCT [h]	Operation [days]	Reference
BOF HSSF	8-14	Full (60 000 L)	RWW	6-11	1.39^{s}	178.08	24-48	782	This study
40% BOF, 60% sand downward flow column	0.39-2.38	Lab (min 0.75 L)	SWW	60	$>10.52^{ns}$	<50	55	250	(Dunets et al. 2015)
40% BOF, 60% sand downward flow column	0.39-2.38	Lab (min 0.75 L)	SWW	60	$6.17\text{-}8.78^{ns}$	<50	7	31	(Dunets et al. 2015)
BOF column	20	Lab	SWW	100-300	8.39^{ns}	NA	8h HRT	306	(Bowden et al. 2009)
BOF downward flow column with gravel at top/bottom	0.1-10	Lab (3.4 L)	SWW	15	3.1^{s}	NA	3	213	(Blanco et al. 2016)
BOF HSSF	6-12	Pilot (42 L)	SWW	9-12	1.05^{ns}	140	70	364	(Barca et al. 2014)
BOF HSSF	20-50	Pilot (84 L)	SWW	9-12	1.01^{ns}	140	70	364	(Barca et al. 2014)
BOF HSSF (after two-stage VF)	20-40	Pilot (6000 L)	RWW	4.4-11	0.61^{ns}	282	44	700	(Barca et al. 2013)

Continued on next page

Table 4.1 – continued from previous page

Set-up	Particle size [mm]	Scale and Volume	Type of wastewater	Influent P [mg P/L]	P capacity [mg P/g media]	Influent alkalinity [mg Ca/L]	EBCT [h]	Operation [days]	Reference
Rapid cooled BOF (25%) and 75% sand HF	NA	Pilot (8 L)	RWW	11.8	0.151	NA	226 (9 days)	196	(Park et al. 2017)
Rapid cooled BOF HF	NA	Pilot (8 L)	RWW	11.8	0.146	NA	226 (9 days)	196	(Park et al. 2017)
50% BOF and 50% gravel downward flow cell	0.5-4	Pilot 13 200 L	RWW	5-10	0.085^{ns}	298	14 days	248	(Hussain et al. 2015)
BOF column	20	Lab	SWW	1-50	NA	NA	4-22h HRT	406	(Bowden et al. 2009)
50% silica sand, 45% limestone, 5% BOF column	0.84	Lab	SWW	3.3	NA	23.8 (effluent)	90	1460	(Baker et al. 1998)
BOF saturated SAT column	1-2	Lab (0.98 L)	RWW	2.3	NA	NA	123 (5 days)	NA	(Cha et al. 2006)
BOF (50%) and soil (50%) saturated SAT column	1-3	Lab (0.98 L)	RWW	2.3	NA	NA	123 (5 days)	NA	(Cha et al. 2006)
BOF (50%) and soil (50%) unsaturated SAT column	1-3	Lab (0.98 L)	RWW	2.6-3.4	NA	NA	55	NA	(Cha et al. 2006)

Continued on next page

Table 4.1 – continued from previous page

Set-up	Particle size [mm]	Scale and Volume	Type of wastewater	Influent P [mg P/L]	P capacity [mg P/g media]	Influent alkalinity [mg Ca/L]	EBCT [h]	Operation [days]	Reference
BOF (25%) and soil (75%) unsaturated SAT column	1-4	Lab (0.98 L)	RWW	2.6-3.4	NA	NA	55	NA	(Cha et al. 2006)

RWW: Real wastewater, SWW: Synthetic wastewater, HSSF: Horizontal subsurface flow wetland, SAT: soil aquifer treatment, s: saturated, ns: not saturated

4.2 Materials and Methods

A full scale horizontal sub-surface flow wetland filled with BOF steel slag media (99,600 kg, d= 8-14 mm, Lafarge Tarmac Trading Ltd, UK) has been operated for 782 days at a sewage treatment works in Leicestershire, UK. The wetland was built according to a typical tertiary design in the UK on a surface area of 100 m^2 (width: 8 m, length: 12.5 m) and 0.6 m depth. The bed was planted with *Phragmites australis* at 4 plants/m^2 which were not harvested throughout the trial. The influent was fed from the effluent of secondary clarifiers and P was supplemented to an influent P concentration of 5.8-9.5 mg P/L (Table 4.2). This would simulate the P concentration in a small sewage treatment works with no or limited P removal where a wetland would normally be installed. The bed was operated at a flow rate of 0.35-0.7 equating to an EBCT of 24-48 hours.

Table 4.2: Wetland influent characteristics

	COD [mg/L]	Total P [mg/L]	ortho-P [mg/L]	Suspended solids [mg/L]	Ca^{2+} [mg/L]	Alkalinity [mg/L]	pH	Fe^{3+}[mg/L]
Average ± Standard deviation	21.25 ± 2.77	7.68 ± 0.95	7.63 ± 1.83	7.27 ± 3.42	60.66 ± 12.33	178.08 ± 16.34	7.42 ± 0.17	0.05 ± 0.07
Number of samples (n)	78	80	122	76	73	15	79	55

4.2.1 Water analysis

Online monitoring was set in place at the wetland influent and effluent for ortho-P, Fe^{3+}, pH, turbidity, flow rate and temperature (influent only). Additional weekly grab samples were taken for analysis of P and COD fractions (solid, colloidal, dissolved), total P (TP), total suspended solids (TSS), conductivity, pH, turbidity, ammonium (NH_4^+-N) and metals[1]. The online analysis of P and Fe was conducted according to colorimetric

[1]Metals that were measured: Ca, Mg, Fe, Al, Si, V, Ti, Cr, Ni, Cu, Zn, As, Se, Ag, Cd, Pb, Hg

techniques at 15 minutes intervals (ABB online analysers, UK). Turbidity and pH were analysed with online sampling probes at 1-minute intervals (Hach, UK). The additional samples were analysed with cell tests according to colorimetric methods for P, COD, Fe and NH_4^+ (Hach, UK). Fractions for P and COD were divided into unfiltered and filtration through 1.2 µm and 10 kDa representing solid, colloidal and dissolved fractions, respectively. Suspended solids were measured according to standard methods. Turbidity was measured with a turbidimeter (Hach 9100, UK) and pH/conductivity were measured with a handheld probe meter (VWR, UK). Metals were analysed with ICP-MS (Perkin-Elmer, UK).

4.2.2 Hydraulic assessment

To assess the change of retention time and possible clogging within the bed tracer tests were conducted by injecting a pulse of a known weight of Rhodamine-WT (Keystone, UK) and measuring the concentration of the chemical in the effluent with a rhodamine detector probe (YSI, Xylem, UK) over a duration of 2 days.

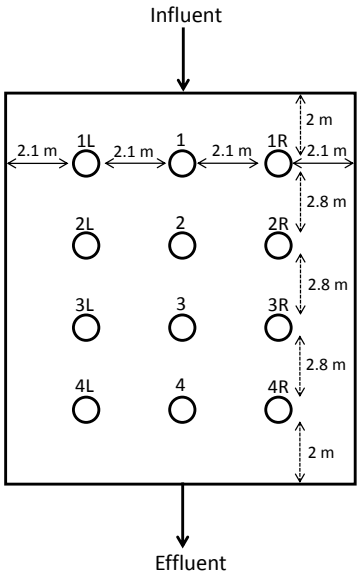

Figure 4.2: Layout of sampling points for samples for SEM/EDX and sequential P extraction

4.2.3 Media and visual plant analysis

Photographs of the wetland appearance were taken weekly to monitor visual change of plant growth over time and with the seasons. Rainfall and ambient temperature have been monitored on site with a weather station.

Sequential P extraction experiments were carried out with steel slag samples following the method described by Letshwenyo (2014) using 1M NH_4Cl, 0.1M NaOH, 0.5M $NaHCO_3$, 1M HCl and concentrated HCl to desorb loosely bound P, Al bound P, Fe bound P, Ca bound P and P in stable residual pools, respectively. Samples of fresh, un-used slag and exhausted slag at the end of the trial were analysed. Fresh steel slag samples were divided into un-used (FU) and washed (FW), i.e. washed three times with 25 mL DI water and air dried for 3 days. The exhausted slag samples were taken from four points in the direction of flow (Figure 4.2). All slag samples (1 g each) were air dried for 24h before commencement of the procedure, shaken for 24h in each extraction solution and washed with 25 mL supersaturated NaCl in-between steps. Analysis was conducted with respect

to 0.45 µm filtered TP measurements. Solutions were also analysed for their metal content and the sum from each extraction solution was taken as the value of total extracted metal.

4.2.4 Precipitation potential

Since precipitation of minerals depends on supersaturation, calculation of saturation indices (SI) values was used to ascertain the possible precipitate that could form (Gustafsson 2016; Stumm and Morgan 1996). The potential for various mineral compounds to precipitate within the constructed wetland was predicted by calculating their SI with Visual MINTEQ version 3.1 (Gustafsson 2016). The SI, which is the ratio of the ion activity product (IAP) of a given mineral by its solubility product (Equation 4.1) provides information on the level of saturation of a given mineral in solution.

$$SI = \frac{[IAP]}{[K_{\mathrm{sp}}]} \tag{4.1}$$

- If SI<0, the solution is undersaturated, and the mineral can dissolve. No precipitation occurs;
- If SI = 0, the solution and mineral are at equilibrium, the solution is saturated with the mineral;
- If SI>0, the solution is supersaturated with respect to the given mineral and precipitation can occur spontaneously.

SI values have been calculated at multiple points (trial days 33, 121, 210, 253, 266, 329, 342, 352, 366, 406, 504, 581, 608, 685 and 749) throughout the trial period. Only minerals with predicted positive SI values have been considered here because these indicate saturation with respect to the mineral. The parameters used to predict the SI included water temperature, pH, calcium, ortho-P, magnesium, vanadium, aluminium, iron, silica,

titanium, alkalinity and NH_4-N. Results from sampling were used as input data and were chosen at dates throughout the whole trial period. It should be noted that, as most of the above parameters could not be measured within the system, maximum ions concentrations and pH values between the influent and effluent of the wetland were used, assuming these would be the concentrations that would at least be measured within the system.

4.3 Results and Discussion

4.3.1 Treatment performance

The reactive media constructed wetland met consents of below 0.5 mg P/L for the first 6 months and was operated for 266 and 353 days before the effluent P concentration rose above the typical P consents of 1 and 2 mg P/L, respectively. During the 782 days of the trial, four distinct phases were identified based on observations of major changes in the effluent P, which lasted for about 6 months each (Figure 4.3).

In *phase* 1 (days 1 to 209, P load from 0 to 0.47 mg P/g slag), the system achieved almost complete P removal with an effluent phosphorus concentration around 0.05 mg P/L (the detection limit). This coincided with a stable elevated pH of between 11 and 12 and a net calcium release of between 35 and 37 mg/L (Figure 4.3a and 4.3b). Such conditions are consistent with rapid dissolution of calcium oxide and subsequently precipitation of the released calcium (Johansson and Gustafsson 2000; Song et al. 2002). Towards the end of this phase of operation the net calcium levels became negative indicative of continued precipitation and growth exceeding the rate of calcium release from the media and so utilising calcium from the incoming wastewater. In addition, other compounds were observed to be released from the media (Figure 4.3b). Most important is the metal vanadium which re-

sulted in effluent concentrations of between 0.35 to 0.7 mg/L compared to an influent level that remained below 1 µg/L throughout. Vanadium is not routinely consented against as it is not expected to be in wastewater. However, potential limiting values around 60 µg/L have been discussed during other reported trials (Fonseca 2017). Accordingly, vanadium leaching from the media poses a non-compliance concern if being considered for operational use. During this phase substantial inhibition of reed development was observed due to competition with a weed identified as *Epilobium hirsutum* (Figure C.2). The plant is known to grow preferably in alkaline conditions whereas the reeds seemed to have stayed dormant until the pH reached an acceptable level below 9 (Figure 4.3a) (Al-Farraj et al. 1984; Pérez-Fernández et al. 2006; Yin et al. 2016). At the back end of the bed no growth was observed.

In *phase* 2 (days 209 to 400, P load between 0.47 and 1.01 mg P/g slag), the EBCT was decreased from 48h to 24h which corresponded to a gradual increase in the effluent P up to 1.96 mg P/L. On day 278 (equivalent to 0.73 mg P/g slag[2]), the EBCT was reverted to 48 hours but interestingly, the effluent P concentration continued to increase to reach a maximum of about 2.24 mg P/L after a P load of 1.01 mg P/g slag (400 days of operation). In parallel, pH in the effluent decreased to values of 8.60-8.73. The initial increase in effluent phosphorus concentration when the contact time was decreased is consistent with previous trials (Barca et al. 2013) although the continued increase when the contact time was reverted back was not expected based on the previous reported trials. The deterioration in removal performance coincided with an increase in the net calcium levels up to a maximum of 16 mg/L and a decrease in the corresponding levels of vanadium which decreased down to below 100 µg/L on average across this phase of the trial. In addition, the effluent P increased, especially after a P load of 0.73 mg P/g slag, coinciding with a

[2]Note: The P retention capacity of 0.73 mg P/g slag at this time already exceeded the final reported capacity by Barca et al. (2013) (Table 4.1).

drop-in temperature from 15°C to 9.5°C suggesting temperature as another impacting parameter on P removal (Figure 4.3b and 4.4b). In comparison, Blanco et al. (2016) reported a pH drop from 12 to 7 until a P load of 4.3 mg P/ g slag was reached. The link between pH and removal has been verified in laboratory trials where steel slag particles have been soaked in sodium hydroxide and showed a significant reduction in P uptake below a pH of 8 (Park et al. 2017). Overall, this phase is indicative of the precipitate coating the media restricting the rate of dissolution. Importantly, the pH and removal remained, albeit at a reduced level to phase 1, indicating that dissolution had slowed and not stopped. During this phase, the weed *Epilobium hirsutum* had overgrown the reeds up to the middle of the bed. At the back of the bed, both reeds and the weed sustained with little growth (Figure C.2).

In *phase* 3 (days 401-600, P load between 1.01 and 1.44 mg P/g slag), the performance was relatively stable with the pH remaining between 8.7 and 9.3 and the effluent P slowly decreasing from 2.76 to 1.24 mg P/L. This change coincided with an increase in the water temperature from 11 to 20°C (Figure 4.3c). Net releases of calcium and vanadium were consistently below 23 and 0.1 mg/L, respectively suggesting a slow but steady release from the media (Figure 4.3b). This indicates a stable period where reasonable P removal can occur, and this is thought to be mainly associated to growth or adsorption onto the precipitate that had previously formed. During this phase, plant growth of reeds increased at the back of the bed and weed growth at the front and middle started to cease (Figure C.2).

In *phase* 4 (days 601 to 782, P load between 1.44 and 1.86 mg P/g slag), the pH was stable with values between 8.89-8.67 and both the calcium and vanadium concentrations remained unchanged compared to phase 3. In contrast, significant difference was observed in relation to the effluent phosphorus concentration which increased up to a maximum of 7.33 mg P/L after 721 days of operation which meant nearly no P removal. From that

point on, the effluent P concentration decreased rapidly again to reach a value of about 5.04 to 5.43 mg P/L at the end of the trial (782 days of operation, P load of 1.86 mg P/g slag) (Figure 4.3a). It should be noted that the influent P concentration was found to fluctuate significantly over this last period with spikes up to 12 mg P/L. Fractionation of the effluent phosphorus revealed that the majority existed as dissolved phosphate denoting that it is unreacted or had desorbed (Figure 4.3c). As in phase 3, the changes appeared to coincide with temperature changes congruent with previous reports of seasonal impacts (Figure 4.4b) (Barca et al. 2013; Herrmann et al. 2014; Shilton et al. 2006). The respective authors have associated the changes to either temperature dependent P removal mechanisms, due to increasing growth of alga raising the pH (Shilton et al. 2006) or the change in the solubility of calcium phosphate with temperature (Barca et al. 2013; Herrmann et al. 2014). This is supported by the fact that the reaction of calcium and phosphate is endothermic which means that the chemical equilibrium would be shifted towards the product side (calcium phosphate precipitates) at higher temperatures and result in higher P removal (Stumm and Morgan 1996). During this phase of operation, most plant growth ceased at the front of the bed and the reeds were established from the middle to the back of the bed (Figure C.2).

The reactive media were observed to also impact on other metals in the wastewater with iron, zinc, nickel, copper, arsenic, silver, cadmium and lead levels reduced by 84%, 35%, 18%, 22%, 41%, 71%, 52% and 15%, respectively. This occurred despite their low initial concentration (on average $<$0.2 mg Fe/L and $<$0.027 mg/L all other metals) and indicates that other precipitates may have been formed other than calcium phosphate. To illustrate, iron fluctuated throughout the whole trial duration with maximum releases and uptakes of 0.47 mg/L and 0.36 mg/L (Figure C.1). An uptake of zinc up to 56.9 µg/L was recorded in phase 1 and 3 while release up to 35.7 µg/L was observed in phase 2. In phase 1, a maximum copper uptake up to 21.7 µg/L was recorded while in phase 2 a release of

3.8 µg/L was noted. For arsenic, most variations were observed in phase 4 with fluctuations between 40.7 µg/L uptake and 40.9 µg/L release. At the end of phase 1 and at the beginning of phase 2 (between days 188 and 265), a silver uptake of 10.52-38.8 µg/L was recorded. For cadmium and lead, uptakes up to 1.8 µg/L and 0.8 µg/L occurred in phase 1 and in phase 2, releases up to 0.32 µg/L and 0.51 µg/L were observed for cadmium and lead, respectively. With metal releases and uptakes varying throughout the phases, the complexity and abundance of possible reactions in the bed is highlighted.

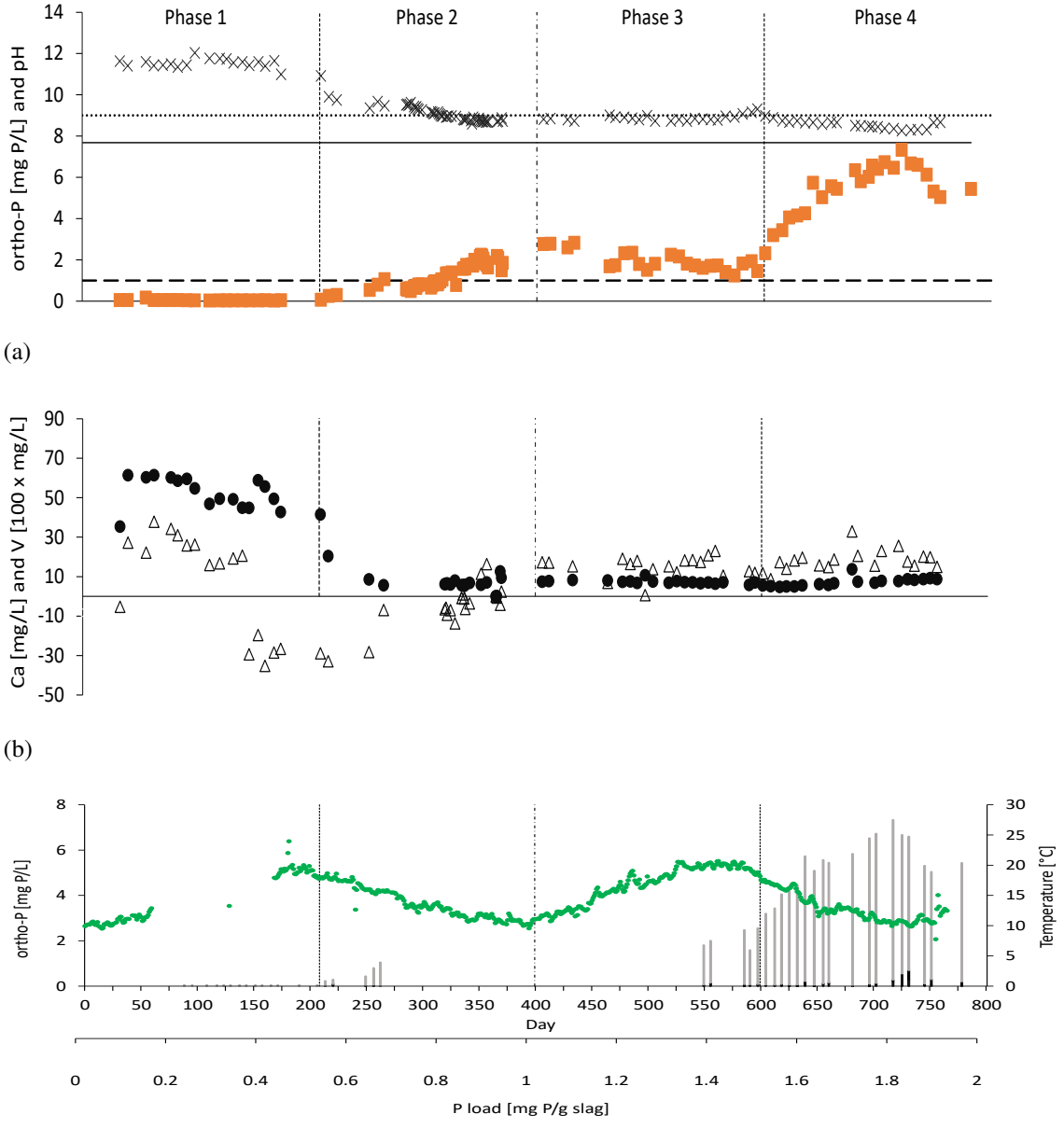

Figure 4.3: Overview of main measured parameters during the whole period of operation. Changes in flow rate (and EBCT) were from 48h to 24h EBCT on day 209 and from 24h to 48h on day 278. (a) Average influent P (—, 7.63 ± 1.83 mg/L), acceptable maximum pH for effluent discharge (·····), target effluent P (– – –), effluent P (■) as ortho-P in mg P/L and effluent pH (x). (b) Release of calcium (△) and vanadium (●). (c) Effluent P fractions: Particulate P (■) and dissolved P (■) and water temperature (●).

Further analysis of the link between pH and effluent phosphorus concentration revealed a decreasing trend (Figure 4.4a). Between pH 10 and 12, effluent P was stable below 0.25 mg/L and with decreasing pH from 10 to 8.3, the effluent P increased nearly exponentially. Overall, it suggests that an effluent phosphate concentration below 2 mg/L only occurred when the pH was above 9. Below this level, the effluent phosphorus concentration changed significantly. In contrast, Park et al. (2017) reported an ideal pH of >8 for P removal above 80% using steel slag which is consistent with the reported optimum pH range of 8-9.5 for calcium phosphate precipitation when the phosphorus concentration is below 5 mg P/L (Kim et al. 2006). The difference in the current dataset suggests a change in removal pathway and a possible P removal mechanism related to adsorption of phosphate to other precipitates (Giannimaras and Koutsoukos 1987). Further, if all removed P is assumed to have reacted to $Ca_5(PO_4)_3OH$, a stable pH between 10.06-11.1 can be predicted for the whole operational time. This only coincides with the actual measured pH in phase 1 suggesting that this might be the main P removal mechanism in that phase but not the subsequent ones.

Importantly, much of the previous work has been conducted in synthetic solution and in the absence of carbonates. In the current case, the wastewater had an alkalinity of 178.1 ± 16.3 mg/L suggesting a relative abundance of carbonates over phosphate. Accordingly, it is suggested that significant proportions of the precipitate are likely to be calcium carbonates. This was confirmed through SEM/EDX analysis of precipitates formed from a wash-out during commissioning when no P was supplemented to the influent (data not shown) and more importantly during analysis of the media taken from the bed (Le Corre Pidou and Jefferson 2019). In fact, in a study by Song et al. (2008) an adverse impact of carbonate ions on calcium phosphate precipitation has been shown at pH 8 which, however, became negligibly small at more alkaline conditions (pH$\geq$9) showing that the pH is a key contributor. It is likely that lower P removal was not only caused by the pH decrease

but also by less Ca^{2+} availability. The latter may have favoured $CaCO_3$ over calcium phosphate precipitation. For instance, Liira and Kõiv (2009) suggested that a doubling of retention time in shale ash columns resulted in supersaturation with respect to calcium carbonate. Despite being different media, steel slag and shale ash are both calcium-rich materials and it can be expected that the comparably high EBCT of this wetland (48h during most of the study) did have an impact on calcium carbonate precipitation. Finally, these results highlight the need to monitor and understand the impact of carbonates on P removal and reactive media performance.

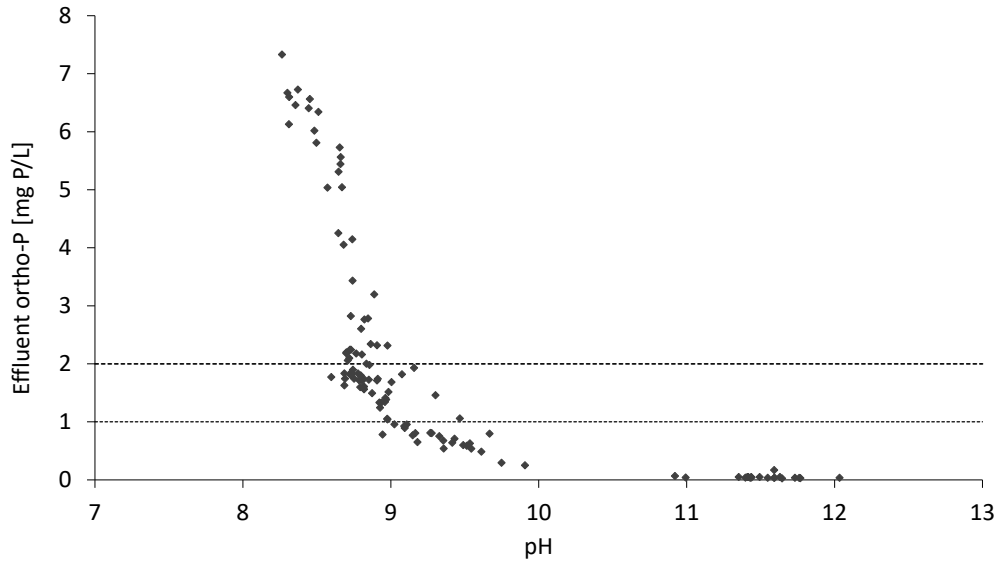

(a)

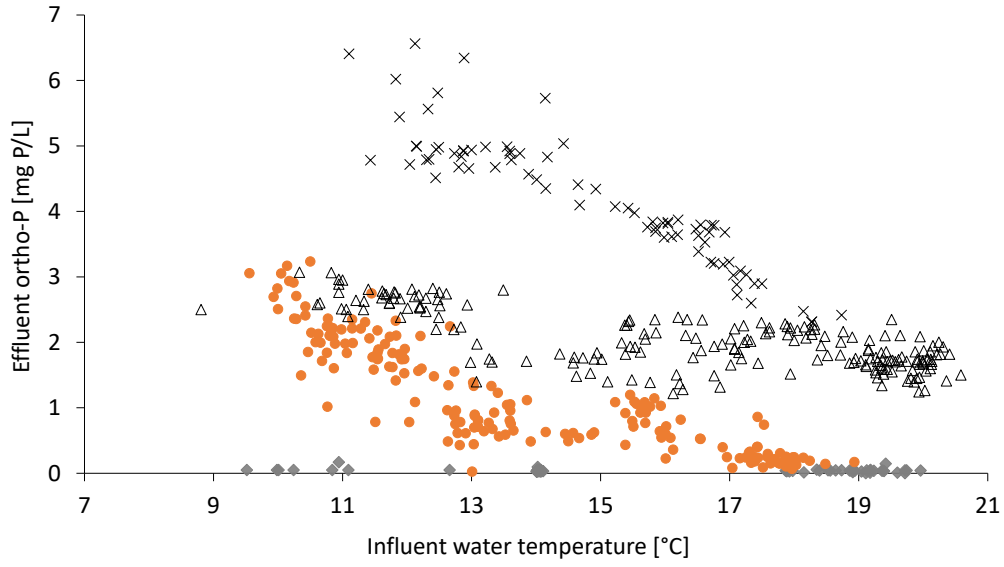

(b)

Figure 4.4: Correlation of (a) effluent P with pH and (b) Effluent P with temperature in phase 1 (◆), phase 2 (●), phase 3 (△) and phase 4 (X).

Further analysis of the media by sequential extraction supported the notion that reactions other than calcium phosphate precipitation were occurring. Compared to fresh slag increases predominantly associated with the stable residual pool, iron bound and loosely bound fractions were observed with overall decrease associated with calcium bound P (Figure 4.5). To illustrate, the iron bound fraction increased from 2% in the fresh media to between 8% and 40% in the used samples. Equivalent changes in the stable residual pool saw an increase from between 0.2% and 0.7% to between 14% and 21%. This suggests that more consideration should be given to the P removal through other mechanisms such as incorporation into other minerals, such as iron based ones, or adsorption.

By the end of the trial, the media had a phosphorus retention capacity of 1.39 mg P/g media (Figure 4.6). Of the available literature only four studies provided higher overall P capacity but all were at significantly smaller scale ($<$3.4 L), synthetic wastewater as feed and high influent P concentrations ($>$15 mg/L). Compared to the more realistic trials, the P retention capacity of this study was the highest reported to date (Table 4.1). At a P load of 1.07 mg P/g media, Barca et al. (2014) reported a slightly higher P retention capacity which may be due to the longer retention time in their system and the use of synthetic wastewater feed. Interestingly, when comparing a trial with real wastewater at similar P load (1 mg P/g media), the current study had an about 1.3 times higher retention capacity (Barca et al. 2013). The differences reflect the potential impacts of the media source, scale and media/wastewater characteristics. Ultimately, this means caution must be applied when translating data between studies, suggesting that pilot trials are critical in understanding the efficacy of reactive media to any specific site.

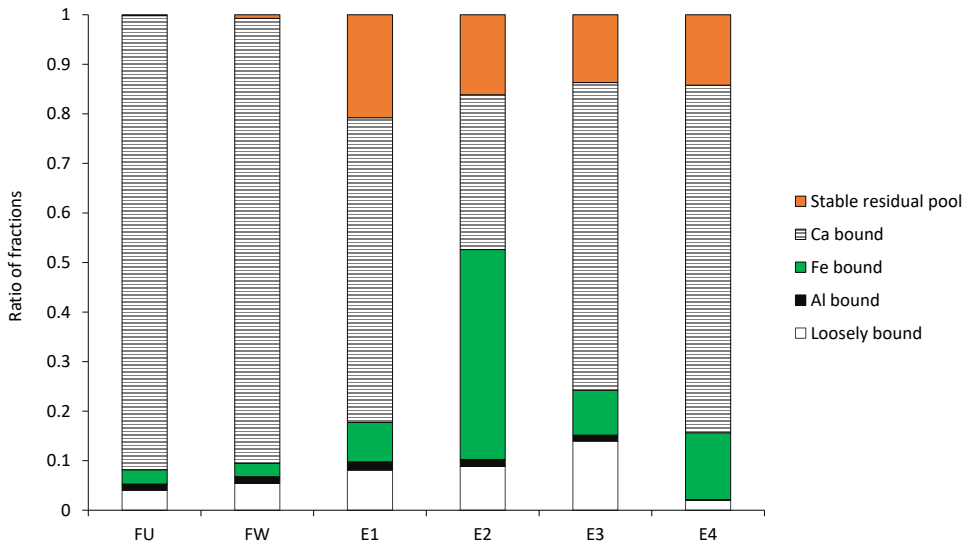

Figure 4.5: Sequential extraction of P bound fractions from fresh unwashed (FU), fresh washed (FW) and exhausted (E) slag from four intersectional points (E1, E2, E3, E4).

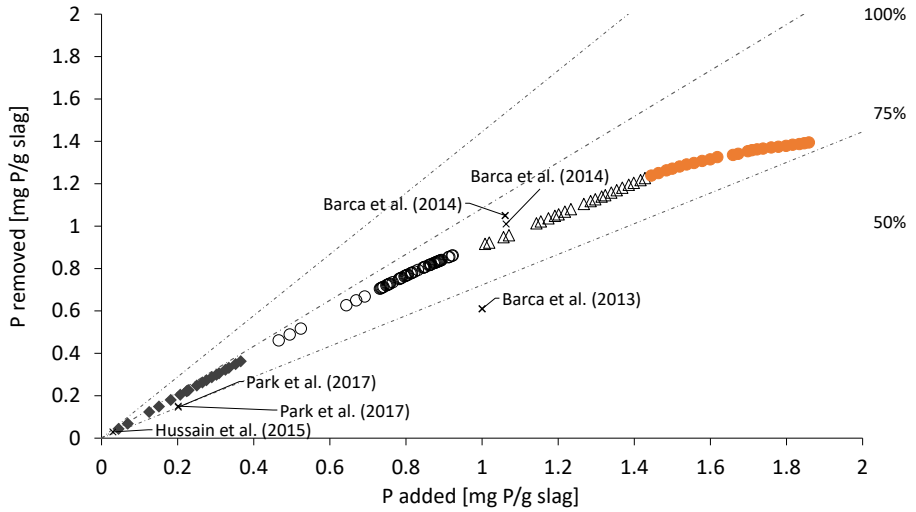

Figure 4.6: Cumulative added and removed P in the reactive media reed bed in Phase 1 (◆), Phase 2 (○), Phase 3(△) and Phase 4 (●) with comparison to literature (where data available). Diagonal lines represent 100%, 75% and 50% P removal.

4.3.2 Saturation indices

For each phase, potential supersaturation of 27 to 34 potential minerals has been identified (Table 4.3). The highest SI values (>5) were mainly obtained for ferric oxides and calcium phosphate compounds with hematite (α-Fe_2O_3), hydroxyapatite (HAP, $Ca_5(PO_4)_3$ OH), magnesioferrite ($MgFe_2O_4$), maghemite (γ-Fe_2O_3), goethite (α-FeO(OH)), lepidocrocite (γ-FeO(OH)), ferrihydrite ($Fe_2O_3 \cdot 0.5\ H_2O$) and Ca_3PO_4 (beta) which suggests more that P would only be removed in calcium based compounds (or adsorbed on Fe based compounds). As Fe concentrations were low in the influent and effluent, ferric phosphate formation was not assessed in this exercise, but the media analysis suggests that Fe was released into the bed and consequently could have contributed to the formation of ferric phosphates and consequently removal of P.

The fact that a big part of the predicted minerals are iron-based ones corresponds with the high amount of extracted iron from the media and with very low effluent concentrations this suggests that iron was trapped within the bed through precipitation and/or adsorption (Table 1.3). Iron oxides have their lowest solubility at neutral to alkaline pH (Kraemer 2004; Lindsay 1991). Therefore, it seems reasonable that alkaline conditions and iron availability from the media, as in this study, would contribute to the precipitation of iron minerals including iron phosphate-based compounds and consequently directly contribute to P removal. With the expected effluent pH being constantly above 10 but in reality decreasing (see previous section), it may be that minerals with “OH” fractions consumed some of the hydroxide from dissolving CaO, therefore contributing to a lower pH. This again highlights the need to have better understanding of the local reactions inside the bed to fully understand the mechanisms.

Table 4.3: Minerals returning a positive SI for Phases 1 to 4 and their respective solubility products at at 25°C (Baker et al. 1998; Hydrochemistry & Water Analysis 2018)

Mineral	Phase 1	Phase 2	Phase 3	Phase 4	pK_{sp} = -log K_{sp}
Hematite (α-Fe_2O_3)	15.48	19.194	19.79	19.46	87.95
Hydroxyapatite ($Ca_5(PO_4)_3OH$)	18.41	15.22	15.44	15.10	54.45
Magnesioferrite ($MgFe_2O_4$)	15.23	14.59	15.30	14.13	
Maghemite (γ-Fe_2O_3)	8.52	12.33	12.64	12.55	
Goethite (α-FeO(OH))	6.57	8.43	8.71	8.56	42.97
Lepidocrocite (γ-FeO(OH))	6.08	7.99	8.14	8.10	
Ferrihydrite (aged) ($Fe_2O_3 \cdot 0.5\ H_2O$)	4.11	5.94	6.31	6.08	
Ferrihydrite ($Fe_2O_3 \cdot 0.5\ H_2O$)	3.60	5.43	5.80	5.57	
$Ca_3(PO_4)_2$ (beta)	5.55	4.94	4.99	4.99	28.94
$Ca_3(PO_4)_2$ (am2)	3.95	3.24	3.60	3.34	
$Ca_4H(PO_4)3 \cdot 3\ H_2O$(s)	2.01	3.17	3.69	3.54	93.95
Chrysotile ($Mg_3(Si_2O_5(OH)_4)$)	12.73	3.10	3.07	1.60	
Dolomite (ordered) ($CaMg(CO_3)_2$)	2.78	2.11	2.23	1.61	17.09
Rutile (TiO_2)	1.57	1.82	0.04		
Kaolinite ($Al_2Si_2O_5(OH)_4$)		1.67	1.36	2.40	
Sepiolite ($Mg_4Si_6O_{15}(OH)_2 \cdot 6\ H_2O$	5.29	1.59	1.67	0.72	
Dolomite (disordered) ($CaMg(CO_3)_2$)	2.19	1.51	1.64	1.01	17.09
Strengite ($FePO_4 \cdot 2\ H_2O$)		1.43	1.52	1.98	26.4
Calcite ($CaCO_3$)	1.56	1.15	1.45	1.05	8.48
Huntite ($Mg_3Ca(CO_3)_4$)	1.91	1.12	0.86		
Aragonite ($CaCO_3$)	1.41	1.00	1.10	0.90	8.34
Sepiolite (A) $Mg_4Si_6O_{15}(OH)_2 \cdot 6\ H_2O$	3.02	0.87			
Diaspore (AlO(OH))		0.86	1.07	1.52	35.09
Vaterite ($CaCO_3$)	0.97	0.55	0.66	0.45	7.91
$Ca_3(PO_4)_2$ (am1)	1.16	0.44	0.81	0.54	
Quartz (SiO_2)		0.38	0.42	0.47	3.98
Magnesite ($MgCO_3$)	0.41	0.38	0.17		8.03
Gibbsite (C) α-$Al(OH)_3$		0.31	0.40	0.64	33.86
Imogolite ($Al_2SiO_3(OH)_4$)		0.19		0.72	
$CaCO_3 \cdot H_2O$(s)	0.22	0.09	0.11		7.33
$Al(OH)_3$ (soil)		0.08		0.32	31.17
$CaHPO_4$(s)		0.05	0.07	0.13	6.91
Halloysite ($Al_2Si_2O_5(OH)_4$)		0.04		0.61	
Chalcedony (SiO_2)		0.02	0.05	0.08	3.55

4.4 Concluding remarks

This study reports on the first long-term, full-scale BOF wetland operated with real wastewater in the UK. An ultimate retention capacity of 1.39 mg P/g media was observed with low effluent phosphorus concentration achieved for around 1 year of operation. The high removal efficiencies were associated with elevated pH and other trace metals inferring rapid dissolution form the media surface. Once this declined, removal also declined and became more responsive to temperature changes.

Ultimately, the experiences outlined from the current study identify some inconsistencies with previously reported studies and the associated mechanism of removal. Current predictions state that the main P removal mechanism is calcium phosphate precipitation with a potential phase transitioning from amorphous to crystalline at a later stage when P removal decreases. From the results in this study it can be assumed that calcium phosphate is one of the P removal mechanisms, but it was also suggested that also calcium carbonate as well as magnesium and iron minerals can precipitate as well, and these minerals may present adsorption sites for P. This highlights the complexity of the system when used under real condition and the need for continuous monitoring of precipitates and minerals inside the bed.

In this study, more P was retained by the bed than in other comparable studies. Especially when P removal deteriorated, factors -apart from pH and calcium concentration- such as temperature, carbonate and other ion concentrations appeared to impact the performance of the wetland. This highlights the need for trials in large scale and under real conditions to better understand the underlying mechanisms.

Overall, the results reported here demonstrate that the removal mechanisms and hence the performance of a steel slag constructed wetland are affected by a wide range of parameters, both operational and environmental, far more complex than often portrayed in

the literature. Ultimately, this emphasizes the need to develop a greater understanding of the different phenomena occurring locally on the media in order the fully understand and optimise the operation of such systems.

4.5 Acknowledgements

The authors gratefully acknowledge financial support from Severn Trent Water. In addition, some of the work reported here was part of the AquaNES project which has received funding from the European Union's Horizon 2020 research and innovation programme under grant agreement no. 689450.

References

Baker, M. J., Blowes, D. W., and Ptacek, C. J. (1998). "Laboratory development of permeable reactive mixtures for the removal of phosphorus from onsite wastewater disposal systems". *Environmental Science and Technology* 32.15, pp. 2308–2316.

Barca, C., Gérente, C., Meyer, D., Chazarenc, F., and Andrès, Y. (2012). "Phosphate removal from synthetic and real wastewater using steel slags produced in Europe". *Water Research* 46.7, pp. 2376–2384.

Barca, C., Meyer, D., Liira, M., Drissen, P., Comeau, Y., Andrès, Y., and Chazarenc, F. (2014). "Steel slag filters to upgrade phosphorus removal in small wastewater treatment plants : Removal mechanisms and performance". *Ecological Engineering* 68, pp. 214–222.

Barca, C., Troesch, S., Meyer, D., Drissen, P., Andreìs, Y., and Chazarenc, F. (2013). "Steel slag filters to upgrade phosphorus removal in constructed wetlands: Two years of field experiments". *Environmental Science and Technology* 47.1, pp. 549–556.

Blanco, I., Molle, P., Sáenz de Miera, L. E., and Ansola, G. (2016). "Basic Oxygen Furnace steel slag aggregates for phosphorus treatment: Evaluation of its potential use as a substrate in constructed wetlands". *Water Research* 89, pp. 355–365.

Bowden, L. I., Jarvis, A. P., Younger, P. L., and Johnson, K. L. (2009). "Phosphorus removal from waste waters using basic oxygen steel slag." *Environmental science & technology* 43.7, pp. 2476–2481.

Cha, W., Kim, J., and Choi, H. (2006). "Evaluation of steel slag for organic and inorganic removals in soil aquifer treatment". *Water Research* 40.6, pp. 1034–1042.

Claveau-Mallet, D., Boutet, É., and Comeau, Y. (2018). "Steel slag filter design criteria for phosphorus removal from wastewater in decentralized applications". *Water Research*.

Dunets, C. S., Zheng, Y., and Dixon, M. (2015). "Use of phosphorus-sorbing materials to remove phosphate from greenhouse wastewater." *Environmental technology* 36.14, pp. 1759–1770.

EU Water Framework Directive (2000). *2000/60/EC*.

Al-Farraj, M. M., Giller, K. E., and Wheeler, B. D. (1984). "Phytometric estimation of fertility of waterlogged rich-fen peats using Epilobium hirsutum L." *Plant and Soil* 81.2, pp. 283–289.

Fonseca, N. (2017). "Sustainable phosphorus removal with BOF steel slag and apatite: mechanisms and challenges". *AquaEnviro- Big P conference*. Manchester, 4th–5th July 2017.

Giannimaras, E. K. and Koutsoukos, P. G. (1987). "The crystallization of calcite in the presence of orthophosphate". *Journal of Colloid And Interface Science* 116.2, pp. 423–430.

Gustafsson, J. P. (2016). *Visual MINTEQ ver. 3.1*. Stockholm.

Herrmann, I., Nordqvist, K., Hedström, A., and Viklander, M. (2014). "Effect of temperature on the performance of laboratory-scale phosphorus-removing filter beds in on-site wastewater treatment". *Chemosphere* 117, pp. 360–366.

Hussain, S. I., Blowes, D. W., Ptacek, C. J., Jamieson-Hanes, J. H., Wootton, B., Balch, G., and Higgins, J. (2015). "Mechanisms of Phosphorus Removal in a Pilot-Scale Constructed Wetland/BOF Slag Wastewater Treatment System". *Environmental Engineering Science* 32.4, pp. 340–352.

Hydrochemistry & Water Analysis (2018). *http://www.aqion.de, Accessed on 26/6/2018.*

Johansson Westholm, L. (2006). "Substrates for phosphorus removal-potential benefits for on-site wastewater treatment?" *Water Research* 40.1, pp. 23–36.

Johansson, L. and Gustafsson, J. P. (2000). "Phosphate removal using blast furnace slags and opoka-mechanisms". *Water Research* 34.1, pp. 259–265.

Kim, E. H., Yim, S. B., Jung, H. C., and Lee, E. J. (2006). "Hydroxyapatite crystallization from a highly concentrated phosphate solution using powdered converter slag as a seed material". *Journal of Hazardous Materials* 136.3, pp. 690–697.

Kraemer, S. M. (2004). "Iron oxide dissolution and solubility in the presence of siderophores". *Aquatic Sciences* 66.1, pp. 3–18.

Le Corre Pidou, K. and Jefferson, B. (2019). *Management of reactive media for phosphorus removal*. Tech. rep. Cranfield Water Science Institute.

Letshwenyo, M. (2014). "Phosphorus removal in passive treatment technologies for tertiary wastewater treatment". PhD thesis. Cranfield University.

Liira, M. and Kõiv, M. (2009). "The phosphorus - binding capacity of hydrated Ca Ca- oil -shale ash : does longer retention time improve the process ?" *Dynamics and Control* 43.September, pp. 3809–3814.

Lindsay, W. L. (1991). "Iron oxide solubilization by organic matter and its effect on iron availability". *Iron Nutrition and Interactions in Plants: "Proceedings of the Fifth International Symposium on Iron Nutrition and Interactions in Plants", 11–17 June 1989, Jerusalem, Israel, 1989*. Ed. by Chen, Y. and Hadar, Y. Dordrecht: Springer Netherlands, pp. 29–36.

Molle, P., Liénard, A., Grasmick, A., and Iwema, A. (2003). "Phosphorus retention in subsurface constructed wetlands: Investigations focused on calcareous materials and their chemical reactions". *Water Science and Technology*. Vol. 48. 5, pp. 75–83.

Park, J., Wang, J. J., Kim, S., Cho, J., Kang, S., Delaune, R., and Seo, D. (2017). "Phosphate removal in constructed wetland with rapid cooled basic oxygen furnace slag". *Chemical Engineering Journal* 327, pp. 713–724.

Park, T., Ampunan, V., Maeng, S., and Chung, E. (2017). "Application of steel slag coated with sodium hydroxide to enhance precipitation-coagulation for phosphorus removal". *Chemosphere* 167, pp. 91–97.

Pérez-Fernández, M. A., Calvo-Magro, E., Montanero-Fernández, J., and Oyola-Velasco, J. A. (2006). "Seed germination in response to chemicals: effect of nitrogen and pH in the media." *Journal of Environmental Biology* 27.1, pp. 13–20.

Shilton, A. N., Elmetri, I., Drizo, A., Pratt, S., Haverkamp, R. G., and Bilby, S. C. (2006). "Phosphorus removal by an 'active' slag filter-a decade of full scale experience". *Water Research* 40.1, pp. 113–118.

Song, K.-G., Kim, Y., and Ahn, K.-H. (2008). "Effect of coagulant addition on membrane fouling and nutrient removal in a submerged membrane bioreactor". *Desalination* 221.1-3, pp. 467–474.

Song, Y., Hahn, H., and Hoffman, E. (2002). "Effects of solution conditions on the precipitation of phosphate for recovery A thermodynamic evaluation". *Chemosphere* 48, pp. 1029–1034.

Stumm, W. and Morgan, J. J. (1996). *Aquatic Chemistry: Chemical Equilibria and Rates in Natural Waters*. 3rd ed. Wiley-Interscience.

Vohla, C., Kõiv, M., Bavor, H. J., Chazarenc, F., and Mander, Ü. (2011). "Filter materials for phosphorus removal from wastewater in treatment wetlands-A review". *Ecological Engineering* 37.1, pp. 70–89.

Yin, X., Zhang, J., Hu, Z., Xie, H., Guo, W., Wang, Q., Ngo, H. H., Liang, S., Lu, S., and Wu, W. (2016). "Effect of photosynthetically elevated pH on performance of surface flow-constructed wetland planted with Phragmites australis". *Environmental Science and Pollution Research* 23.15, pp. 15524–15531.

Chapter 5

Recycling and reuse of alginate in an immobilised algae system

Olga Murujew[1], Rachel Whitton[1], Linhua Fan[2], Felicity Roddick[2], Bruce Jefferson[1], Marc Pidou[1,*]

[1] Cranfield University, College Road, Cranfield, Bedfordshire, MK43 0AL, UK

[2] RMIT University, GPO Box 2476, Melbourne 3001, Australia

[*]Corresponding author: m.pidou@cranfield.ac.uk

Abstract

A significant operational cost in the up-scaling of immobilised algae systems will be the gelling agent alginate. To reduce expenditure of this consumable a proof-of-concept is given for an alginate recycling method using sodium citrate as a dissolving agent. Using algae beads made from virgin and recycled alginate yielded comparable phosphorus removal rates from real wastewater. At lab-scale, an alginate recovery of 69.1% can be achieved which would result in a net operational costs reduction of 34%.

Keywords: Alginate, immobilised algae, reuse

5.1 Introduction

Tertiary P removal with algae is a promising development because it offers efficient and combined nutrient removal of nitrogen (N) and phosphorus (P) compounds (Infante et al. 2013; Liu et al. 2012). Algae technologies are divided into suspended and non-suspended systems and within those categories into open and enclosed to the environment. In suspended systems the algal biomass is free flowing either in a high-rate algal pond (HRAP) or a photobioreactor (PBR). Implementation into tertiary treatment systems remains challenging due to large footprint (HRAP), algal biomass separation (both) and treatment resilience (both) (Whitton et al. 2015). Switching to immobilised systems significantly reduces these issues with the algae either grown attached to a surface as a biofilm or immobilised as beads in a matrix of a polysaccharide such as alginate, carrageenan or chitosan (De-Bashan et al. 2010; Whitton et al. 2015).

Although the concept for immobilised algae reactors (IBRs) is still in its infancy, reports on small scale studies using different algal species and operational parameters have been published (Chevalier and Noüe 1985; Filippino et al. 2015; Mallick 2002; Vallero 2010). Immobilised algae systems are typically characterised by high algal concentrations of selected species without risk of cross contamination, leading to very short hydraulic residence times and hence small footprints which use artificial lights to enable effective treatment at all times (De-Bashan et al. 2010; Whitton et al. 2015). To illustrate, HRAPs are typically operated at hydraulic retention times (HRT) of up to 10 days; whereas immobilised algae reactors (IBR) can be operated at HRTs as low as 3 hours (Whitton et al. 2018). An advantage that all algae technologies share is the generation of a useful product, the algal biomass, which can be utilised as a protein biomass, a fertiliser or as an

energy crop for feeding into digestion to offset energy from the operation of the system (Ometto et al. 2014, 2013).

Accordingly, immobilised algae reactors are a promising technology not only for efficient nutrient removal but also when targeting sustainable alternatives with added value such as energy recovery. Research from lab to pilot scale has shown that effluent P concentrations of 0.1 mg/L can be achieved along with ammonia levels below 0.1 mg/L and nitrate below 0.5 mg/L (Whitton et al. 2016, 2018). Successful up-scaling of the IBR technology requires the development of an optimized reactor design and provision of infrastructure and logistics to produce algae beads at a large scale. Additionally, such an innovative technology needs to be cost competitive to conventional options and to date, no IBR operation at full-scale has been reported (Whitton et al. 2018).

The key component of the technology are the immobilised algal beads which are produced when a concentrated algal suspension is homogeneously mixed in a low concentrated sodium alginate solution. Droplets of this mixture are then continuously added to a curing solution, calcium chloride, in which the alginate solidifies forming algae beads. The gelation of alginate, as used in the algae beads production process, is based on an ion transfer of sodium and calcium ions and is generally described by the egg-box structure (Ching et al. 2017) (Figure 5.1). Previous studies have shown systems work as a batch process in relation to the beads such that they need replacing every 15-30 days representing a significant operating cost. In fact, a previous economic analysis revealed that if the beads where used once and then digested that the annual cost of beads would represent up to 85% of the total operating cost and would limit the economic attractiveness of the technology. However, the batch cycle is based on the algae and not the alginate and so it is posited that the alginate could be recovered and reused to significantly reduce the operating cost profile of the technology.

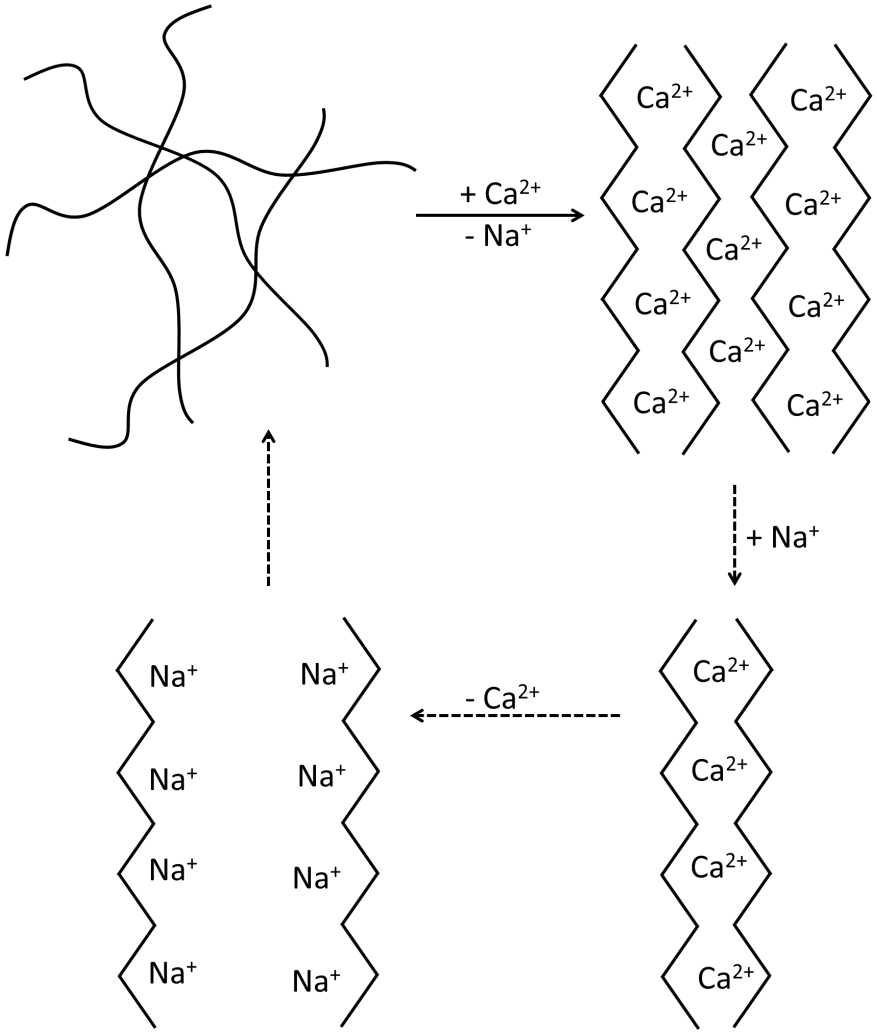

Figure 5.1: Egg-box model with expected ion transfer mechanism based on Ching et al. 2017.

Although Ca-alginate gel beads are insoluble in water, it has been known that dissolution is possible using compounds with strong attraction towards calcium ions, e.g. complexing agents like EDTA (Velings and Mestdagh 1995). The reaction was shown to be reversible by placing the beads in a sodium phosphate buffer solution at pH 7.4 returning the alginate back to its sodium form (Bajpai and Sharma 2004). Similarly, Qin et al. (2006) converted calcium alginate fibres to alginic acid and subsequently sodium alginate by using hydrochloric acid and sodium hydroxide, suggesting that the reaction may be a

simple ion exchange.

These publications, however, refer to a medical rather than a wastewater treatment context and do not include the utilisation of algae. Wastewater related research on alginate recovery has to date focused on its recovery from granular activated sludge (Van Der Hoek et al. 2016). Therefore, a practical method on alginate recycling from immobilised algae beads is still lacking and will be presented in this work. The aim is to give a proof-of-concept for a practical alginate recycling method by demonstrating the potential of re-using dissolved algae beads for re-immobilisation, as well as showing un-compromised performance in wastewater treatment and therefore contributing to an economic benefit for the up-scaling of immobilised algae systems.

5.2 Materials and Methods

Production of algae beads

Beads were made from 2% (w/v) sodium alginate solution (Sigma-Aldrich, product number 71238) and 2% calcium chloride solution (Sigma-Aldrich, ACS reagent >99%, Lot MKBP4041V) following the method described by Whitton (2016) using a peristaltic pump (Gilson Miniplus 3, 3mm ID tubing, 12 rpm) and a nozzle to generate uniform beads (Figure 5.2). The distance of the nozzle to the solution surface was kept at 25 cm. Beads were either made with only alginate (empty beads, EB) or alginate with algae cells (algae beads, AB). After preparation, beads were stirred in $CaCl_2$ for an additional 1 h. Removing of excess water was done by drying over vacuum for 5 minutes.

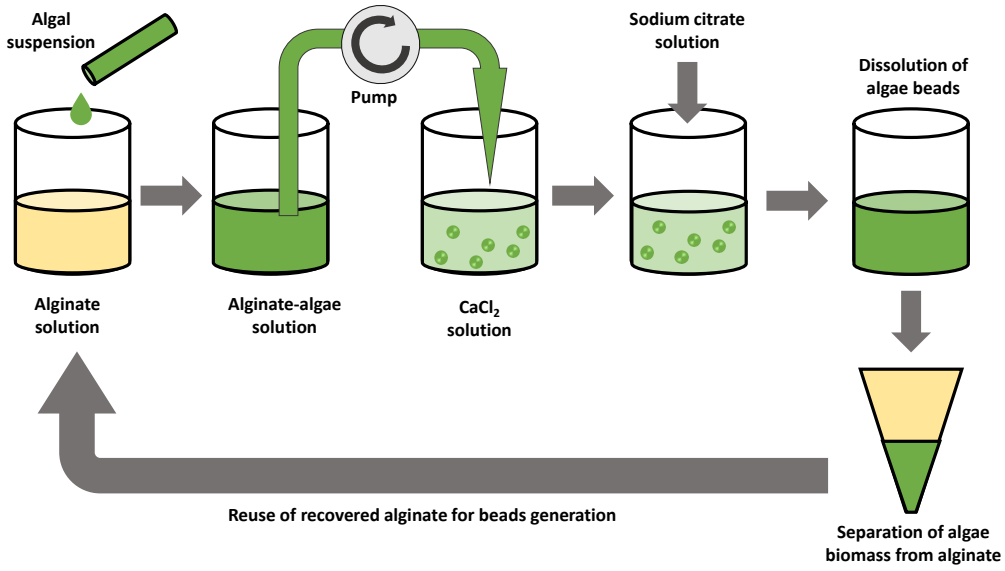

Figure 5.2: Diagram of beads preparation and dissolution

Alginate recovery method

Dissolution

Preliminary tests were run to identify the most suitable chemical for beads dissolution. Three sodium salts were tried: NaCl, Na_2CO_3 and trisodium citrate (Na-citrate) solutions were made up to at least 0.5 M to have excess sodium ions. Algae beads were weighed to 1 g (61-67 beads), added to 25 mL of each of the sodium solutions and magnetically stirred for 20 to 150 minutes.

In the following experiments, beads (EB and AB) were dissolved by stirring for 1-2 h in trisodium citrate solution (Merck, Batch No MC1M610493) which was made up to 0.5 M. To choose a suitable volume for dissolution, preliminary tests were run and a ratio of 1:2 Na-citrate:sodium alginate was shown to be suitable. Sodium alginate powder was supplemented into the recovered alginate (RA) solutions to overcome the dilution incurred by dissolution and it is mentioned when done so. Addition of sodium alginate to RA was 1% of the RA volume.

After dissolution of the algae beads, the algal biomass was separated with vacuum filtration. However, this procedure was omitted in later experiments due to time restrictions and inefficiency of filtrated alginate yield. A centrifugation method, detailed below, was subsequently used for the separation of the algal biomass from the alginate for the continuous P removal experiments only.

Re-immobilisation

The recovered alginate was used for re-immobilisation following the previously described method for beads production. Beads made from recovered alginate were measured, counted, weighed and imaged with scanning electron microscopy (SEM). Finally, beads recovery rates were calculated based on comparison of produced beads per volume of

alginate with virgin alginate (VA) and recovered alginate (RA).

Characterisation

VA and RA were assessed on their viscosity as well as on the surface morphology and compressibility of the beads formed. The dynamic viscosity of alginate was measured with a rheometer (HR-3 Discovery, US) using a cone-and-plate geometry (60 mm diameter, 2°cone angle, 120 s soak time, 25°C) against an increasing shear rate from 0 to 500 s^{-1}. Detailed surface morphology of beads was imaged with a SEM (FEI Quanta 200 ESEM, FEI, USA) operated under low vacuum mode. Prior to SEM imaging, beads were frozen for 5 h at -20°C, then freeze-dried at -55°C overnight and stored in a desiccator. The strength/compressibility of beads was measured with a TA-XT texture analyser (Arrow Scientific, Australia). A compressibility test was conducted with a cylindrical probe of 3 mm diameter which lowered down onto a bead until a resistance force of 5 g was detected from which on the probe moved down at a speed of 0.01 mm/s, flattening or rupturing the bead until the bottom of the sample dish. Force, measured in grams, and strength, in kg/mm, were recorded against distance and time. Measurements were taken in triplicates.

Phosphorus removal in continuous operation

The nutrients removal performance of algae beads produced with VA and RA was tested in continuously operated reactors (Algem^{TM} Labscale Photobioreactor, Stewartby, UK). These reactors were chosen based on previous research on immobilised algae (Whitton et al. 2016). The flow rate was set to a 24-hour hydraulic retention time (HRT) and the reactors were filled with 600 mL wastewater and 10 beads/mL (Abdel Hameed 2007). Constant light was set at a photon irradiance of 200 $\mu molm^{-2}s^{-1}$ and the temperature was controlled at 20°C. The algae strain for these experiments was *Scenedesmus obliquus* and

beads were produced with an aimed cell concentration of 10^5 cells/bead. The wastewater used in these experiments was a secondary effluent from a STW in Leicestershire, UK. For the trial, the wastewater was supplemented with NH_4Cl and KH_2PO_4 from average 0.1 and 0.3 to 3 mg NH_4-N/L and 1 mg P/L, respectively, to obtain controlled testing conditions. The NO_3^--N concentration was not altered as it was on average 2.39 mg/L in the influent.

During the experimental runs, samples were taken every 1-2 days and analysed for pH (Jenway 3510 pH metre, Staffordshire, UK) and for ortho-P, total P (TP), filtered ortho-P (0.45 µm), NH_4-N and NO_3-N with colorimetric cell tests (Merck, UK). Algal growth was monitored by dissolving 10 beads in 5 mL Na-citrate solution (2% w/v) and determining cell numbers using a haemocytometer and a light microscope (Olympus CX41, Essex, UK).

RA beads were made from algae beads that had undergone a previous trial with wastewater for 19 days. VA beads were run in parallel to the RA beads to have a side-by-side performance comparison. Both were run in duplicates and for a total of 17 days.

Alginate recovery was performed following the previously described method. Beads from the initial trials with VA (quadruplicate) were combined, washed with DI water and dissolved in 150 mL trisodium citrate solution. This volume was chosen based on the total weight of the beads (174.60 g). Algal biomass and alginate were separated by centrifugation for 15 minutes at 4000 rpm (Thermo Scientific, Sorvall Legend RT Plus, UK). The volume of the recovered alginate was 270 mL and 2.7 g of sodium alginate were added prior to addition of algal cells to produce the AB with RA with an aimed cell concentration of 10^5 cells/bead. Beads (RA and VA) were then made as described previously.

5.3 Results and Discussion

5.3.1 Identifying a chemical for dissolution of algae beads

Visual observation of the three test solutions revealed obvious differences. In the case of NaCl, no observable dissolution occurred within 150 minutes with slight changes in the size of the beads observed at 30 and 40 minutes including a swelling of the beads after 40 minutes (Figure D.1). In the case of Na_2CO_3, the beads started dissolving after 30 minutes and were completely dissolved after 40 minutes. However, in conjunction with the dissolution process, an increase in turbidity of the solution was visually apparent. The formation of a precipitate is congruent with the formation of calcium carbonate due to the ion activity product of calcium carbonate (0.09 mol^2/L^2) being greater than the solubility product of $CaCO_3$ ($3.31 \cdot 10$ 8 mol^2/L^2, (Gebauer 2008)). Further, low calcium carbonate solubility of 0.13 mg/mL at pH 7.5 was exceeded with concentrations of 4.5 mg/L Ca^{2+} and 8.3 mg/L CO_3^{2-} in the solutions (Goss et al. 2007). In contrast, dissolution using sodium citrate was observably rapid and did not result in precipitation of any material. In fact the beads began to become visually smaller after 10 minutes and were fully dissolved after 20 minutes. During the dissolution tests, pH decreased from 7 to 6 when using sodium citrate and it increased to 12 with Na_2CO_3 which is likely due to the alkaline nature of carbonate.

Considering the beads to dissolving solution ratio of 1:25[1] and the respective molar ion ratios in the solutions, sodium ions were in excess of calcium ions by 106, 139 and 209 times for NaCl, Na_2CO_3 and $Na_3C_6H_5O_7$, respectively. However, dissolution effectiveness also appears sensitive to the anion component related to its attractiveness to calcium in relation to its charge and steric interactions providing differences in the free energy of

[1] Density was assumed to be 1 g/mL as measurements resulted to be 1.001 ± 0.024 g/mL.

reaction. For instance, citrate, carbonate and chloride anions have ionic charges of -3, -2 and -1, respectively, which suggests that the high charge of the citrate anion attracted Ca^{2+} cations more strongly than the other two.

With sodium citrate resulting in the fastest dissolution of algae beads, this chemical was chosen to be used in the more detailed experiments.

5.3.2 Quality and quantity assessment of recycled alginate

Assessing the quantity of recovered alginate gives an important indication for the efficiency of recycling and any possible losses. On average 17 algae beads can be produced from one millilitre of fresh alginate (VA) (Table 5.1). Comparing this to the production rate from recovered alginate (11.7 beads/mL), a recovery rate of 69.1% can be calculated. In the case of empty beads, a recovery rate of 77.1% was determined.

Table 5.1: Beads production from virgin and recycled alginate with and without algae incapsulation

	Beads production [beads/mL alginate solution]		
	Virgin alginate ± SD	Recovered alginate ± SD	Recovery rate ± SD
Empty beads n = 14	17.7 ± 2.7	13.7 ± 1.7	77.1 ± 8
Algae beads n = 6	17.1 ± 1.6	11.7 ± 2.0	69.1 ± 15

SD: Standard deviation

Visual differences can be observed with respect to the recovered alginate beads appearing to be a paler green colour compared to the beads made from fresh alginate (Figure 5.3). The colour change may have been caused by white calcium citrate residues reflecting the light (Figure D.2). For a further qualitative assessment of the beads, images were made from the virgin and recovered alginate with SEM (Figure 5.4). The surface structure looks similar for VA and RA beads and no recognizable difference can be seen between empty and algae beads either (Figure 5.4a and 5.4b).

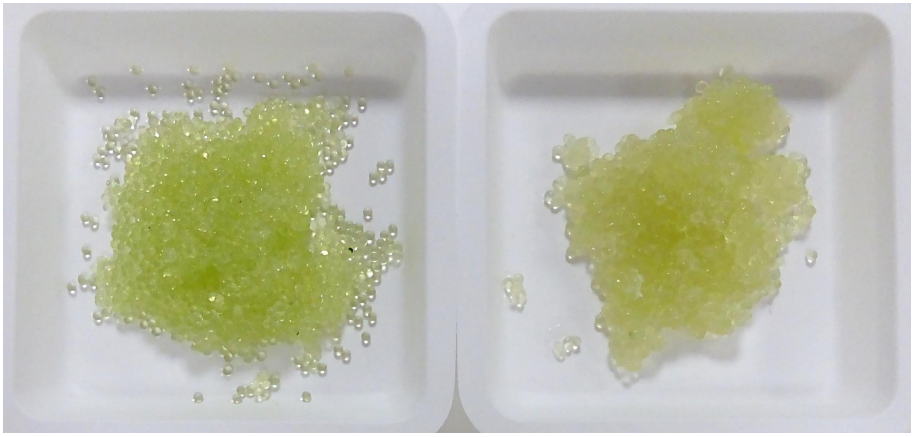

Figure 5.3: Photograph of VA (left) and RA beads (right).

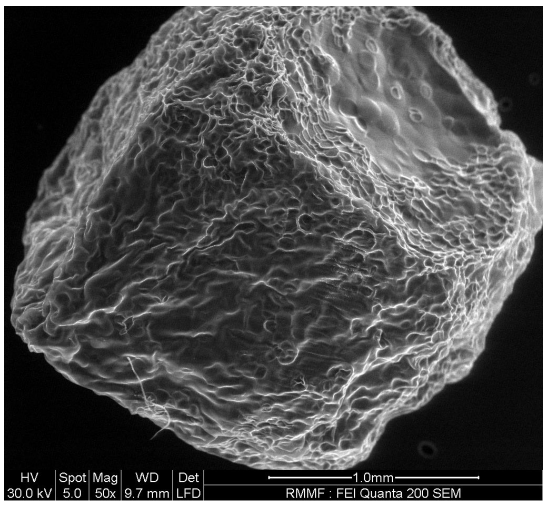

(a)

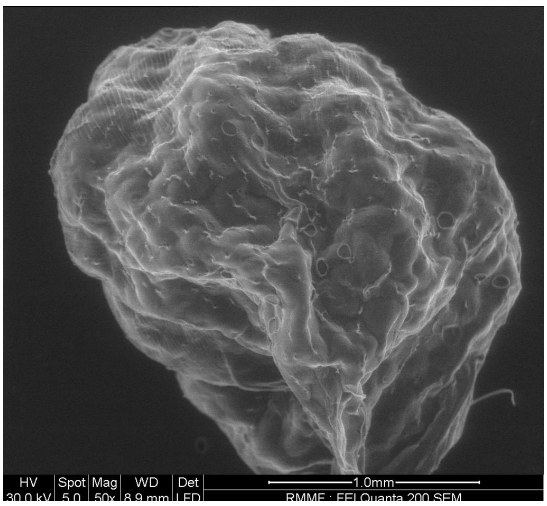

(b)

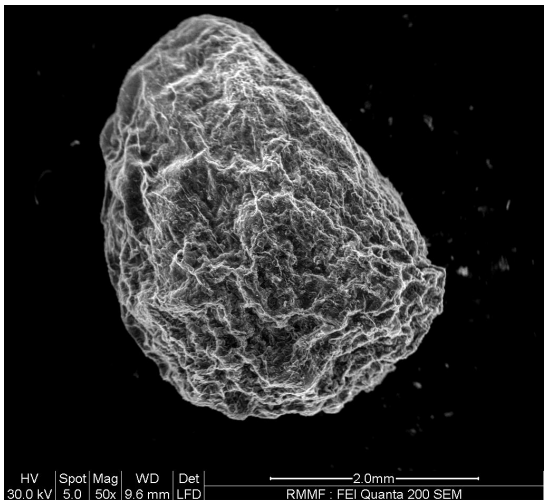

(c)

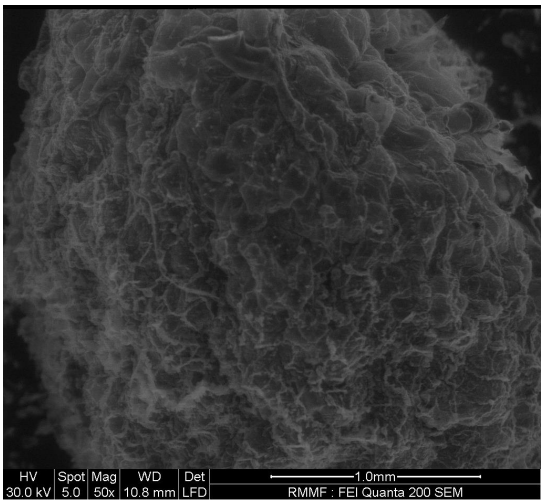

(d)

Figure 5.4: SEM images of (a) VA empty bead, (b) VA algae bead, (c) RA empty bead, (d) RA algae bead at 50x magnification.

With dissolution of beads in sodium citrate, a dilution of the original alginate concentration is expected which may have an influence on the properties of the recycled alginate and therefore re-immobilised beads. This was assessed by viscosity and mechanical strength measurements. The viscosity can have an influence on the gelation reaction and the size of the beads whereas the strength of beads can be an indicator for the longevity of the beads when used in a mixed reactor for wastewater treatment. The expected concentrations of RA solutions were calculated from the volume of sodium citrate and the weight of beads. The viscosity of three RA solutions was compared to a concentration series (0.5% - 2%) of VA in water and trisodium citrate (Table 5.2). For both VA solutions, viscosity increases with alginate concentration. When alginate is dissolved in sodium citrate, this increase occurs at a slower rate. Comparison to RA indicates a clear difference with a higher apparent viscosity in the case of the RA. To illustrate, the viscosity for the RA varied between 0.827 and 0.879 Pa.s for concentrations of 1.17% and 1.23% compared to viscosities of 0.037 and 0.170 Pa.s for VA concentrations of 1 and 1.5%, respectively, in trisodium citrate. Accordingly, the RA exhibited a viscosity of a more highly concentrated VA with a concentration of between 1.5 and 2%.

Despite differences when comparing viscosities of different VA concentrations with RA, beads could be formed from RA and did sustain in a P removal trial run (more detailed description in section 5.3.3) clearly demonstrating that the changes in viscosity observed had no impact on the beads production process.

Table 5.2: Viscosity in Pa.s at 7.6 s^{-1} of made up alginate solutions in water and trisodium citrate compared to recovered alginate solutions.

Viscosity of alginate solutions in Pa.s				
VA concentration [%]	VA in water ± SD	VA in trisodium citrate ± SD	RA concentration [%]	RA solution ± SD
0.5	0.027 ± 0	0.011 ± 0		
1	0.035 ± 0.001	0.037 ± 0.001	1.17	0.827 ± 0.116
1.5	0.312 ± 0.002	0.170 ± 0.002	1.2	0.848 ± 0.174
2	1.021 ± 0.026	0.498 ± 0.003	1.23	0.879 ± 0.064
2.5	1.856 ± 0.019	1.120 ± 0.032		

SD: Standard deviation

Compressibility of a set of beads was measured to identify differences in mechanical strength of VA and RA beads as this can determine the life of beads (or duration of batches) when used in wastewater remediation. The force and strength to which beads resisted was recorded against compressive distance (i.e. a probe pushing down on one bead at a set speed). Peak force and strength values were determined at those points where irreversible deformation of beads occurred (Table 5.3; Figure 5.5). No significant difference in applied force was observed up to a compression of 0.5 mm beyond which the profiles differed significantly (Figure 5.5). It is noticeable that the presence of algae cells within the beads did not seem to impact the mechanical strength profiles of beads in either VA and RA systems. The maximum forces that beads withstood were 104.33 g and 100.87 g for empty and algae VA beads, respectively. In comparison, algae beads made from recovered alginate and supplemented with virgin alginate had a maximum force of 52.72 g which was about half of the VA beads but significantly higher than the peak forces for empty and algae RA beads. The results for the latter two were 26.72 g and 25.53 g for EB and AB RA beads, respectively. The peak strength values show a similar trend in a sequence of VA, RA supplemented with VA and RA alone (Table 5.3). Overall, this indicates that recovered alginate has a higher viscosity but lower mechanical

strength than VA, but this can be enhanced by supplementing the recovered material with VA. The current results are reinforced by comparison to medical trials with alginate fibres for wound dressings where calcium alginate showed more swelling when dissolved and solidified again (Qin et al. 2006). Both observations are congruent with a loosening of the egg-box-shape structure due to additional citrate in the mixture causing a repelling effect and larger distances of polymer chains between each other. The implication is that long term repeated recycling of the alginate may cause structural problems which need further investigation and may require a certain amount of fresh alginate to always be included.

Table 5.3: Force and strength of beads (n=3, ± 1 Standard deviation).

	EB VA	AB VA	AB RA (supp)	EB RA	AB RA
Peak Force [g]	104.33 ± 64.73	100.87 ± 38.53	52.72 ± 3.41	26.72 ± 14.84	25.53 ± 19.53
Peak Strength [kg/mm]	0.035 ± 0.022	0.034 ± 0.013	0.018 ± 0.001	0.009 ± 0.005	0.009 ± 0.007

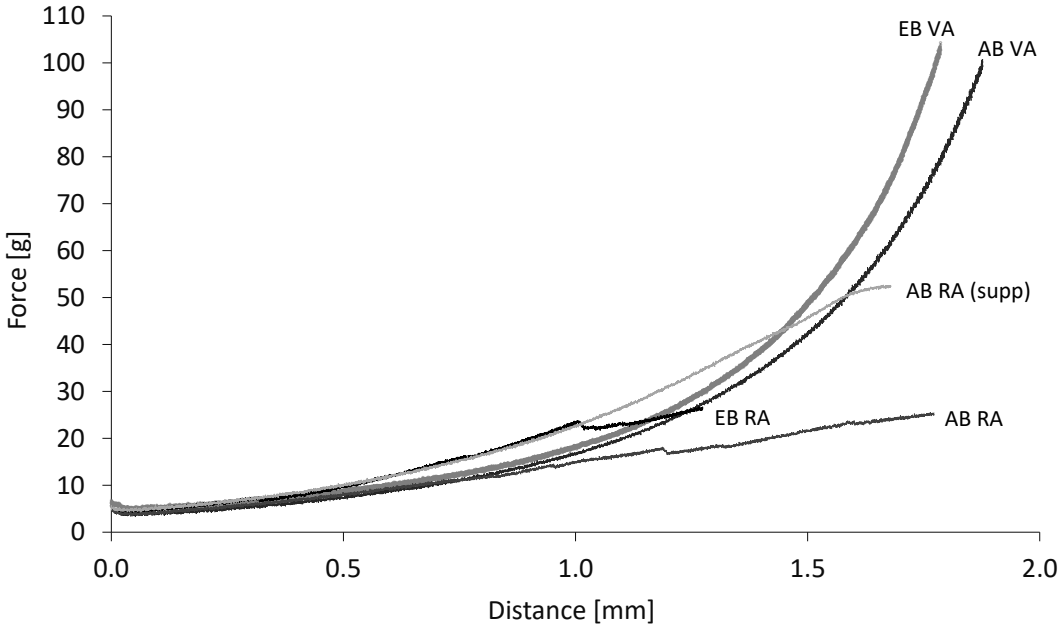

Figure 5.5: Force of beads with distance. EB: empty beads, AB: algae beads, VA: virgin alginate, RA: recovered alginate, supp: supplemented with additional alginate.

5.3.3 Phosphorus removal in continuous operation

To obtain a realistic representation of alginate recycling, fresh algae beads were used in a lab-scale photobioreactor trial which lasted 19 days. The alginate from used beads from this experiment was then recycled to re-immobilise a second set of beads. These were then used in parallel to a new batch of VA beads to compare their performances against each other. The influent ortho-P concentration was on average 0.97 mg P/L over the whole trial period. Both VA and RA beads followed the same trend (Figure 5.6). From day 1 until 7, P concentrations decreased from 0.58 and 0.54 mg P/L to 0.09 and 0.07 mg P/L for VA and RA, respectively (Figure 5.6a). In a previous study with a similar influent P concentration and at 20h HRT, minimum effluent P concentrations below 0.01 mg/L (which was below detection limit) were reported (Whitton et al. 2018). Between days 7 and 17, effluent P steadily increased to finally reach 1.31 and 0.9 mg P/L for VA and RA, respectively. It is notable that the final concentrations were near or above the influent concentration on day 17 at which point the test was stopped. The influent pH was on average 7.61. The pH increased with both VA and RA beads such that between days 1 and 8, the pH varied between 7.6 and 8.5 for the VA beads before decreasing slowly to a final value of 7.0 on day 17 (Figure 5.6b). In the case of RA, a maximum pH of 8.8 was reached on day 3 which then decreased slowly to the final pH of 7.5. An elevated effluent pH has been shown to be partly caused by alkalinisation through uptake of NO_3^--N and a net decrease of H^+ (Whitton et al. 2018).

Ammonia concentrations in the influent were 2.57 mg NH_4^+-N/L on average with very low concentrations of 1.24, 0.1 and 0.28 mg NH_4^+-N/L on days 3, 13 and 17, respectively, when new batches of feed water were supplemented. Both VA and RA beads achieved very low ammonia concentrations consistently below 0.1 mg NH_4^+-N/L with VA having one spike of 1.99 mg NH_4^+-N/L on day 5 (Figure 5.6b). The nitrate influent concentration

was 2.39 mg NO_3^--N/L on average with an unsteady trend overall. Both VA and RA beads resulted in effluent nitrate concentrations of 0.5 mg NO_3^--N/L and each having one peak on day 5 at 1.68 and 2.75 mg NO_3^--N/L for VA and RA, respectively (Figure 5.6c). The ammonia and nitrate removal rates are comparable to previous studies with algae beads, where consistently low ammonia (<0.001 mg/L) and nitrate (0.4 mg/L) effluent concentrations were achieved with a 20h HRT and similar influent concentrations (Whitton et al. 2018).

Algal cell concentrations grew rapidly to a plateau of 1.24-1.26·10^6 cells/bead between days 5 and 10 in the case of VA (Figure 5.6d). The cell concentration then decreased to 5.8·10^5 cells/bead on day 17. In the case of RA, algal cells grew to a maximum of 1.53·10^6 cells/bead on day 8 and after that rapidly decreased to a final concentration of 3.5·10^5 cells/bead. The parallel trials of VA and RA beads showed similar results suggesting that recycling of alginate is possible for use in wastewater remediation without a negative impact on performance. However, the period at which low P levels (<0.5 mg/L) were achieved (up to day 7) was notably shorter when comparing to previously reported studies where low levels were maintained until up to 20 days (R. Whitton et al. 2018). Although this difference cannot be explained, it can be expected to come from variations in wastewater composition.

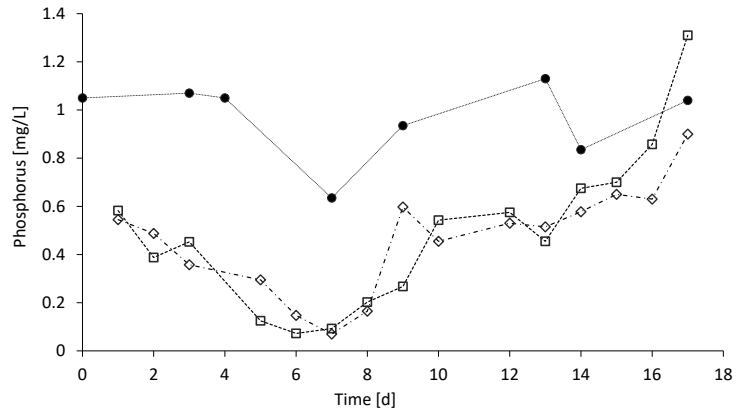

(a)

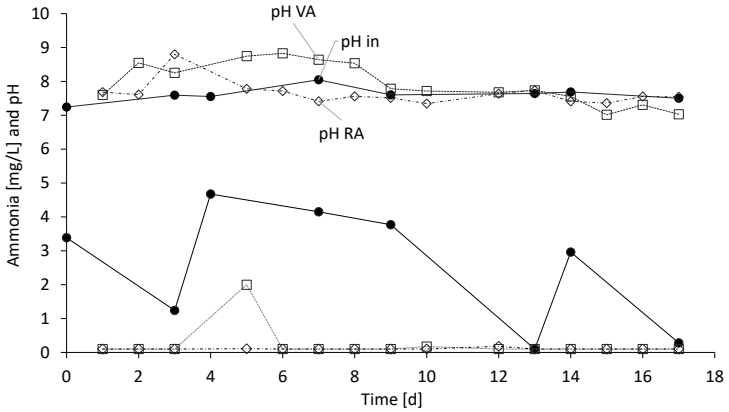

(b)

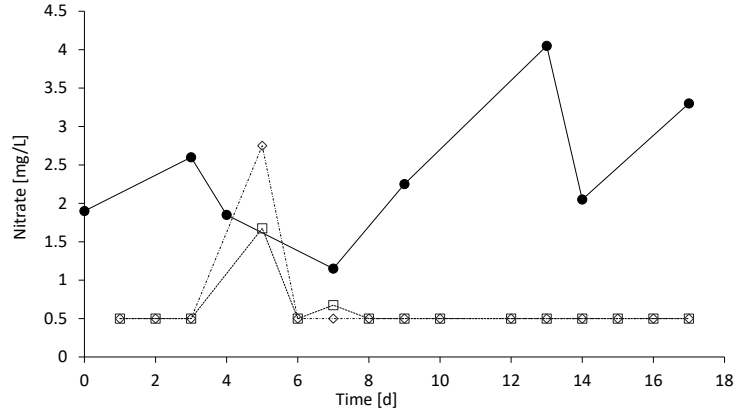

(c)

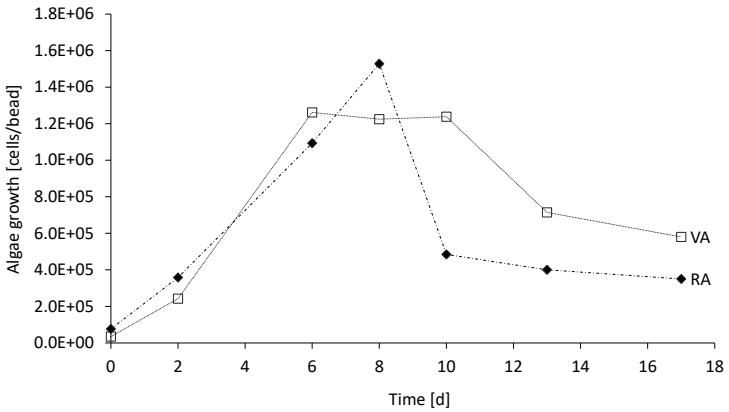

(d)

Figure 5.6: Performance of VA and RA beads in continuous photobioreactors. Influent (●), VA effluent (□), RA effluent (◇) (a) P concentration (b) NH_4-N and pH (c) NO_3-N (d) Algae growth

5.3.4 Economic assessment for alginate recovery

The results obtained in this work were used to evaluate the economic impact of alginate recycling on IBR operation for 1 year at a wastewater treatment plant of 1000 PE. Only the costs for bead making, dissolution and re-immobilisation were considered as part of the net operational expenditure (nOPEX) and the costs for $CaCl_2$ and machinery for bead making were not considered here as they will be the same in both scenarios (Table 5.4). The comparison considered a scenario with and without alginate recovery. A sensitivity analysis was further undertaken where beads' life, virgin alginate costs and recovery rates were varied (+/-50% of original value) and their respective impact on nOPEX was studied.

Table 5.4: Parameters used in economic analysis

Parameter		Unit	Sensitivity
Cost of sodium alginate	33.04	£/kg	+/-50%
Beads' life/ Batch duration	20	Days	
Recovery rate for alginate	60	%	
Cost of trisodium citrate	0.924	£/kg	Fixed values
Production of algae beads	17	Beads/ mL alginate	
Flow rate (1000 PE)	180	m^3/d	
HRT (IBR)	24	h	

When all parameters are fixed, nOPEX can be reduced by 50% when recovery of alginate is implemented. For a variation of beads' life (i.e. one batch duration) between 10 and 30 days, the same reduction of 50% will apply. Although increasing beads life, and thus decreasing number of annual batches, will reduce overall operational costs, this effect will be at the same rate in both scenarios, whether with or without recovery, because

alginate is still used in both cases.

The cost for sodium alginate is likely to vary depending on its origin/source (Kube et al. 2019) and with current research developments on alginate like polymers, recovery from granular sludge the costs may decrease in the future (Lin et al. 2010; Van Der Hoek et al. 2016). Cost variations of sodium alginate between £16.52 and £49.55 per kilogram will first impact the whole IBR process even without alginate recovery. With a 60% alginate recovery rate, nOPEX will be reduced between 39% and 53% for the lowest and highest alginate costs, respectively (Figure 5.7). In this cost scenario, there is also a breakeven alginate cost of £4.75/kg below which a system without alginate recovery may be more economically beneficial than with recovery with the onset of the use of wastewater derived alginate like polymers. Therefore, it is realistic to assume that in the future the IBR process may become economically viable even without alginate recovery.

Changes of the recovery rate of alginate will have the biggest impact on nOPEX. Between 30% and 90% recovery rate, the costs can be reduced by 20% to 80%, respectively. As opposed to alginate costs, the recovery rate can be controlled to a certain point by improving the operational conditions. Therefore, it appears that an improved alginate recovery method will be most valuable for the advancement of the IBR process towards full-scale application.

5.4 Conclusions

The objective of this work was to give a proof-of-concept of the recycling of alginate in an immobilised algae system. The results showed that recycled alginate beads at a recovery rate of 69% can be produced. Although RA beads showed a lower mechanical strength than VA beads, both were used for wastewater remediation and achieved a similar treatment performance. At current costs of chemicals, recovery of alginate can bring a

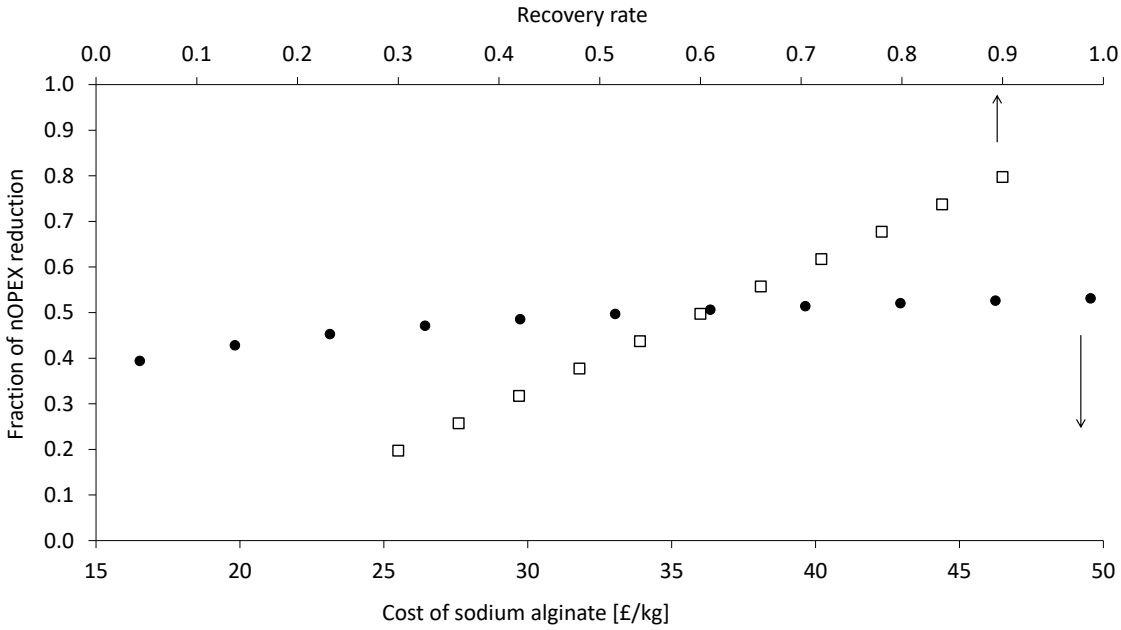

Figure 5.7: Development of nOPEX cost reduction with variation of sodium alginate costs (●) and recovery rate (□).

34% net operational cost reduction which can be increased with further improvements in recovery. These can be achieved through a more thorough assessment of the required concentration of the dissolving agent (in this case sodium citrate) to reduce costs and dilution rates. It will be also economically beneficial to determine the minimum amount of sodium alginate supplementation needed for sufficient beads' strength and performance in wastewater treatment. This work has shown that alginate recovery in an IBR system can be beneficial for process operations and economics and it therefore contributed to move the development towards full-scale application.

5.5 Acknowledgements

Funding for this study was gratefully received by Severn Trent Water and the Royal Society of Chemistry Water Science group in form of the Alan Tetlow Memorial Bursary. The

authors gratefully acknowledge the facilities, and the scientific and technical assistance, of the Australian Microscopy & Microanalysis Research Facility at the RMIT Microscopy & Microanalysis Facility, the facilities and technical support by Nadia Zakhartchouk at the Separation Science and Mass Spectrometry Facility, the facilities and the technical support by Muthu Pannirselvam at the Rheology and Materials Characterisation Laboratory and finally the facilities of the Food Research and Innovation Centre at RMIT University.

References

Abdel Hameed, M. S. (2007). "Effect of algal density in bead, bead size and bead concentration on wastewater nutrient removal". *African Journal of Biotechnology* 6.10, pp. 1185–1191.

Bajpai, S. K. and Sharma, S. (2004). "Investigation of swelling/degradation behaviour of alginate beads crosslinked with Ca2+ and Ba2+ ions". *Reactive and Functional Polymers* 59.2, pp. 129–140.

De-Bashan, L. E. and Bashan, Y. (2004). "Recent advances in removing phosphorus from wastewater and its future use as fertilizer (1997-2003)". *Water Research* 38.19, pp. 4222–4246.

Chevalier, P. and Noüe, J. de la (1985). "Efficiency of immobilized hyperconcentrated algae for ammonium and orthophosphate removal from wastewaters". *Biotechnology Letters*.

Ching, S. H., Bansal, N., and Bhandari, B. (2017). "Alginate gel particles–A review of production techniques and physical properties". *Critical Reviews in Food Science and Nutrition* 57.6, pp. 1133–1152.

Filippino, K. C., Mulholland, M. R., and Bott, C. B. (2015). "Phycoremediation strategies for rapid tertiary nutrient removal in a waste stream". *Algal Research*.

Gebauer, D. (2008). “Stable Prenucleation Calcium Carbonate Clusters”. *Science* 322.December, pp. 1819–1823.

Goss, S. L., Lemons, K. A., Kerstetter, J. E., and Bogner, R. H. (2007). “Determination of calcium salt solubility with changes in pH and P CO2 , simulating varying gastrointestinal environments”. *Journal of Pharmacy and Pharmacology* 59.11, pp. 1485–1492.

Infante, C., León, I., Florez, J., Zárate, A., Barrios, F., and Zapata, C. (2013). “Removal of ammonium and phosphate ions from wastewater samples by immobilized Chlorella sp.” *International Journal of Environmental Studies* 70.1, pp. 1–7.

Kube, M., Mohseni, A., Fan, L., and Roddick, F. (2019). “Impact of alginate selection for wastewater treatment by immobilised Chlorella vulgaris”. *Chemical Engineering Journal* 358.April 2018, pp. 1601–1609.

Lin, Y., Kreuk, M. de, Loosdrecht, M. C. van, and Adin, A. (2010). “Characterization of alginate-like exopolysaccharides isolated from aerobic granular sludge in pilot-plant”. *Water Research* 44.11, pp. 3355–3364.

Liu, K., Li, J., Qiao, H., Lin, A., and Wang, G. (2012). “Immobilization of Chlorella sorokiniana GXNN 01 in alginate for removal of N and P from synthetic wastewater.” *Bioresource Technology* 114, pp. 26–32.

Mallick, N. (2002). “Biotechnological potential of immobilized algae for wastewater N, P and metal removal: A review”. *BioMetals*.

Ometto, F., Quiroga, G., Pšenička, P., Whitton, R., Jefferson, B., and Villa, R. (2014). “Impacts of microalgae pre-treatments for improved anaerobic digestion: thermal treatment, thermal hydrolysis, ultrasound and enzymatic hydrolysis.” *Water Research* 65, pp. 350–61.

Ometto, F., Whitton, R., Coulon, F., Jefferson, B., and Villa, R. (2013). "Improving the Energy Balance of an Integrated Microalgal Wastewater Treatment Process". *Waste and Biomass Valorization* 5.2, pp. 245–253.

Qin, Y., Hu, H., and Luo, A. (2006). "The conversion of calcium alginate fibers into alginic acid fibers and sodium alginate fibers". *Journal of Applied Polymer Science* 101.6, pp. 4216–4221.

Vallero, D. (2010). "CHAPTER 1 – Environmental Biotechnology: An Overview". *Environmental Biotechnology: A biosystems approach*. 2nd. Academic Press, pp. 1–44.

Van Der Hoek, J. P., De Fooij, H., and Struker, A. (2016). "Wastewater as a resource: Strategies to recover resources from Amsterdam's wastewater". *Resources, Conservation and Recycling* 113, pp. 53–64.

Velings, N. M. and Mestdagh, M. M. (1995). "Physico-chemical properties of alginate gel beads". *Polymer Gels and Networks* 3.3, pp. 311–330.

Whitton, R. L. (2016). "Algae Reactors for Wastewater Treatment". PhD thesis. Cranfield University.

Whitton, R., Le Mével, A., Pidou, M., Ometto, F., Villa, R., and Jefferson, B. (2016). "Influence of microalgal N and P composition on wastewater nutrient remediation". *Water Research* 91, pp. 371–378.

Whitton, R., Ometto, F., Pidou, M., Jarvis, P., Villa, R., and Jefferson, B. (2015). "Microalgae for municipal wastewater nutrient remediation: mechanisms, reactors and outlook for tertiary treatment". *Environmental Technology Reviews* 4.1, pp. 133–148.

Whitton, R., Santinelli, M., Pidou, M., Ometto, F., Henderson, R., Roddick, F., Jarvis, P., Villa, R., and Jefferson, B. (2018). "Tertiary nutrient removal from wastewater by immobilised microalgae: impact of wastewater nutrient characteristics and hydraulic retention time (HRT)". *H2Open Journal* 1.1, pp. 12–25.

Chapter 6

Implications of the work: Implementation of advanced tertiary P removal

The overall aim of the research was "to understand how to resolve the bottlenecks associated with implementation of tertiary P technologies when meeting sub 1 mg P/L concentrations". This work looked at technologies that have not previously been tested and/or implemented in the UK including ballasted coagulation, pile cloth media filtration, ultrafiltration and a reactive media constructed wetland. It was shown that the type of solid-liquid separation can be the decisive factor in coagulation based tertiary P removal when meeting sub 1 mg/L consents. Further, it was demonstrated that P removal in reactive media constructed wetlands follow more complex pathways than originally expected and new knowledge gained on the process will help further developments towards implementation. Finally, the study on alginate recovery established a method for alginate recycling and reuse and highlighted potential cost savings that can move the immobilised algae process further towards large scale implementation.

6.1 Which tertiary P removal technology should be adopted when meeting sub 1 mg/L effluent P consents?

With tertiary treatment being the last stage at a WWTW before discharge, it is important to not only comply with stricter P consents but also with ferric and aluminium consents. This can become critical when very low P concentrations need to be achieved at high coagulant doses. Based on the insights gained in this work a qualitative comparison of emerging tertiary P removal technologies has been conducted to inform a tertiary P removal strategy for sub 1 mg P/L (Table 6.1). The technology readiness level (TRL) describes the current development stage of a technology with 9 being the highest. P targets describe what level a technology can meet and were based on the findings in this work (Chapters 2-4). The P target for the immobilised algae reactor (IBR) was based on previous research on pilot scale (Whitton et al. 2018). Energy demand and costs were given qualitatively based on literature and supplier's information (Remy et al. 2014). The sustainability rating is based on the added value of a technology, i.e. circular economy potential, and whether it uses additional chemicals (i.e. coagulant, cleaning chemicals). The rating is given numerically with values between 1 and 5, where 5 indicates the highest sustainability.

Table 6.1: Qualitative rating of tertiary P removal technologies against achievable P target, energy demand, costs and sustainability

Technology	TRL	P target [mg/L]	Energy demand	Costs	Footprint	Sustainability
Ballasted coagulation	9	0.1	Medium	Medium	Medium	2
Pile cloth filtration	9	0.5	Medium	Low	Small	2
Membrane filtration	9	0.1	High	High	Large	1
Steel slag constructed wetland	6	1	Low	Low	Large	4
Immobilised algae reactor	5	0.1	Low	High	Small	5

Ballasted coagulation is a technology for large WWTW due to its required infrastructure and ability to handle large wastewater loads. It is a technology at the highest TRL 9 and has been shown in this work to achieve effluent P targets of 0.1 mg P/L (Chapter 2 and 3). In this system the coagulation-flocculation is optimised through generating larger and heavier flocs -by adding polymer and ballast- and operating at short retention times below 15 minutes, thus removing solids before floc breakage occurs (Chapter 3) (Table 6.2). Compared to the whole life costs of a continuous sand filter at a medium size works (20,000 PE), it will be a cost competitive choice. The energy demand can be rated within the medium range and in fact, high rate sedimentation was reported to have the lowest energy demand when compared to a microsieve or an UF membrane (Remy et al. 2014). Due to its short retention time, it can have a smaller footprint than an alternative with longer retention times. Due to continuous use of coagulant and polymer, the sustainability has been rated at the lower end. Based on this assessment, ballasted coagulation can be recommended for tertiary P removal for medium to large WWTWs with 0.1 mg P/L targets.

The pile cloth media filtration technology requires low maintenance and is the least expensive of the tested technologies making it a suitable choice for small to medium WWTWs. In this work it has been shown to be able to sustainably achieve a 0.5 mg P/L target, and at optimised dose and flocculation conditions it will meet a 0.3 mg P/L target (Chapter 2). Since the performance of the pile cloth filtration mostly deteriorated at higher influent P concentrations rather than higher flows, optimum coagulant to P ratios need to be established and a minimum Fe:P ratio of 2.29 is required (Table 6.2). Being at a medium robustness this technology appears to be best suited for small WWTWs where higher solids content predominates (compared to the test with high TSS influent) and at which the cloth filter performs better. The capital and operational costs for this technology are low and a medium sized footprint will be required depending on whether upstream coagulation-

flocculation tanks exist yet. The pile cloth media filter cannot be recommended for larger WWTWs where typically consents below 0.3 mg/L will be expected, and the technology has not to been fully optimised yet. Therefore, a recommendation for implementation at small WWTWs is given. Since this is a coagulation-based technology, the sustainability is rated towards the lower end.

Ultrafiltration at tertiary P removal stage can achieve sub 0.1 mg P/L levels if the operational conditions and coagulant type are optimised (Table 6.2). This has been shown in this work when coagulant was changed from ferric chloride to alum (Chapter 2) and can be confirmed by literature (Langer and Scherman 2013). Ultrafiltration was observed to operate towards the effluent target requiring a 20% lower Fe:P ratio than the cloth filtration, yet it was one of the least robust technologies. Although it is a total filtration technology, the membrane appeared to not have optimised coagulation-flocculation conditions. However, this technology appeared less robust compared to the other tested solid liquid separators and given the high costs and energy demand that comes with it, ultrafiltration cannot be recommended for tertiary P removal at this stage. It might be a viable choice, though, at sites where other contaminants are regulated, and total filtration is required.

Table 6.2: Qualitative rating of tertiary P removal solids liquid separation technologies

Technology	Robustness	P target [mg/L]	Retention times	Dynamic resilience	Fe:P ratio for 0.3 mg/L P target	Optimised flocculation
Ballasted coagulation	High	0.1	Short	High	1.4	Yes
Pile cloth filtration	Medium	0.5	Medium	Low-Medium	2.29	No
Membrane filtration	Medium	0.1	Medium	Medium-High	1.83	No

On the side of novel alternatives, reactive media constructed wetland (CW) is at TRL 6, i.e. not yet implementation-ready (Table 6.1). Based on this work, a steel slag CW would be able to meet an annual average of 1 mg P/L (Chapter 4) with potential to meet sub 0.1 mg P/L in the future after optimisation of the process. This technology would be

a choice for small treatment works with sufficient area for the large footprint of the wetland. Overall, the CW would consume little energy and incur low operational costs. The sustainability is rated highly due to reuse of waste media, yet the potential health hazards from dissolving vanadium needs to be considered.

It has been shown in laboratory and pilot scale work that an immobilised algae reactor (IBR) can meet 0.1 mg/L effluent P levels (Whitton et al. 2018). Although this technology is still in its infancy (TRL 5), it has potential for small WWTWs because of its low energy demand and small footprint. Moreover, this technology has a high sustainability rating because the algal biomass recovered from the used beads can be converted to energy (as biogas) through anaerobic digestion (Gomez San Juan et al. 2017). However, at this stage the IBR is not yet cost-competitive and therefore not a suitable choice for a tertiary P strategy. Nevertheless, this work presented an opportunity for reducing overall net operational costs by 34% through recycling and reuse of alginate progressing the IBR further towards large scale implementation as a future tertiary P removal alternative (Chapter 5).

6.2 What is the future perspective for novel non-coagulant technologies?

Currently, depth and cloth filters are used at small WWTWs to achieve stricter P consents because no alternatives are currently available but the use of chemical free technologies that fit the industry's simple technology/low maintenance strategy for small WWTW is strongly desired. Compared to the benchmarked sand filter evaluated in this thesis, the tested pile cloth filter will be 60% cheaper when implemented at a small WWTW (Severn Trent Water 2018).

For future alternatives, a reactive media wetland has been shown to achieve very low effluent P concentrations during the first full-scale, long-term trial highlighting its potential (Table 6.3). Although challenges for this technology remain, it can be easily implemented, once reaching higher TRL, at sites with already existing wetlands by replacing gravel with the reactive media and would be 22% cheaper than a pile cloth filter at similar scale (Severn Trent Water 2018). Insights towards the complexity of predominating P removal mechanisms were given based on the research undertaken. This means that the technology will need to be further developed and understood before considering implementation.

The future perspective of the IBR relies on cost reduction and demonstration of its viability at scales beyond the laboratory where promising performance has been shown (Whitton 2016). In this work, the technology was progressed towards larger scale through proving that alginate recycling can be achieved, resulting in lower operational costs. For small WWTWs, an IBR is particularly interesting because it is a complete remediation technology not only removing P but also N (Whitton et al. 2018). At this stage, the IBR would be 14 times more expensive than a reactive media wetland considering a small WWTW (2000 PE) which highlights the need for further research and development (Severn Trent Water 2018).

Table 6.3: Future perspective of novel tertiary P removal technologies

	Steel slag constructed wetland	Immobilised algae reactor
Viability for P removal	Very low effluent P possible but cannot be maintained	Very low effluent P possible[a]
Progress towards full-scale	First full-scale, long-term trial	Opportunity to reduce operational costs
Remaining challenges	Management of P removal and pH, Understanding pathways	Demonstrate performance at large scale

[a] Based on R. L. Whitton (2016)

References

Gomez San Juan, M., Ometto, F., Whitton, R., Pidou, M., Jefferson, B., and Villa, R. (2017). "Energy Recovery from Immobilised Cells of Scenedesmus obliquus after Wastewater Treatment". *Lecture Notes in Civil Engineering*, pp. 266–271.

Langer, M. and Scherman, A. (2013). *Feasibility of the Microsieve technology for advanced phosphorus removal Project acronym: OXERAM 2*. Tech. rep. Berlin: Kompetenzzentrum Wasser Berlin gGmbh.

Remy, C., Miehe, U., Lesjean, B., and Bartholomäus, C. (2014). "Comparing environmental impacts of tertiary wastewater treatment technologies for advanced phosphorus removal and disinfection with life cycle assessment". *Water Science and Technology* 69.8, pp. 1742–1750.

Severn Trent Water (2018). *Low Phosphorus Trials*. Tech. rep. Confidential.

Whitton, R. L. (2016). "Algae Reactors for Wastewater Treatment". PhD thesis. Cranfield University.

Whitton, R., Santinelli, M., Pidou, M., Ometto, F., Henderson, R., Roddick, F., Jarvis, P., Villa, R., and Jefferson, B. (2018). “Tertiary nutrient removal from wastewater by immobilised microalgae: impact of wastewater nutrient characteristics and hydraulic retention time (HRT)”. *H2Open Journal* 1.1, pp. 12–25.

Chapter 7

Conclusions and future work

7.1 Conclusions

In this thesis, previously identified bottlenecks associated with the implementation of tertiary P removal technologies were addressed and the following conclusions can be derived for each of the objectives.

Objective A. Compare the robustness and efficacy of commercial coagulation-based technologies with different solid liquid separation processes in meeting sub 1 mg P/L consents under UK conditions.

- The choice of solid liquid separation technologies at tertiary treatment impacts the final P concentrations.
- Ballasted coagulation is the most robust of the three tested technologies at steady state and dynamic operation.
- Sufficient P removal relies on upstream flocculation settings and coagulant to influent P ratio (minimum 2.29 Fe:P molar ratio) in a pile cloth drum filter.

- Under optimised coagulation conditions, i.e. flocculation and coagulant choice and dose, an ultrafiltration membrane can achieve P removal to sub 0.3 and even 0.1 mg/L levels. However, because of the high operational costs, UF will likely not be suitable for tertiary P removal.

Objective B. Analyse the impact of different polymers and their doses on P removal and floc properties in a ballasted coagulation process.

- In a ballasted coagulation system, anionic polymers result in better P removal compared to cationic polymers.
- P removal does not deteriorate even at polymer doses as low as 0.01 mg/L.
- At higher polymer doses, larger more open flocs were formed resulting in lower effluent turbidity.
- Polymer act as connectors between coagulant-wastewater-ballast flocs rather than as the primary precipitating agent.
- Flocs made in a ballasted coagulation system break faster than plain coagulant-wastewater flocs, but it was seen that floc strength is not the essential factor for efficient P removal if the retention time in the system remains short (5 minutes in jar tests, 5.5-10 minutes at demo scale).

Objective C. Validate existing understanding of the efficacy of reactive media in large scale, long-term constructed wetlands trials for P removal.

- Full-scale reactive media systems behave differently from their laboratory and pilot counterparts.
- Although the technology is not at a sufficient technology readiness level yet, steel slag wetlands are a promising alternative for P removal at small wastewater treatment sites.

- The physico-chemical processes in this system are more complex than previously described and were also found to vary throughout the life of the bed.

- P removal in a steel slag constructed wetland does not mainly occur through calcium phosphate precipitation but is also influenced by internal as well as external factors such as pH, temperature and ion concentrations (Ca, CO_3^{2-}, Mg, Fe etc.).

Objective D. Evaluate the potential to recover and reuse alginate in an immobilised algal bio-reactor process.

- It is possible to recycle and reuse alginate from used algae beads in an immobilised algae system with a recovery rate of 69%.

- Algae beads made from recycled alginate had a lower mechanical strength, which can be mitigated by supplementation with fresh alginate, but performed similarly to beads made from virgin alginate in a continuous trial.

- Recycling and reuse of alginate will result in at least 34% net operational cost reduction in an immobilised algae system.

7.2 Future work

Since it was seen that the choice of tertiary P removal technologies impacts the final P concentration, experiments under controlled conditions to evaluate the impact of a range of parameters including coagulant choice and dose, wastewater characteristics and coagulation-flocculation settings will be needed to fully optimise such systems. This would be done by keeping parameters constant while varying one of them, e.g. coagulant dose response tests for different coagulants using the same wastewater and upstream

conditions, and by analysing P removal and floc characteristics. As such floc characteristics may be tailored for the respective solid liquid separation technologies and ultimately optimise the coagulation/separation process. This research would generate more understanding of underlying P removal mechanisms.

The experiments with a range of polymers in ballasted coagulation showed that polymer doses below 1 mg/L are still sufficient for P removal to low levels. To further reduce chemical consumption, it would be important to understand what the minimum possible coagulant and polymer doses are while still meeting effluent P consents. This can be done through further controlled dose response experiments with analysis of P removal and floc properties. In addition to that, with the limited understanding of P removal mechanisms when reaching very low P levels, thorough analysis on P speciation will bring more insights towards the underlying mechanisms. Since the work on the impact of polymers in ballasted coagulation was carried out in jar tests which are an idealised environment, validation of these results at larger scale and under real conditions is needed. This could be done with a similarly scaled plant where different polymers at varying doses are tested and floc analysis is incorporated. Finally, to optimise the choice of polymers and understand their behaviour under these conditions, a full structural analysis of the chemicals is needed.

The work with a reactive media wetland showed that the impact on P removal is more complex than previously thought. Future research on reactive media wetlands may include monitoring within the bed to better understand precipitation potentials of occurring ions. Better understanding and longer lifetimes of reactive media wetlands may become possible through pre-treatment of the media. Three potential avenues for reactive media need to be addressed. First, pre-conditioning of the media could be done through coating of the media with CO32- to slow down the dissolution of CaO, vanadium and other metals, maintain a near-neutral pH and generate adsorption sites for phosphate species. This

could be achieved through immersion of steel slag media in solutions with high carbonate concentrations. Secondly, with better P removal observed at higher pH, solutions to control pH without external chemical dosing will be required. This may be trialled in column or field experiments by reverting part of the initially alkaline effluent stream back through the wetland. This way a high pH could be maintained for a longer period. Options to control the alkaline pH at the effluent would need to be explored as well. This may be conducted by mixing of alkaline effluent with a fraction of the influent in continuous experiments. Third, it will be worthwhile exploring the regeneration potential of media to extend the life of reactive media wetlands. Regeneration experiments may be conducted by immersion of exhausted media in a highly alkaline (pH 14) or acid solutions for a fixed duration. Afterwards, this media could be tested on its P removal capacity in batch or continuous trials. Since reactive media wetlands are aimed to be circular economy solutions, the practicality of these approaches with an outlook towards full-scale needs to be considered. As such, additional consumption of chemicals, especially hazardous ones, may result in a rebound effect in sustainability aims. Nevertheless, this does not diminish the valuable knowledge more understanding on the physico-chemical mechanisms would generate.

Alginate recycling from used algae beads was shown to be possible without deterioration in subsequent P removal tests. In further research, alginate recycling can be improved through optimisation of the concentration of the dissolving agent by testing a lower range of concentrations. Further, a detailed study examining algae-alginate separation with filtration or centrifugation against no separation could highlight the most viable process, economically and operationally. To bring alginate recovery further, a detailed study implementing more than one recycling cycle could be conducted within continuous P removal trials. Finally, it would be worthwhile exploring the compounds (e.g. micropollutants) that recycled alginate retains from wastewater and whether this might impact

subsequent P removal.

Appendix A

Table A.1: Pilot and full-scale results on tertiary P removal with high rate sedimentation, depth filtration and surface filtration.

	Technology	Scale	Influent P mg TP/L	Effluent P mg TP/L	Coagulant	Coagulant dose mg Me/L	Dose ratio	Hydraulic setting	Additional chemicals	Reference
High rate sedimentation	BCM	Full	-	0.026	PACl	4	-	68 L/S	-	(Keaney et al. 2012)
	BCM	Pilot	1	0.039 (Alum), 0.025 ($FeCl_3$), 0.036 (PACl)	Alum, $FeCl_3$, PACl	12 (Alum), 24 ($FeCl_3$), 20 (PACl)	13.78 (Alum), 13.29 ($FeCl_3$), 22.96 (PACl)	3.2 L/s	0.7-0.8 mg/L polymer	(Lee et al. 2015)
	BCS + MMF	Pilot	0.22	0.031	$FeCl_3$	14	35.23	80 m/h	1 mg/L polymer	(DeBarbadillo et al. 2010)
Depth filtration	GM	Full	0.39	0.15	Alum	2.4	7.07	7.3 m/h	-	(Mueller et al. 1999)
	CUF-SF	Pilot	2.3	0.14	PASS	5.7	2.85	11 m/h	NaOCl	(Bratby 2016)
	CUF-SF	Pilot	1.5	0.06	PASS	5.7	4.36	11 m/h	NaOCl	(Bratby 2016)
	CG-SF	Pilot	1-4	0.014	$Fe_2(SO_4)3$	6-10	0.69-1.66	948 m^3/d	-	(Ragsdale 2007)
	CUF-SF	Pilot	0.135	0.017	$FeCl_3$	7	28.70	4.4-9.8 m/h	-	(Hook and Ott 2001)
Surface filtration	UF (0.02 µm)	Pilot	0.22	0.15	Alum	14.7	76.72	16.8 LMH	Cleaning chemicals	(DeBarbadillo et al. 2010)
	UF (0.04 µm)	Pilot	0.78-0.81	0.017-0.043	Alum	7.9	11.20	22.4-63.6 LMH	Cleaning chemicals	(Bill et al. 2011)

Continued on next page

Table A.1 – continued from previous page

	Technology	Scale	Influent P mg TP/L	Effluent P mg TP/L	Coagulant	Coagulant dose mg Me/L	Dose ratio	Hydraulic setting	Additional chemicals	Reference
	MicroF (0.1 µm)	Pilot	0.352	0.021	FeCl3	8	12.58	90 LMH	Cleaning chemicals	(Langer and Scherman 2013)
	MS (10 µm)	Pilot-Full	0.323	<0.08	PACl	2	7.11	10-25 m^3/h	0.6-1.7 mg/L polymer	(Langer and Scherman 2013)
	MicroF	Pilot	0.15	0.03	$FeClSO_4$	1.4	5.17	-	-	(Bratby 2016)

BCM: ballasted coag with magnetite. Co: co-precipitation. Post: post-precipitation. 2p dose: two point dosing. BCS: ballasted coag with sand. MMF: multi-media filter. SF: Sandfilter. GM: granular media. CUF: continuous upflow. CG: continuous gravity. UF: Ultrafiltration. MicroF: Microfiltration. MS: microsieve. BNR: Biological nutrient removal

A.1 Cloth filter effluent turbidity

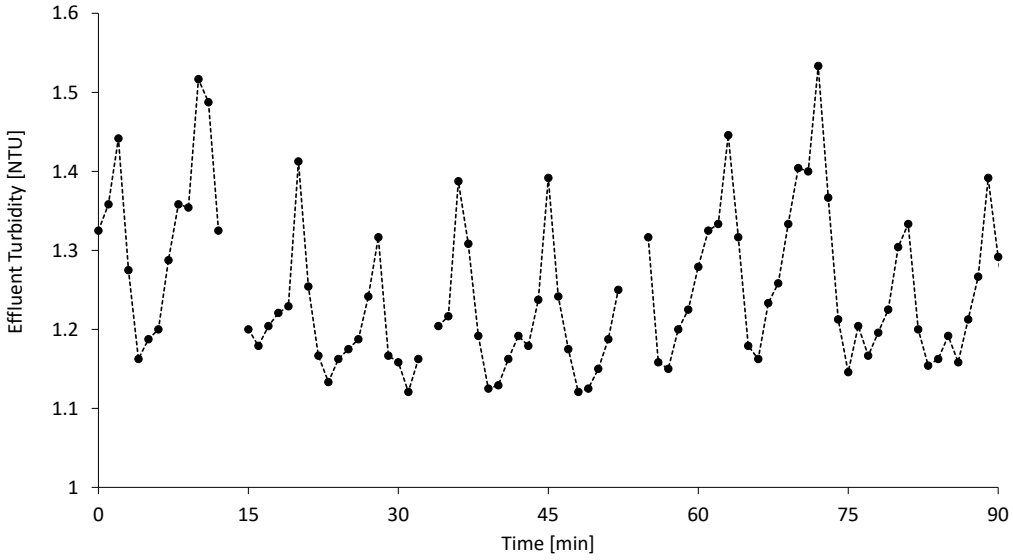

Figure A.1: Effluent turbidity variation during operation of cloth filter. Timeline is taken during steady-state operation.

Appendix B

B.1 Zeta potentials of polymers

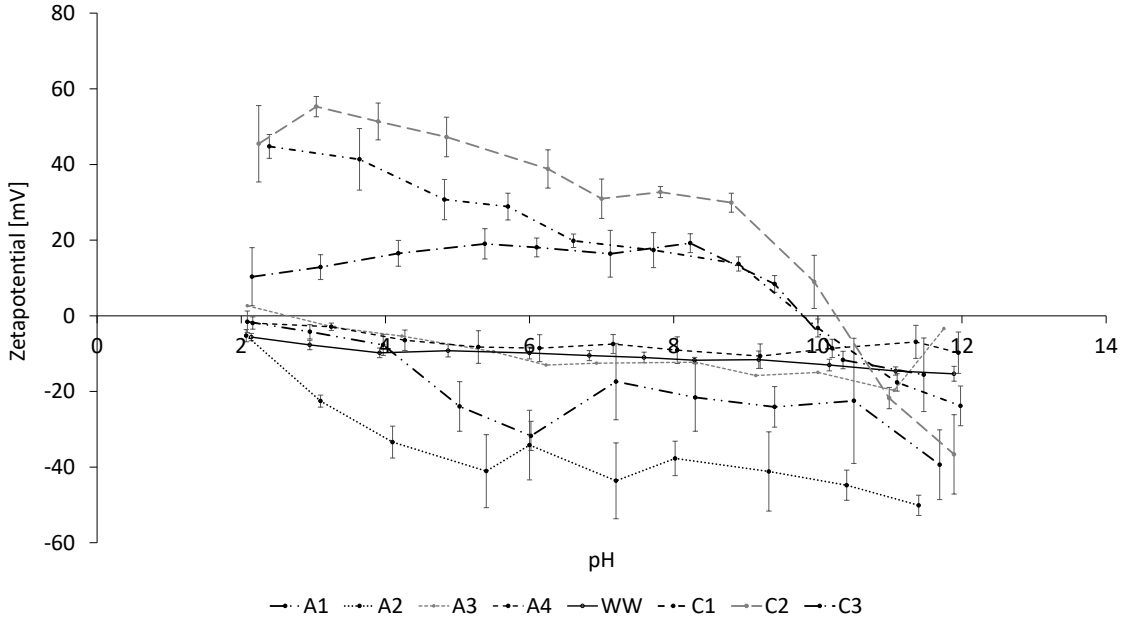

Figure B.1: Zeta potential for wastewater and polymers. C2: ——, C1: -·-·- , C3: ------ , A4: ——, Wastewater: ···-···- , A3: - - - - - , A1: ····· , A2: –·–·– .

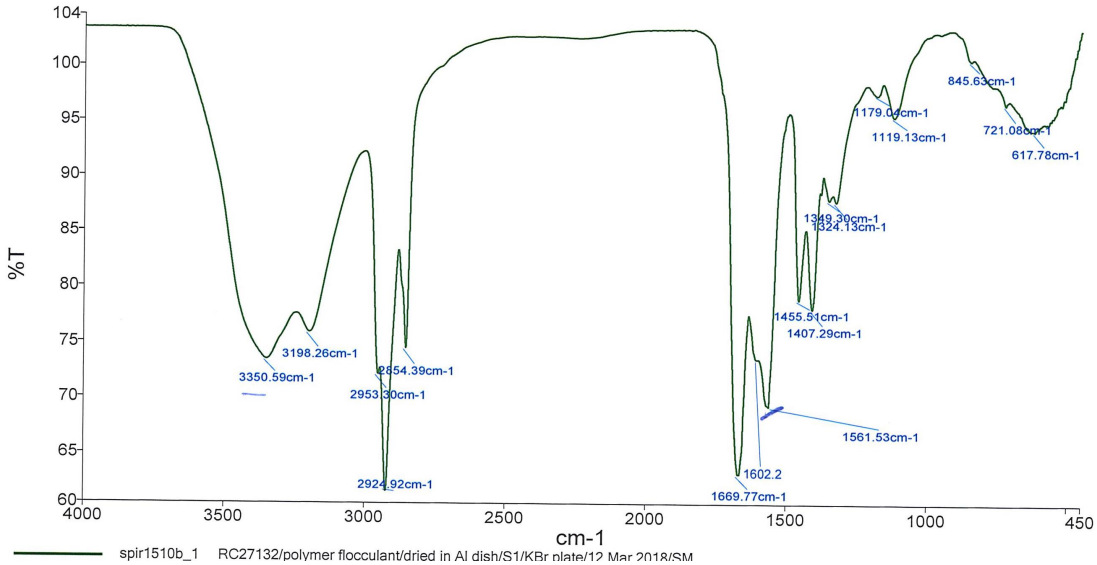

Figure B.2: FTIR spectrum of A2

B.2 FTIR spectra of polymers

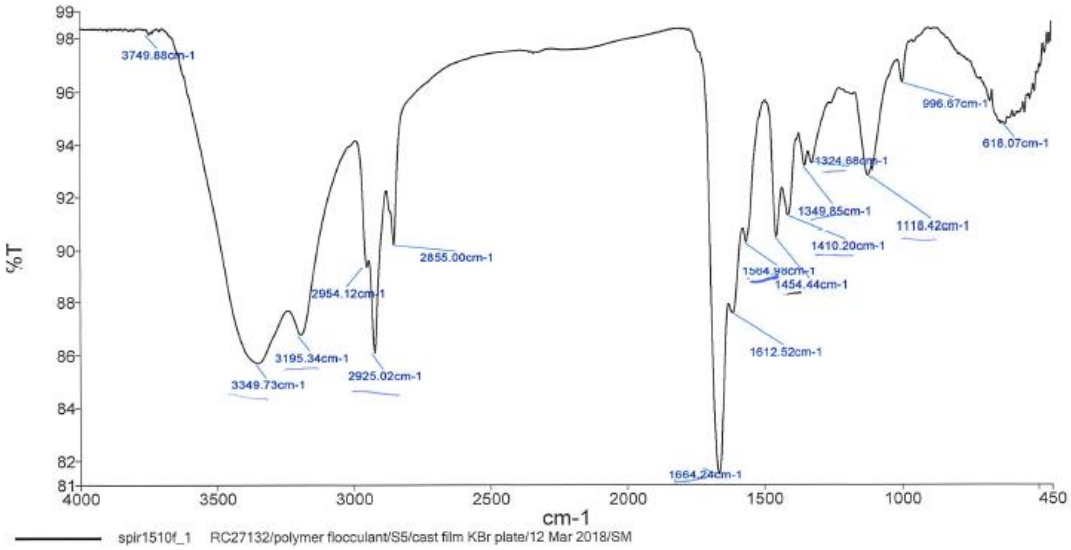

Figure B.3: FTIR spectrum of A3

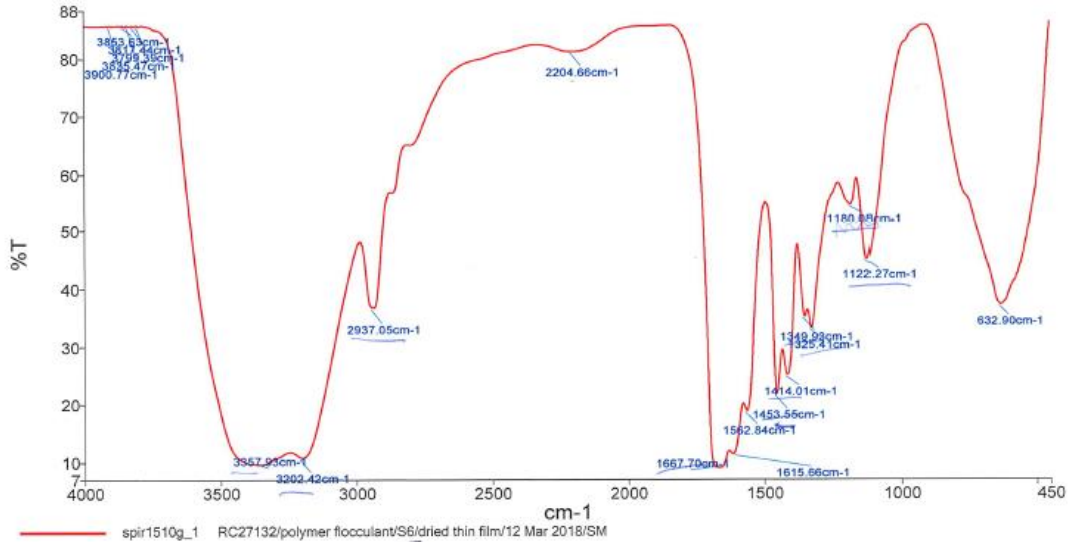

Figure B.4: FTIR spectrum of A4

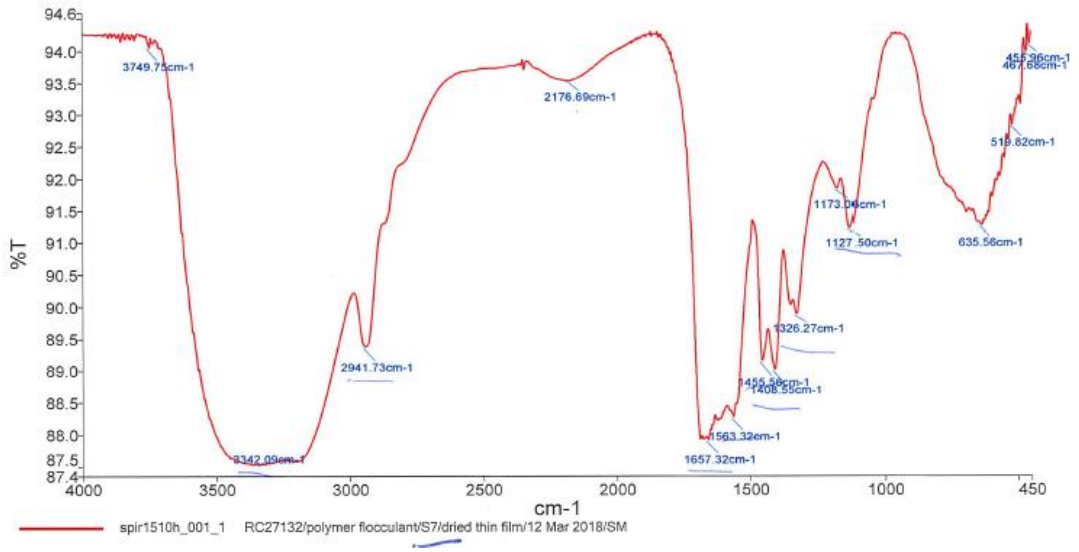

Figure B.5: FTIR spectrum of A1

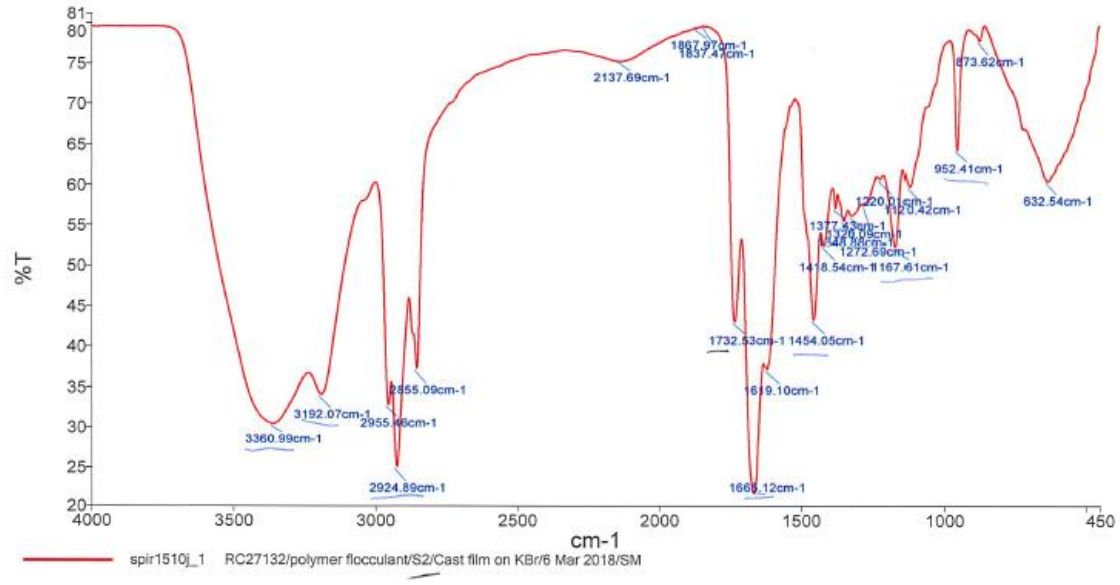

Figure B.6: FTIR spectrum of C1

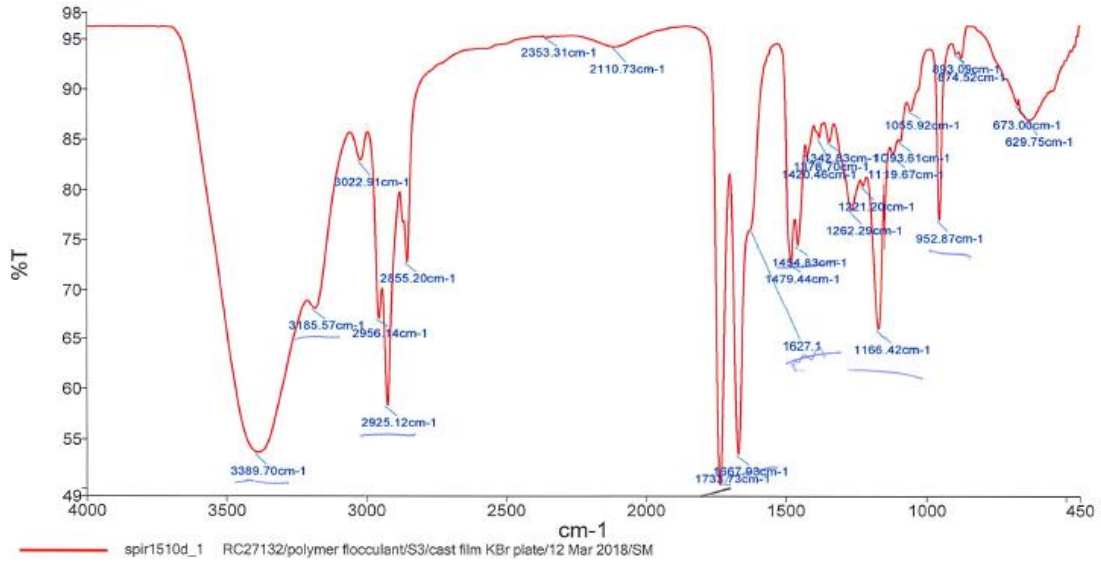

Figure B.7: FTIR spectrum of C2

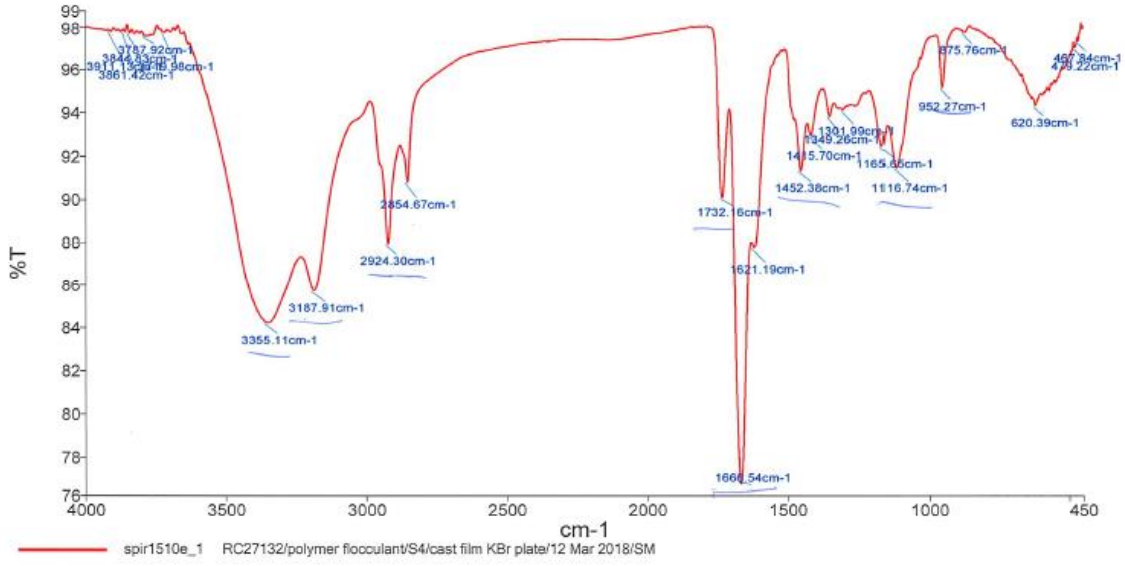

Figure B.8: FTIR spectrum of C3

Appendix C

C.1 Release and uptake of metals

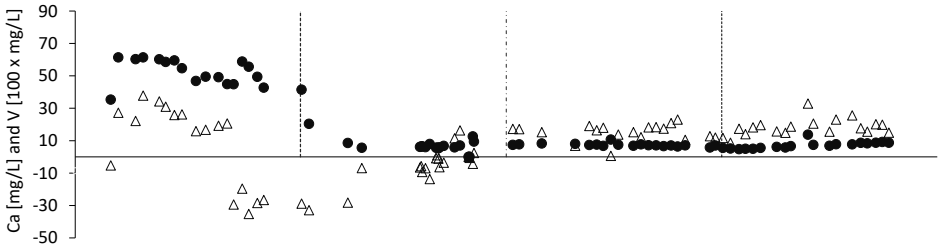

Figure C.1: Release of iron, zinc, nickel, copper, arsenic, silver and cadmium throughout the trial operation.

C.2 Plant growth and media analysis

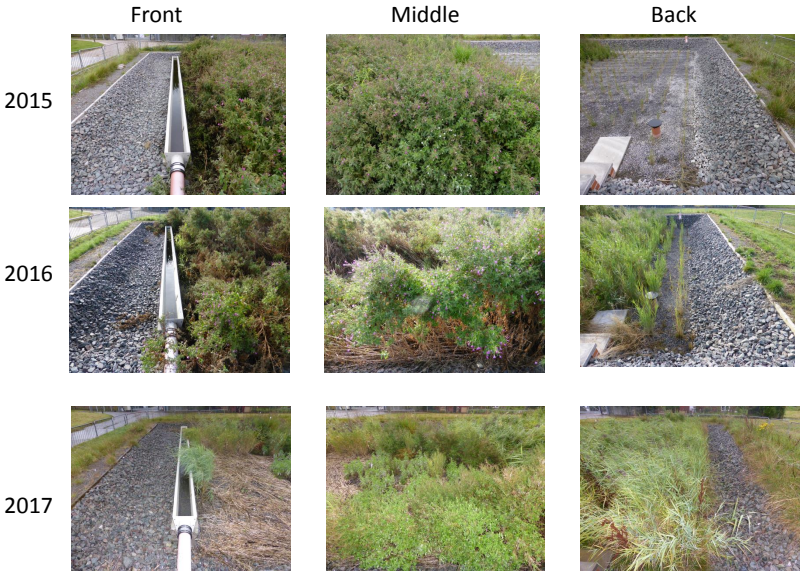

Figure C.2: Photographs of front, middle and back section of reed bed during September in years 2015 (Phase 2), 2016 (Phase 3) and 2017 (beyond Phase 4).

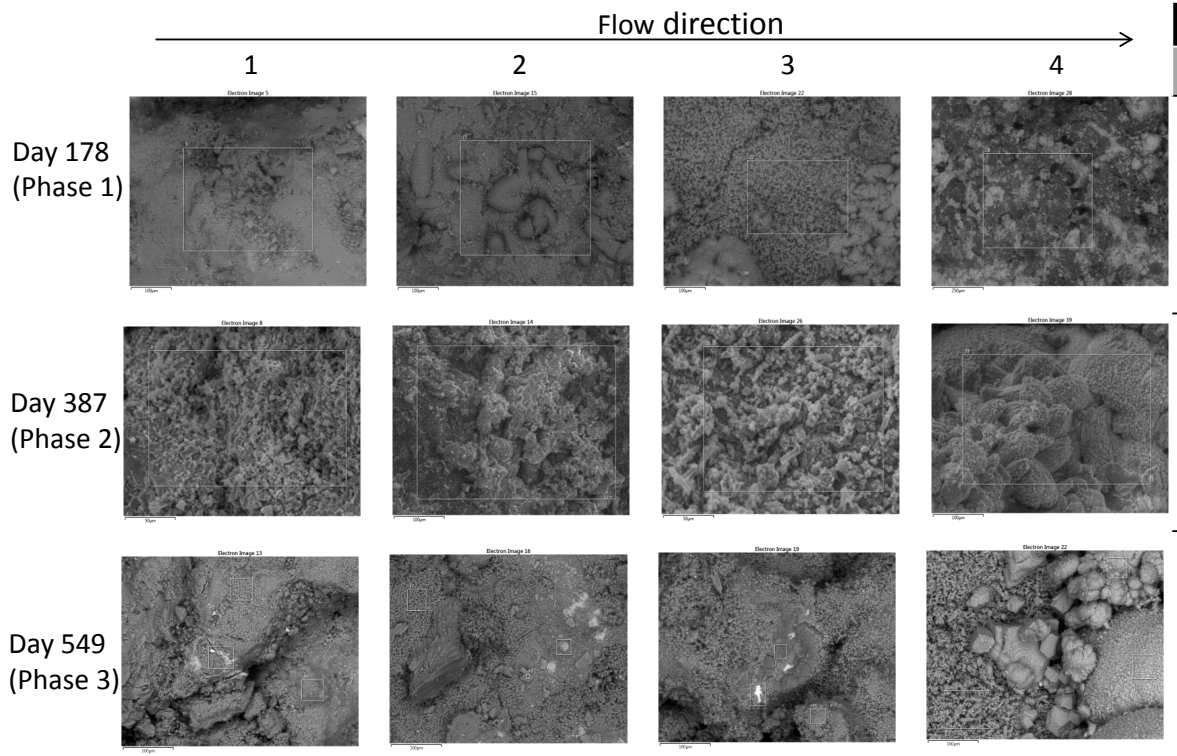

w% (n= 4)				
C	O	Ca	P	Fe
10.1 ± 3.8	48.7 ± 1.1	32.1 ± 3.5	2.2 ± 1.9	2.6 ± 1.0
8.2 ± 0.4	49.6 ± 1.9	31.4 ± 1.2	3.0 ± 1.7	3.2 ± 2.4
9.4 ± 1.1	45.8 ± 1.1	33.8 ± 2.8	2:2 ± 0.7	5.5 ± 3.3

Figure C.3: SEM images throughout intersectional points on days 178 (Phase 1), 387 (Phase 2) and 549 (Phase 3) with averaged weight percentage (w%) from EDX elemental analysis.

C.3 Tracer test

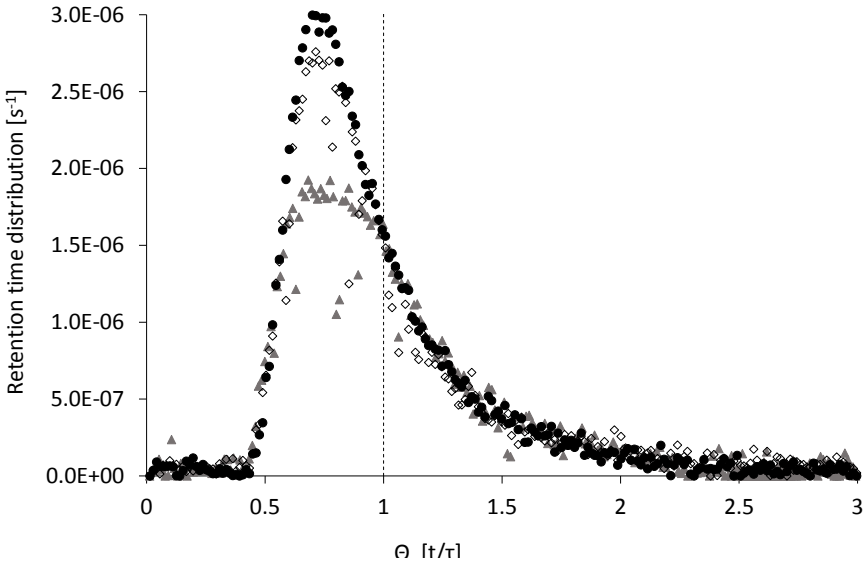

Figure C.4: Results from tracer tests done in Phase 1 (▲), Phase 3 (◇) and Phase 4 (●)

C.4 Extracted metals from media

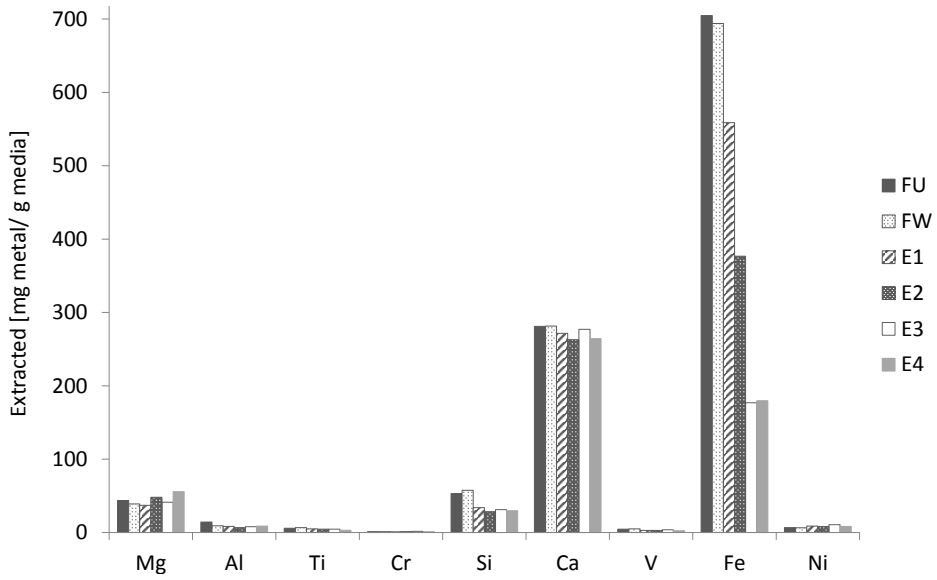

Figure C.5: Extraction of metals from fresh unwashed (FU), fresh washed (FW) and exhausted (E) slag from four intersectional points (E1, E2, E3, E4).

Table C.1: List of minerals returning a positive SI for Phases 1 to 4 sorted by their main cation and in each section by descending SI value.

Main cation	Phase 1	Phase 2	Phase 3	Phase 4
Ca	Hydroxyapatite	Hydroxyapatite	Hydroxyapatite	Hydroxyapatite
	Ca3(PO4)2 (beta)	Ca3(PO4)2 (beta)	Ca3(PO4)2 (beta)	Ca3(PO4)2 (beta)
	Ca3(PO4)2 (am2)	Ca3(PO4)2 (am2)	Ca4H(PO4)3:3H2O(s)	Ca4H(PO4)3:3H2O(s)
	Ca4H(PO4)3:3H2O(s) (OCP)	Ca4H(PO4)3:3H2O(s)	Ca3(PO4)2 (am2)	Ca3(PO4)2 (am2)
	Calcite	Calcite	Calcite	Calcite
	Aragonite	Aragonite	Aragonite	Aragonite
	Ca3(PO4)2 (am1)	Vaterite	Ca3(PO4)2 (am1)	Ca3(PO4)2 (am1)
	Vaterite	Ca3(PO4)2 (am1)	Vaterite	Vaterite
	CaCO3xH2O(s)	CaCO3xH2O(s)	CaCO3xH2O(s)	CaHPO4(s)
		CaHPO4(s)	CaHPO4(s)	
Fe	Hematite	Hematite	Hematite	Hematite
	Maghemite	Maghemite	Maghemite	Maghemite
	Goethite	Goethite	Goethite	Goethite
	Lepidocrocite	Lepidocrocite	Lepidocrocite	Lepidocrocite
	Ferrihydrite (aged)	Ferrihydrite (aged)	Ferrihydrite (aged)	Ferrihydrite (aged)
	Ferrihydrite	Ferrihydrite	Ferrihydrite	Ferrihydrite
	Strengite	Strengite	Strengite	
Mixed	Magnesioferrite	Magnesioferrite	Magnesioferrite	Magnesioferrite
	Chrysotile	Chrysotile	Chrysotile	Kaolinite
	Sepiolite	Dolomite (ordered)	Dolomite (ordered)	Dolomite (ordered)
	Sepiolite (A)	Kaolinite	Sepiolite	Chrysotile
	Dolomite (ordered)	Sepiolite	Dolomite (disordered)	Dolomite (disordered)
	Dolomite (disordered)	Dolomite (disordered)	Kaolinite	Sepiolite
	Huntite	Huntite	Huntite	Imogolite
	Sepiolite (A)			Halloysite

Continued on next page

Table C.1 – continued from previous page

Main cation	Phase 1	Phase 2	Phase 3	Phase 4
	Imogolite			
	Halloysite			
Mg	Artinite	Magnesite	Magnesite	
	Brucite			
	Mg(OH)2 (active)			
	Magnesite			
Si	Quartz	Quartz	Quartz	
	Chalcedony (SiO2)	Chalcedony (SiO2)	Chalcedony (SiO2)	
Al		Diaspore	Diaspore	Diaspore
		Gibbsite (C)	Gibbsite (C)	Gibbsite (C)
		Al(OH)3 (soil)		Al(OH)3 (soil)
				Boehmite
Ti	Rutile	Rutile	Rutile	

Appendix D

D.1 Dissolution of algae beads

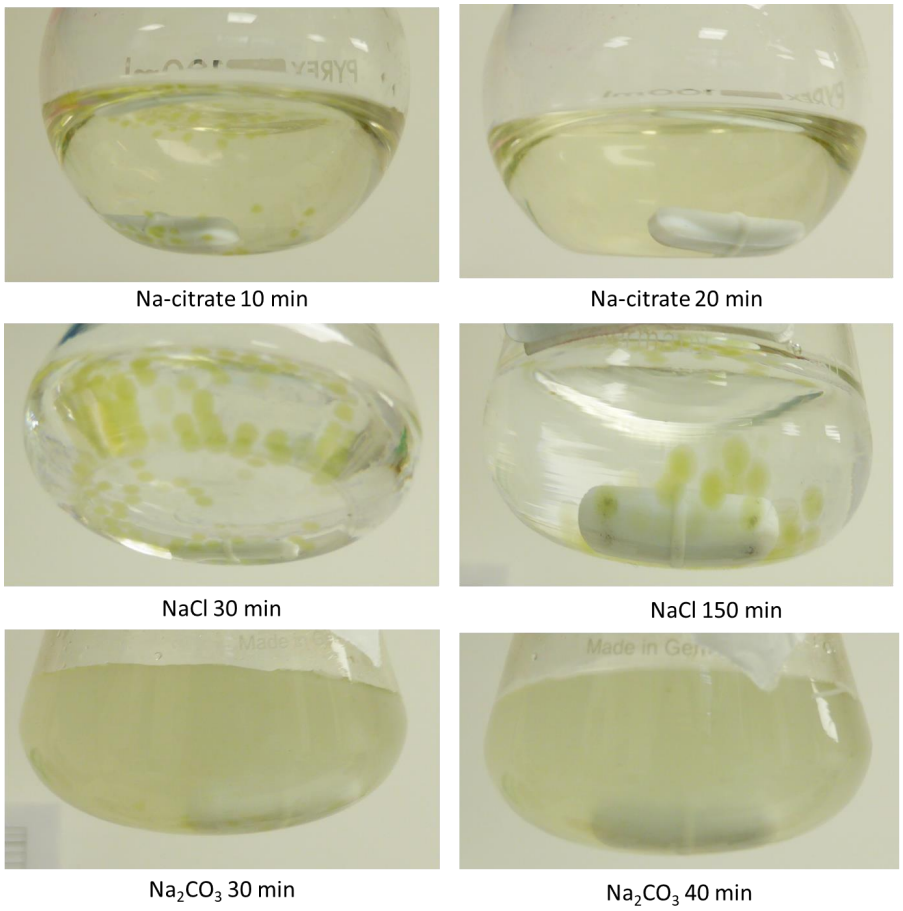

Figure D.1: Algae beads in respective dissolution solutions.

D.2 Re-immobilisation of algae beads

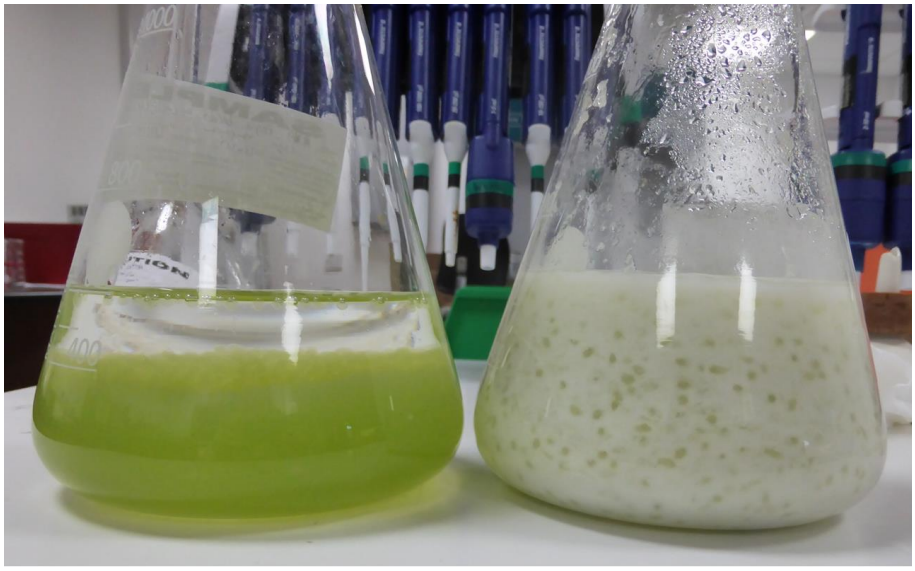

Figure D.2: Algae beads made from VA (left) and RA (right) after stirring.